博士論文

論文題目　**Studies on two novel interaction partners of Arabidopsis heterotrimeric G protein β subunit (AGB1): Adaptor protein 3μ (AP-3μ) and Nonphototropic hypocotyl 3 (NPH3)**
（シロイヌナズナのヘテロ三量体 **G** タンパク質 **β** サブユニット **(AGB1)**の新規相互作用因子：細胞内小胞輸送因子 **AP-3μ** と青色光信号伝達因子 **NPH3** に関する研究）

氏名　ガンサップ　ジラーポン

Table of Contents

Chapter 1

General Introduction

Heterotrimeric G proteins (G proteins) are conserved among eukaryotes and are responsible for the transmission of extracellular signals perceived by G protein-coupled receptors (GPCRs) to intracellular effectors (Pierce *et al*., 2002). G proteins consist of three subunits, Gα, Gβ and Gγ. In animals, GPCRs are activated upon binding of their ligands and promote the exchange of GDP to GTP on Gα, which leads to a conformational change of Gα and dissociation of the heterotrimer into Gα and a Gβγ dimer. Gα and Gβγ are active and independently regulate the activities of effector molecules, which transmit the ligand-binding signals from GPCRs to downstream pathways to affect numerous cellular behaviours (Jones and Assmann, 2004; Wettschureck and Offermanns, 2005). In plants, G proteins have structural similarities to the corresponding molecules in animals but transmit signals by atypical mechanisms and effector proteins to control growth, cell proliferation, defence, stomate movements, channel regulation, sugar sensing and some hormonal responses (Urano *et al*., 2013). Furthermore, the numbers and kinds of GPCR signaling components in plants differ somewhat from those in animals. For example, compared with the presence of multiple G protein subunits in mammals (e.g. 23 Gαs, 5 Gβs, and 12 Gγs in humans), Arabidopsis contains only 1 Gα (GPA1) (Ma *et al*., 1990), 1 Gβ (AGB1) (Weiss *et al*., 1994), and 3 Gγs proteins (AGG1, AGG2, and AGG3) (Mason and Botella, 2000; Mason and Botella, 2001; Chakravorty *et al*., 2011). Soybean (*Glycine max*) contains 4 Gαs, 4 Gβs, and 10 Gγs proteins (Bisht *et al*., 2010; Choudhury *et al*., 2011). Similarly,

humans have approximately 1,000 G-protein coupled receptors (GPCRs), whereas only a few divergent GPCRs have been identified in Arabidopsis (Gookin *et al*., 2008). These facts suggest that plants have plant-specific mechanisms for G protein signaling.

Studies on loss-of-function alleles and gain-of-function overexpression lines of G protein subunits suggest that the G proteins modulate hormonal and stress responses, and play regulatory roles in many growth and developmental processes (Jones and Assmann, 2004; Chen, 2008). *agb1* mutants are characterized by aberrant leaf and flower shape, increased production of lateral root primordial and shorter hypocotyls and siliques (Lease *et al*., 2001; Ullah *et al*., 2001; Ullah *et al*., 2003). Additionally, seed germination and early seedling development of *agb1* mutants are hypersensitive to ABA. Because plants lacking AGB1 have greater ABA hypersensitivity than plants lacking GPA1, AGB1 has been suggested to be the predominant regulator of G protein-mediated ABA signaling (Pandey *et al*., 2006). ABA was shown to be bound by GTG1 and GTG2, which are Gα-interacting receptors on the plasma membrane (Pandey *et al*., 2009). A quantitative proteomics-based analysis of WT and *gtg1gtg2* mutants revealed that the majority of ABA-responsive proteins require the presence of GTG proteins (Alvarez *et al*., 2013), supporting the importance of the G proteins in ABA signal transduction.

The multiple phenotypes of *agb1* mutants suggest that AGB1 is a key factor of several signaling pathways. So far some genetic and/or physical AGB1-interaction partners have been identified and characterized, for example a Golgi-localized hexose transporter SGB1(Wang *et al*., 2006), an N-MYC downregulated-like1 (NDL1) (Mudgil *et al*., 2009), and an acireductone dioxygenase-like protein, ARD1 (Friedman *et al*., 2011). An interactome analysis revealed the involvement of G-proteins in cell wall modification (Klopffleisch *et al*., 2011). However, the molecular mechanisms

underlying the AGB1-mediated signaling are unclear (Klopffleisch *et al*., 2011).

A yeast two-hybrid screen was performed to identify interacting partners of the Arabidopsis G protein β subunit AGB1 (Tsugama *et al*., 2012a). Some novel interacting partners of AGB1 were identified, for example, a plasma membrane 2C-type protein phosphatase PP2C52 (Tsugama *et al*., 2012a; Liu *et al*., 2013), a U-box E3 ubiquitin ligase PUB20 (Kobayashi *et al*., 2012), and a bZIP protein VIP1, which is a regulator of osmosensory signaling (Tsugama *et al*., 2012b; Tsugama *et al*., 2013a). In this study, two novel AGB1-interacting proteins, an adaptor protein 3μ (AP-3μ, At1g56590) and a phototropin-interacting protein nonphototropic hypocotyl 3 (NPH3, At5g64330), were functionally characterized. Furthermore, the physiological roles of the interaction between AGB1 and AP-3μ or NPH3 were examined.

Chapter 2

The Arabidopsis adaptor protein AP-3μ interacts with the G protein β subunit AGB1 and is involved in abscisic acid regulation of germination and post-germination development.

2.1 Introduction

To identify interacting partners of AGB1, a yeast two-hybrid screen was performed (Tsugama *et al*., 2012a). One of the AGB1-interacting proteins found in the screen was an adaptor protein, AP-3μ (At1g56590). Adaptor proteins (APs) are key regulators of endocytosis and secretory pathways. Five different heterotetrameric AP complexes (AP-1, AP-2, AP-3, AP-4, and AP-5) have been characterized so far in eukaryotes. The AP-3 complex, which consists of two large subunits (δ and β3), a medium subunit (μ3), and a small subunit (σ3) (Boehm and Bonifacino, 2002; Dell' Angelica, 2009), participates in protein sorting at the trans-Golgi network (TGN) and/or endosome (Cowles *et al*., 1997; Dell' Angelica *et al*., 1997; Stepp *et al*., 1997; Kretzschmar *et al*., 2000).

In Arabidopsis, each subunit of the AP-3 complex is encoded by a single-copy gene (Bassham *et al*., 2008). Loss-of function mutants of several subunits of the AP-3 complex have been shown to be the suppressors of *zigzag1* (*zig1*), which is abnormal in both shoot gravitropism and morphology due to the lack of a vesicle trafficking regulator, SNARE VTI11 (Niihama *et al*., 2009). The AP-3 complex also plays a role in vacuolar function in Arabidopsis, including mediation of the transition between storage and lytic vacuolar identity (Feraru *et al*., 2010; Zwiewka *et al*., 2011). However, it is unclear whether the AP-3 complex also has roles in stress and hormonal responses.

Here I show that AP-3μ physically interacts with AGB1 in yeast and *in vitro*, as well as *in planta*. Genetic interaction between *AP-3μ* and *AGB1* is also examined using *agb1/ap-3μ* double mutants.

2.2 Materials and methods

2.2.1 Plant material and culture conditions

Arabidopsis thaliana ecotype Columbia-0 (Col-0) was used throughout the experiments. Seeds of *ap-3μ-2* (Niihama *et al*., 2009), *ap-3μ-4*, *agb1-1* (Lease *et al*., 2001), *agb1-2* (Ullah *et al*., 2003), *ap-3δ*, and *chc1-2* (Kitakura *et al*., 2011) mutants were obtained from the Arabidopsis Biological Research Center (ABRC) with stock numbers of SALK_064486C, CS859652, CS3976, CS6536, SALK_144344C, and CS25142 respectively. The genetic backgrounds for all the mutant lines are Col-0. Except *agb1-1* mutant, T-DNA insertion was confirmed by genomic PCR analysis (Table 1). Seeds were surface sterilized and sown on 0.8% agar containing 0.5× Murashige and Skoog (MS) salts (Wako, Japan), 1% (w/v) Suc, and 0.5 g/L MES, pH 5.8, with 0, 0.25, 0.5, 1.0 or 2.0 μM ABA or 400 mM mannitol or 150 mM NaCl or 9.2% polyethylene glycol, chilled at 4°C in the dark for 3 d (stratified), and germinated at 22°C. Plants were grown at 22°C under 16-h-light/8-h-dark conditions.

2.2.2 Yeast two-hybrid (Y2H) analysis

A Y2H screen using AGB1 as a bait was performed as described previously (Tsugama *et al*., 2012a). The construct of pGAD-AP-3μ was generated as described below.

A cDNA clone of *AP-3μ* (*AT1G56590*) (clone name: RAFL09-80-A11) was obtained from RIKEN BRC Experimental Plant Division (Seki *et al*., 2002). This clone had an 11-bp deletion (corresponding to position 247-257 from the start codon) in the putative full-length ORF of *AP-3μ* derived from a putative full-length cDNA clone of *AP-3μ* (GenBank accession: BX814222). To obtain the full-length ORF of *AP-3μ*, the 5'

region of *AP-3μ* ORF was amplified by PCR using the RIKEN cDNA clone as template and the following primer pair: 5'-CTCGGATCCATATGCTTCAATGTATCTTTCTC-3' and 5'-GCAACTCTGCAAAGGAACTCGATTGCCATCAACGGTGGC-3'. The 3' region of *AP-3μ* cDNA was amplified by PCR using the RIKEN cDNA clone as template and the following primer pair: 5'-TCGAGTTCCTTTGCAGAGTTGCTGATGTTTTGTCTGAG-3' and 5'-CAGGAAACAGCTATGACCATGA-3'. The two kinds of PCR products (corresponding to the 5' and 3' regions of *AP-3μ* cDNA) were mixed and used as template for PCR using the following primer pair: 5'-CTCGGATCCATATGCTTCAATGTATCTTTCTC-3' (*Bam*HI site is underlined) and 5'-CAGGAAACAGCTATGACCATGA-3'. The resultant PCR products contain the full-length ORF and the 3' untranslated region (UTR) of *AP-3μ*. The PCR products were digested with *Bam*HI, and inserted into the *Bgl*II-*Sma*I site of pGADT7-Rec (Clontech, Japan), generating pGAD-AP-3μ.

To confirm the result of the Y2H screen, pGBK-AGB1 and pGAD-AP-3μ were co-introduced into the *Saccharomyces cerevisiae* strain AH109. After transformation, at least 4 colonies grown on the SD media lacking leucine and tryptophan (SD/-Leu/-Trp), were streaked on the SD/-Leu/-Trp and the SD media lacking leucine, tryptophan, and histidine.

2.2.3 *In vitro* pull-down assay

Polyhistidine-tagged AGB1 (His-AGB1) and polyhistidine-tagged AGG1 (His-AGG1), were expressed in *Escherichia coli* and purified as previously described (Tsugama *et al*., 2012a). The constructs of pGEX-5X-AP-3μ and pGEX-5X- AP-3μ^{DN},

which express GST-fused AP-3μ (GST-AP-3μ) and GST-fused AP-3μ^{DN} (GST-AP-3μ^{DN}) respectively, were generated as described below.

To express GST-fused AP-3μ (GST-AP-3μ), the open reading frame (ORF) of *AP-3μ* was amplified by PCR using pGAD-AP-3μ as template and the following primer pair: 5′-CGCGGGATCCGGATGCTTCAATGTATCTTTCTCATCTCCGAT-3′ and 5′-GGCGCCCGGGTACAACCTGACATCGAACTCACCAGC-3′ (*BamH*I and *Sma*I sites are underlined). The PCR products were digested by *BamH*I and *Sma*I, and cloned into the *BamH*I-*Sma*I site of pGEX-5X-1 (GE Healthcare, UK), generating pGEX-5X-AP-3μ.

To express GST-fused AP-3μ^{DN} (GST-AP-3μ^{DN}), the open reading frame (ORF) of *AP-3μ*^{DN} was amplified by PCR using pGAD-AP-3μ as template and the following primer pair: 5′-AATTCCCGGGAATGCTTCAATGTATCTTTCT -3′ and 5′-AATTGGATCCACAAACGAGGAGGGATAGTTTGAAG-3′ (*Xma*I and *BamH*I sites are underlined). The PCR products were digested by *Xma*I and *BamH*I, and cloned into the *Xma*I-*BamH*I site of pGBKT7 (Clontech, Japan), generating pGBK-AP-3μ^{DN}. pGBK-AP-3μ^{DN} was digested by *Sma*I and *Not*I, and the resultant ORF fragments of AP-3μ^{DN} were inserted into the *Sma*I-*Not*I site of pGEX-5X-1 (GE Healthcare, UK) in-frame to the coding sequence of glutathione S-transferase (GST), generating pGEX-5X- AP-3μ^{DN}.

To induce GST-AP-3μ or GST-AP-3μ^{DN}, pGEX-5X-AP-3μ or pGEX-5X-AP-3μ^{DN} was transformed into the *Escherichia coli* strain, BL21 (DE3). The transformed *E. coli* cells were cultured at 37°C in LB medium until OD_{600} reached 0.5, and incubated at 28 °C for 3 h after an addition of IPTG to a final concentration of 0.1 mM. The cells were then harvested by centrifugation and resuspended in 1× PBS

(phosphate-buffered saline: 137 mM NaCl, 8.10 mM $Na_2HPO_4 \cdot 12H_2O$, 2.68 mM KCl, 1.47 mM KH_2PO_4, pH 7.4) with 2 mg/ml lysozyme (Wako, Japan). The cell suspension was frozen at −80 °C and thawed at room temperature. Freezing and thawing were repeated two more times to lyse the cells, and 2 units of recombinant DNase I (Takara, Japan) was added to the solution. The solution was incubated at room temperature until the solution became fluid due to DNA degradation. The solution was then centrifuged at 12000 ×g for 5 min and the supernatant was used as crude protein extracts.

GST-AP-3μ or GST-AP-3μ^{DN} in the crude extracts was bound to Glutathione Sepharose 4 Fast Flow (GE Healthcare, UK) following the manufacturer's instructions, and the resin was washed 4 times by 1× PBS (phosphate-buffered saline: 137 mM NaCl, 8.10 mM $Na_2HPO_4 \cdot 12H_2O$, 2.68 mM KCl, 1.47 mM KH_2PO_4, pH 7.4). After removing 1× PBS, the resin was resuspended in solution containing purified His-AGB1 and incubated at room temperature for 60 min with gentle shaking. The resin was then washed 4 times by 1× PBS and resuspended in 20 mM reduced glutathione in 50 mM Tris–HCl, pH 8.0. The suspension was incubated at room temperature for 15 min to release GST-AP-3μ or GST-AP-3μ^{DN}. The slurry of the resin was centrifuged for a few min at 12000 ×g. GST-AP-3μ or GST-AP-3μ^{DN} and His-AGB1 in the supernatant were analyzed by immunoblotting using an anti-GST antibody (diluted 4,000-fold; GE Healthcare, UK) and HisProbe-horseradish peroxidase (HRP) (diluted 2,000-fold; Thermo Fisher Scientific, USA). After the reaction of an anti-GST antibody, HRP-linked rabbit antibodies against Goat IgG (diluted 5,000-fold; MBL, Japan) were used as second antibodies. Signals were detected with SuperSignal West Pico Chemiluminescent Substrate (Thermo Fisher Scientific, USA).

2.2.4 Bimolecular fluorescence complementation (BiFC) assay

To express cYFP (the C-terminal half of YFP)-fused AP-3μ, the open reading frame (ORF) of *AP-3μ* was amplified by PCR using pGAD-AP-3μ as template and the following primer pair: 5′-CCGGTCTAGAATGCTTCAATGTATCTTTCTC-3′ and 5′-GGCGCCCGGGTACAACCTGACATCGAACTCACCAGC-3′ (*Xba*I and *Sma*I sites are underlined). The PCR products were cloned into the *Sma*I site of pBluescript II SK$^-$. The resultant plasmid was digested by *Xba*I, and the resultant ORF fragments of AP-3μ were inserted into the *Spe*I site of pBS-35SMCS-cYFP (Tsugama *et al*., 2012a), generating pBS-35S-AP-3μ-cYFP. To express nYFP (the N-terminal half of YFP)-fused AGB1, pBS-35S-nYFP-AGB1 (Tsugama *et al*., 2012a) was used. A mixture of an nYFP construct and a cYFP construct (500 ng each) was used for particle bombardment to co-express proteins of interest in onion epidermal cells. Particle bombardment and fluorescence microscopy were performed as previously described (Zhang CQ *et al*., 2008). Images were processed using Canvas X software (ACD Systems).

2.2.5 Subcellular localizations of GFP- and mCherry-fused proteins

The constructs of pBI121-35S-GFP, pBI121-35S-AP-3μ-GFP, pBI121-35S-mCherry and pBI121-35S-AGB1-mCherry were generated as described below.

To create plasmids for expressing GFP-fused protein, pBS-35SMCS-GFP (Tsugama *et al*., 2012c) was digested by *Sma*I and *EcoR*I to obtain the DNA fragment containing GFP-Nos terminator. This fragment was inserted into the *Sma*I-*EcoR*I site of a pre-digested pBI121, which GUS-Nos terminator fragment was removed, generating pBI121-35S-GFP.

The open reading frame (ORF) of *AP-3μ* was amplified by PCR using pGAD-AP-3μ as template and the following primer pair: 5′-CCGGTCTAGAATGCTTCAATGTATCTTTCTC-3′ and 5′-GGCGCCCGGGTACAACCTGACATCGAACTCACCAGC-3′ (*Xba*I and *Sma*I sites are underlined). The PCR products were digested by *Xba*I and *Sma*I, and cloned into the *Xba*I-*Sma*I site of pBI121-35S-GFP, generating pBI121-35S-AP-3μ-GFP.

To create plasmids for expressing mCherry-fused protein, the ORF of mCherry was amplified by PCR using pmCherry-N1 (Clontech, Japan) as template and the following primer pair: 5′-ATATCCCGGGTATGGTGAGCAAGGGCGAGGAGGATAACATG-3′ and 5′-AATTCCCGGGTTACTTGTACAGCTCGTCCATGCCGCCGGT-3′ (*Sma*I site is underlined). The PCR fragments were digested by *Sma*I and inserted into the *Sma*I site of pBI121, generating pBI121-35S-mCherry. The open reading frame (ORF) of *AGB1* was amplified by PCR using pGBK-AGB1 (Tsugama *et al*., 2012a) as template and the following primer pair: 5′-GGCCTCTAGAATGTCTGTCTCCGAGCTCAAAGAACGCCAC-3′ and 5′-TTAAGGATCCAATCACTCTCCTGTGTCCTCCAAACGCCCAT -3′ (*Xba*I and *BamH*I sites are underlined). The PCR products were digested by *Xba*I and *BamH*I, and cloned into the *Xba*I-*BamH*I site of pBI121-35S-mCherry, generating pBI121-35S-AGB1-mCherry.

A mixture of pBI121-35S-AP-3μ-GFP and pBI121-35S-AGB1-mCherry (1 μg each) or pBI121-35S-GFP and pBI121-35S-mCherry (for control) was used for particle bombardment to co-express AP-3μ-GFP and AGB1-mCherry or GFP alone and mCherry alone in onion epidermal cells. Particle bombardment and fluorescence

microscopy were performed as previously described (Zhang CQ *et al*., 2008). For ABA treatment, the bombarded onion epidermal cells were incubated in 0.5× MS containing 100 μM ABA for 1 h before microscopy observation. Images were processed using Canvas X software (ACD Systems).

2.2.6 Measurement of germination and greening rates

Germination and greening rates were compared between seed lots that were produced, harvested, and stored under identical conditions. Seeds were sown and grown as described in the section Plant material and culture conditions.

Germination is defined here as emergence of the radicle through the seed coat. Cotyledon greening is defined as obvious cotyledon expansion and turning green. Germination and greening rates were scored daily for 9 days after seeds were transferred to the light at 22°C. The experiments were repeated at least twice. The data shown are averages of all the experiments ± SD.

2.2.7 Semi-quantitative RT-PCR and quantitative real-time RT-PCR

The expression of *AP-3μ* mRNA in the wild type and the *ap-3μ* mutants was tested by semi-quantitative RT-PCR. Plants of each genotype were grown for 2 weeks and sampled. Total RNA was prepared using the GTC method (Chomczynski and Sacchi, 1987) and cDNA was synthesized from 4.6 μg of total RNA with PrimeScript Reverse Transcriptase (Takara, Japan) using an oligo (dT) primer. The primer sequences used for the RT-PCR are given in Table 2. The expressions of the ABA-responsive genes (*RAB18*, *RD29A*, and *AHG1*) in the wild-type and the *ap-3μ* mutants were tested by quantitative real-time RT-PCR. Plants of each genotype were

grown for 18 days on 0.8% agar containing 0.5× Murashige and Skoog (MS) salts (Wako, Japan), 1% (w/v) Suc, and 0.5 g/L MES, pH 5.8, with 0 or 1.0 μM ABA and sampled. Total RNA was prepared using RNeasy Plant Mini Kit (Qiagen, Netherlands) and cDNA was synthesized from 2 μg of the total RNA with High Capacity RNA-to-cDNA Kit (Applied Biosystems, USA) according to the manufacturer's instructions. The reaction mixtures were diluted 20 times with distilled water and used as a template for PCR. The primer sequences are given in Table 2 (Tsugama *et al*., 2012b; Nishimura *et al*., 2007). Quantitative real-time RT-PCR was performed using SYBR® *Premix Ex Taq*™ II (Perfect Real Time) (Takara, Japan) and the StepOne Real-Time PCR System (Applied Biosystems, USA).

Table 1. Primer pairs used for genomic PCR.

Gene	Primer sequence (5' > 3')
AP-3μ	PF1: CCGGTCTAGAATGCTTCAATGTATCTTTCTC PR1: AATTGGATCCACAAACGAGGAGGGATAGTTTGAAG
AP-3δ	Fw: GGGCACTGCTCATTGAT Rv: GTGGTTAATGCTGGTC
CHC1	Fw: GGTGGATAGTGAGCTCATCT Rv: CTTTCTCGGGAACTAGGATCTG

Table 2. Primer pairs used for RT-PCR analyses.

Gene	Primer sequence (5' > 3')
AP-3μ	PF2: CCCGTGTGTCCGCTACAGACC PR2: TGGGATTCGCCCGATTGTCCA
UBQ5	Fw: GACGCTTCATCTCGTCC Rv: CCACAGGTTGCGTTAG
RAB18	Fw: TCCAGCTCTAGCTCGGAGGATGA Rv: GGATCCCATGCCGCCCATCG
RD29A	Fw: GCCGGAATCTGACGGCGGTT Rv: CCCGTCGGCACATCCTTGTCG
AHG1	Fw: AGGATGGATGAGATGGCAAC Rv: CCTCCCTCGGATCACAGTTA
Actin	Fw: GGTAACATTGTGCTCAGTGGTGG Rv: AACGACCTTAATCTTCATGCTGC
AGB1	Fw: TGGGATGTAACTACTGGTCTCA Rv: CAGCACGAGTGTCCCACAA
AP-3δ	Fw2: GAGATCCGACGAAACATATTTCTAA Rv2: TGCTGGTCTTATCTTCGTCACT
CHC1	Fw: GGTGGATAGTGAGCTCATCT Rv: CTTTCTCGGGAACTAGGATCTG

2.3 Results

2.3.1 AP-3μ interacts with AGB1

To identify interacting partners of AGB1, a yeast two-hybrid screen of the Arabidopsis leaf library using full-length AGB1 as bait was performed. Even on high-stringency selection media (SD/QDO), more than 3600 positive clones were obtained. Using yeast colony PCR with an *AGG1*- or *AGG2*-specific primer, we found that 60–70% of these clones expressed AGG1 (data not shown). Plasmid inserts from non-AGG1 clones were then amplified by colony PCR using a vector-specific primer pair, and sequenced. Around 400 clones were sequenced, and three of them expressed adaptor protein AP-3μ (GenBank accession: BX814222; At1g56590). Yeast cells could grow on the selection medium when both AP-3μ and AGB1 were present, but not when either of them was absent, indicating that AP-3μ and AGB1 interact with each other in yeast cells (Fig. 1).

To confirm that AP-3μ binds directly to AGB1, I studied their interactions using a GST pull-down assay. His-AGB1 was detected only when it was reacted with AP-3μ, indicating that AGB1 and AP-3μ interact *in vitro* (Fig. 2). Although the C-terminal 18 amino acids of AP-3μ are needed for recruiting cargo into the forming vesicle (Owen and Evans, 1998), they are not needed for the interaction with AGB1 because His-AGB1 was also detected when it was reacted with AP-3μ^{DN}, which lacks the C-terminal 18 amino acids (Fig. 2B right).

In a bimolecular fluorescence complementation (BiFC) assay, YFP (yellow fluorescence protein) fluorescence was recovered in the cytosol and the nucleus when nYFP-AGB1 (AGB1 fused to the N-terminal half of YFP) and AP-3μ-cYFP (AP-3μ fused to the C-terminal half of YFP) were coexpressed (Fig. 3), suggesting that they

interact in the cytosol and nucleus in plant cells.

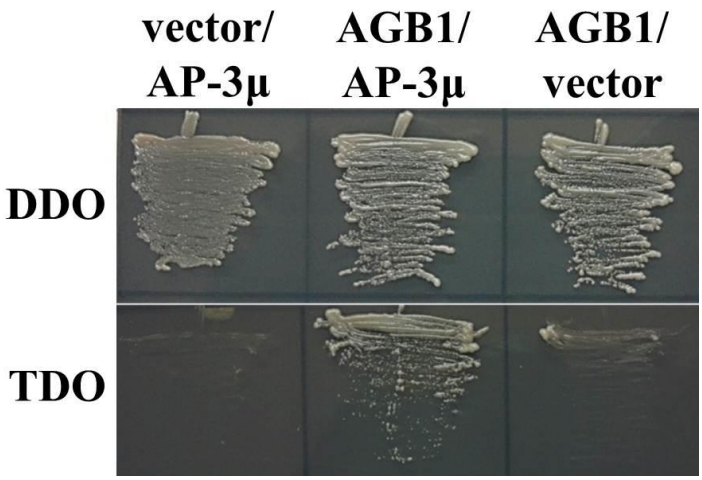

Figure 1. Interaction between AP-3μ and AGB1 in yeast. Yeast two-hybrid assay. The combinations of the plasmids used for transformation of the yeast strain AH109 are indicated at the top of the panel. vector: a pGBKT7 plasmid or a pGADT7-Rec plasmid containing no insert; AGB1: pGBKT7-AGB1; AP-3μ: pGADT7-Rec-AP-3μ (full-length ORF). Yeast cells were cultured on DDO (SD/-Trp/-Leu or control) and TDO (SD/-Trp/-Leu/-His) plates to check activation of the reporter gene, HIS3. At least 4 colonies were tested and a representative result is shown.

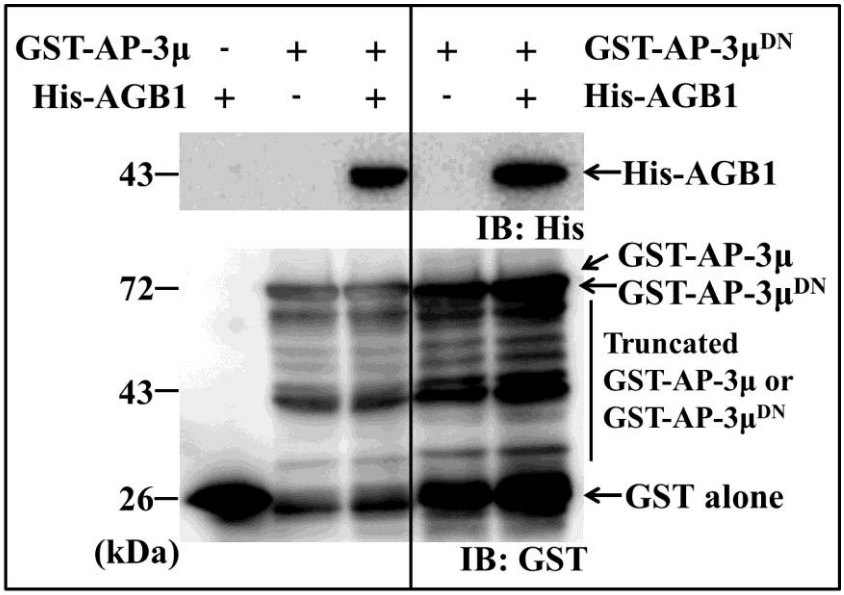

Figure 2. Interaction between AP-3μ and AGB1 *in vitro*. *In vitro* GST pull-down assay. GST-fused AP-3μ (GST-AP-3μ) or GST-fused AP-3μ^{DN} (GST-AP-3μ^{DN}), respectively and His-tagged AGB1 (His-AGB1) were expressed in *E. coli* and used for the analysis. The presence or absence of each protein in the reaction mixture is shown as + or -, respectively. Experiments were performed 4 times and a representative result is shown. Antibodies used for immunoblotting are shown as IB: His and IB: GST.

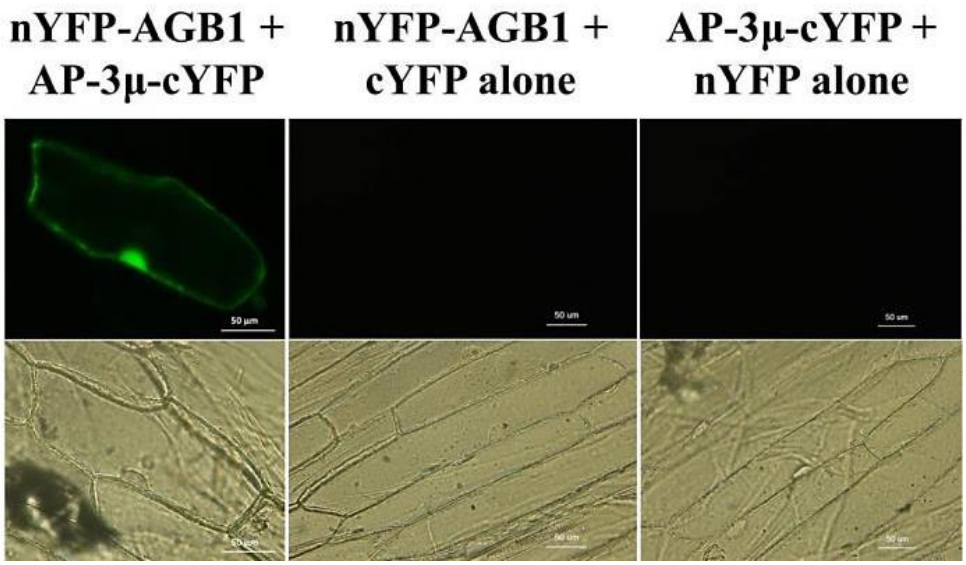

Figure 3. Interaction between AP-3µ and AGB1 *in planta*. BiFC in onion epidermal cells. The ORF of AGB1 was cloned in frame behind the coding sequence of the N-terminal region of YFP (nYFP) to express nYFP-fused AGB1 (nYFP-AGB1), and the ORF of AP-3µ was cloned in frame in front of the coding sequence of the C-terminal region of YFP (cYFP) to express cYFP-fused AP-3µ (AP-3µ-cYFP). Both constructs were introduced into onion epidermal cells. cYFP alone and nYFP alone were used as controls. More than 20 cells were observed and a representative cell is shown. Scale bar = 50 µm.

2.3.2 Subcellular localizations of AP-3μ and AGB1

When co-expressed in onion epidermal cells, GFP-fused AP-3μ (AP-3μ-GFP) was detected in the cytoplasm and nucleus, while mCherry-fused AGB1 (AGB1-mCherry) was detected in the cytoplasm, nucleus, and the plasma membrane (Fig. 4A), suggesting the possibility that AP-3μ and AGB1 are co-localized in the cytoplasm and nucleus. This result is consistent with the above-described cytoplasmic and nuclear BiFC between AP-3μ and AGB1 (Fig. 3). ABA treatment did not affect the patterns of signals of either AP-3μ-GFP or AGB1-mCherry (data not shown).

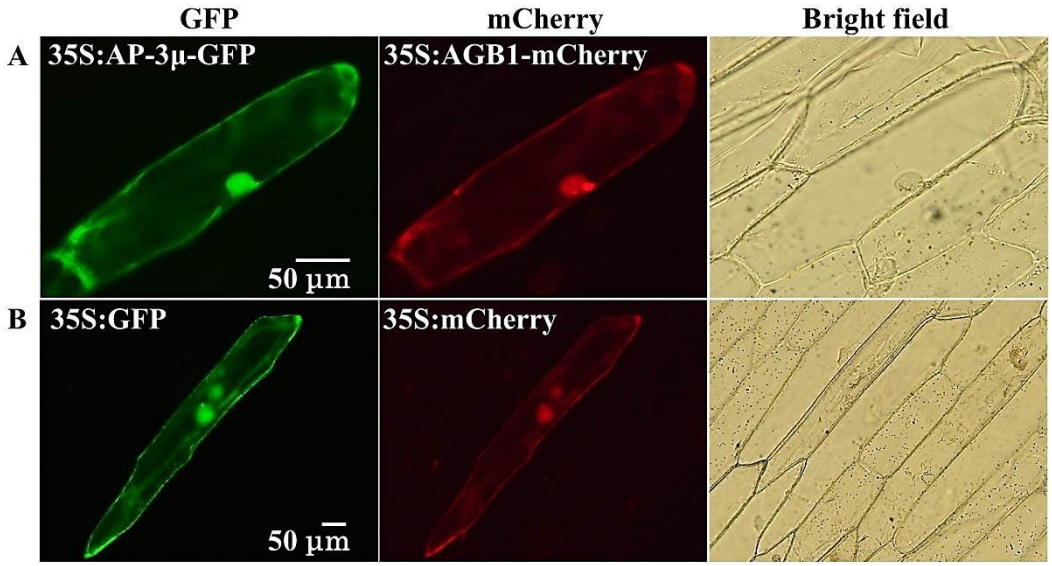

Figure 4. Subcellular localizations of AP-3µ and AGB1. GFP-fused AP-3µ (AP-3µ-GFP) and mCherry-fused AGB1 (AGB1-mCherry) (A) or GFP alone and mCherry alone (B) were transiently co-expressed in onion epidermal cells under the control of 35S promoter (35S:). More than 10 cells were observed, and a representative cell is shown in each panel. Scale bars = 50 µm.

2.3.3 *ap-3μ* mutants show ABA hyposensitive phenotypes in seed germination and post-germination growth

To examine the physiological role of AP-3μ in plants, I obtained two different mutant lines, *ap-3μ-2* (SALK_064486C) and *ap-3μ-4* (CS859652), which carry T-DNA insertions in intron 5 and exon 8 of the *AP-3μ* gene, respectively (Fig. 5A). Genomic PCR analyses verified that the T-DNA alleles were homozygous (Fig. 5B). RT-PCR using the primer combinations PF2+PR2, confirmed the absence of full-length transcripts (Fig. 5A and C).

In the presence of 0.5 to 2.0 μM ABA, *ap-3μ* seeds germinated earlier than did wild type seeds (Fig. 6A-D). The effect of ABA on the post-germination growth of seedlings was analyzed by determining the percentages of seedlings with fully expanded green cotyledons (greening rate) at 0.5-2.0 μM ABA. Greening rates of *ap-3μ* seedlings in the presence of 0.5 and 1.0 μM ABA were higher than those of wild type seedlings (Fig. 6E-G and Fig. 7). On the contrary, *agb1* mutants were hypersensitive to ABA during both germination and post-germination growth, as described previously (Pandey *et al*., 2006). In the presence of 2.0 μM ABA, the wild type and each mutant line were able to germinate, but none of them formed green cotyledons (Fig. 6D and 6H).

In the presence of ABA, which prevents the degradation of the seed storage proteins during germination (Garciarrubio *et al*., 1997), the basic subunit of 12S globulin, which is a seed storage protein, degraded faster in *ap-3μ* mutant seedlings than in wild type seedlings. In contrast, the basic subunit of 12S globulin was most preserved in *agb1* mutants (Fig. 8). These results suggest that the *ap-3μ* mutants are less sensitive to ABA than the wild type. However, no difference between wild type and *ap-3μ-4* mutant was observed in the inhibition of root growth by ABA (Fig. 9).

I investigated the expression profiles of *RAB18*, *RD29A*, and *AHG1*, which are ABA-induced marker genes. ABA-induced gene expression was reduced in *ap-3μ* mutants, as determined by the transcript levels of the marker genes (Fig. 10). It has been reported that the expressions of *RAB18* and *RD29A* are highly induced in *agb1* mutant compared to the wild type (Pandey *et al*., 2006). The expressions of the ABA-induced marker genes in *ap-3μ* mutant and *agb1* mutant are consistent with the ABA sensitivities of these mutants. No effect of ABA on expression of *AP-3μ* transcripts was observed. The expression of *AGB1* in the wild type did not change upon ABA treatment, as described previously (Pandey *et al*., 2006), while the expression of *AGB1* in *ap-3μ* mutant was up-regulated and higher than that in the wild type in the presence of ABA (Fig. 10, left panel).

ABA also has roles in the responses to environmental stresses, including desiccation and high salinity (Busk and Pages, 1998; Leung and Giraudat, 1998). However, when seeds and seedlings were exposed to various osmotic stresses (400 mM mannitol, 150 mM NaCl, or 9.2% polyethylene glycol), no difference was observed between the wild-type and *ap-3μ* with respect to seed germination, seedling growth, or seedling development (Fig. 11, 12, and 13). These data suggest that AP-3μ is not involved in the responses to either osmotic stress or salt stress.

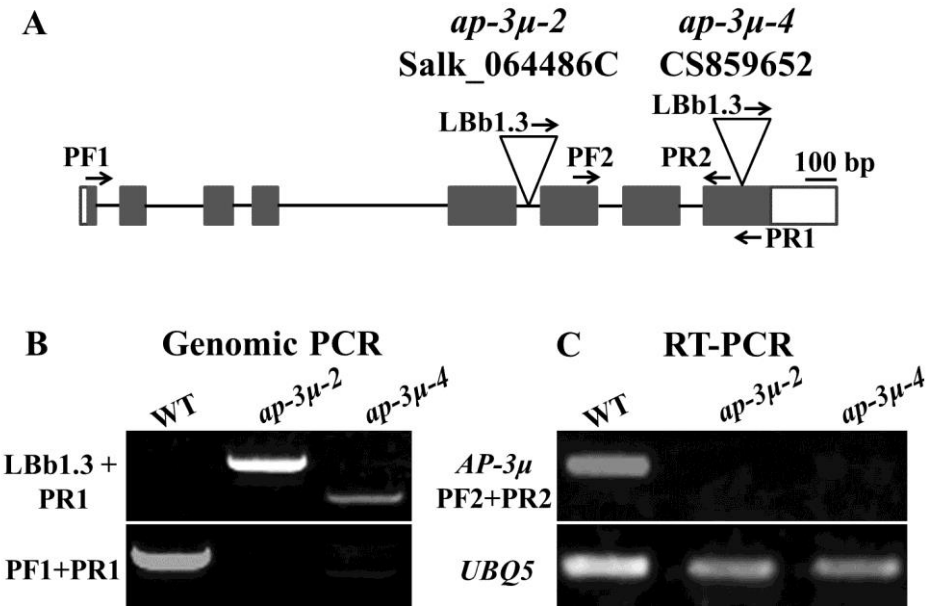

Figure 5. T-DNA insertional mutants of AP-3µ. (A) Schematic representation of the *AP-3μ* gene. Gray boxes and white boxes represent exons and UTR regions, respectively. The positions of the *ap-3μ-2* and *ap-3μ-4* T-DNA insertions are indicated. Primer pairs used in genomic PCR screening and primer pairs used in RT-PCR to assess *AP-3μ* transcripts are indicated. (B) Genomic PCR analyses verified homozygosity for the T-DNA alleles (C) RT-PCR analysis of *AP-3μ* transcript levels in *ap-3μ* mutants compared with wild type. *UBQ5* was used as an internal control.

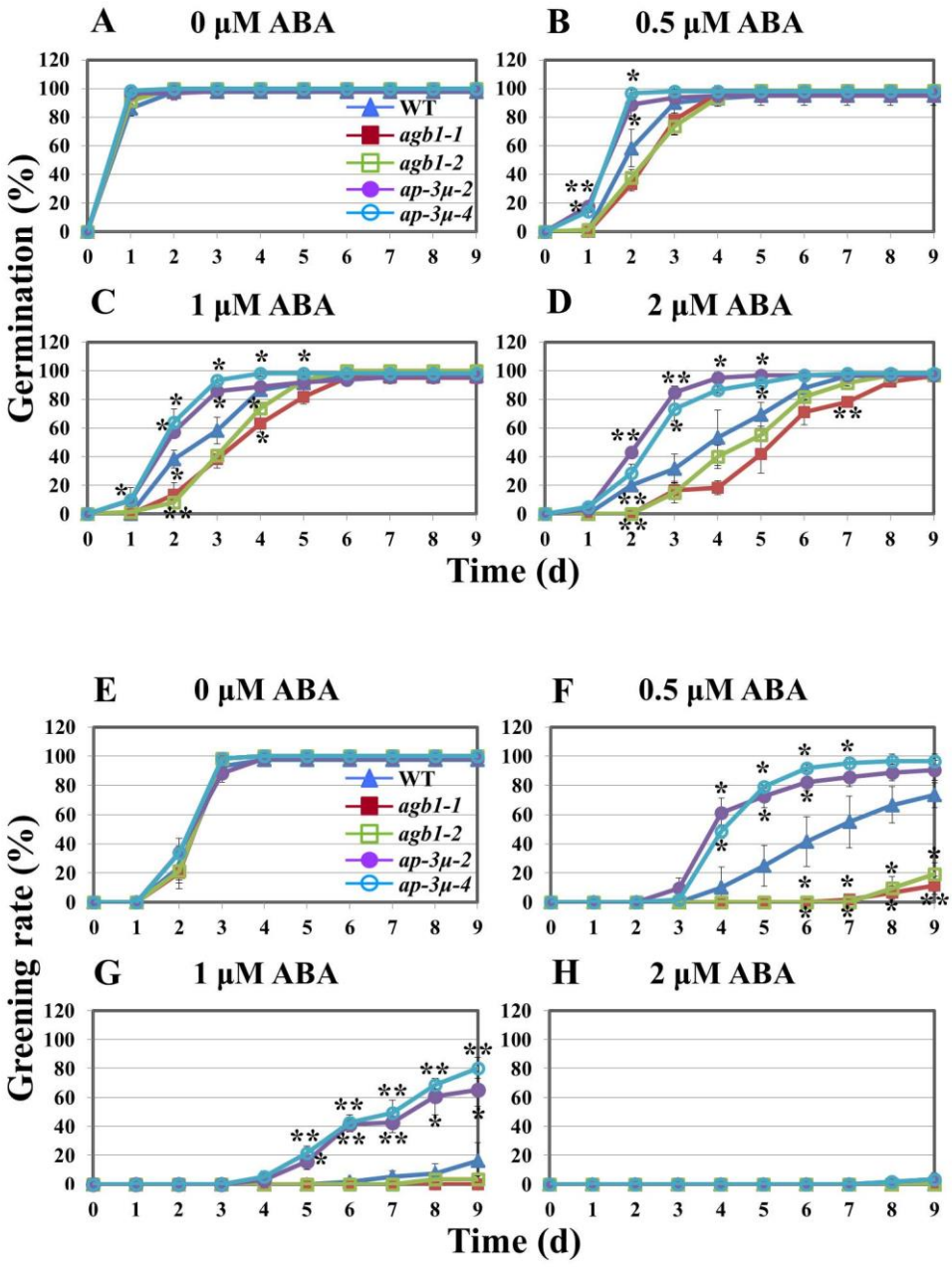

Figure 6. Seed germination and post-germination development of *ap-3µ* mutants are hyposensitive to ABA. (A) to (D) Germination rates of the wild type (WT) seeds and *agb1-1*, *agb1-2*, *ap-3µ-2*, and *ap-3µ-4* mutant seeds in the presence of 0 (A), 0.5 (B), 1 (C) or 2 µM ABA (D). Germinated seeds were counted at the indicated time points (days after stratification). (E) to (H) Percentages of seedlings with fully expanded green

cotyledons (greening rates) of WT and *agb1-1*, *agb1-2*, *ap-3μ-2*, and *ap-3μ-4* mutants in the presence of 0 (E), 0.5 (F), 1 (G) or 2 μM ABA (H). Seedlings with fully expanded green cotyledons were counted at the indicated time points (days after stratification). The experiment was repeated three times and data were averaged. n = 20/genotype for each experiment. The error bars represent SD. *, $p < 0.05$, **, $p < 0.005$ as determined by *t* test in comparison between wild type and each mutants.

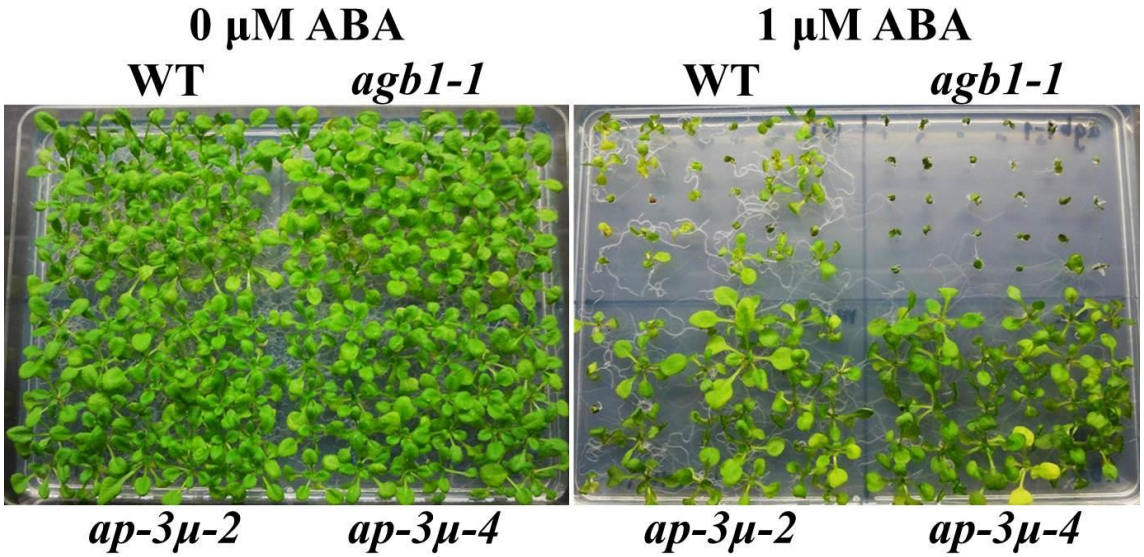

Figure 7. *ap-3μ* mutants are hyposensitive to ABA in post-germination growth. Plants were grown on the media containing 0 and 1 μM ABA. Photographs were taken 20 days after germination.

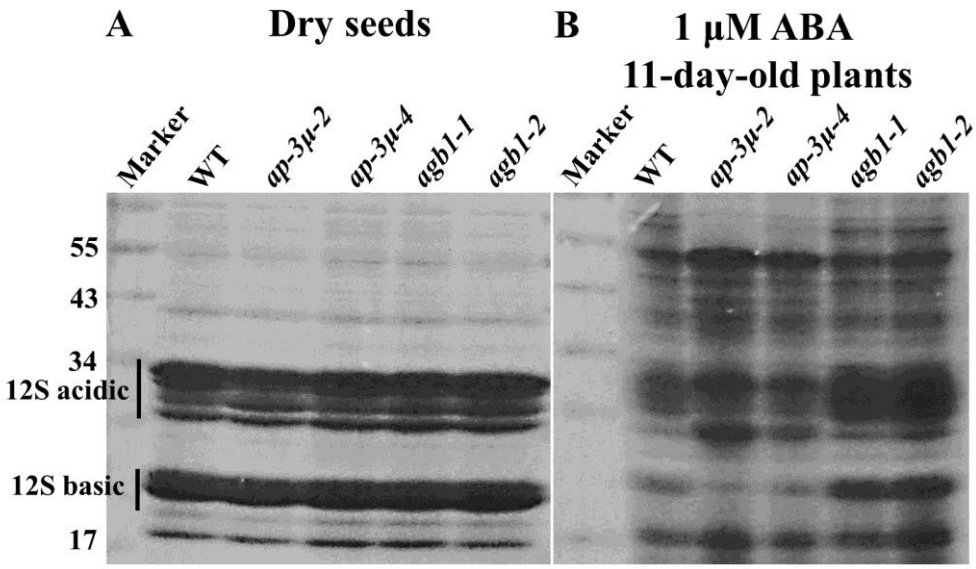

Figure 8. The degradation of seed storage proteins occurs faster in *ap-3μ* mutants than in the wild type in the presence of ABA. Total proteins were extracted from dry seeds (A) and 11-day-old plants grown in the presence of 1 μM ABA (B), and separated by SDS-PAGE. The Arabidopsis storage protein clusters are indicated (acidic and basic subunits of 12S globulin). Experiments were performed 3 times and a representative result is shown.

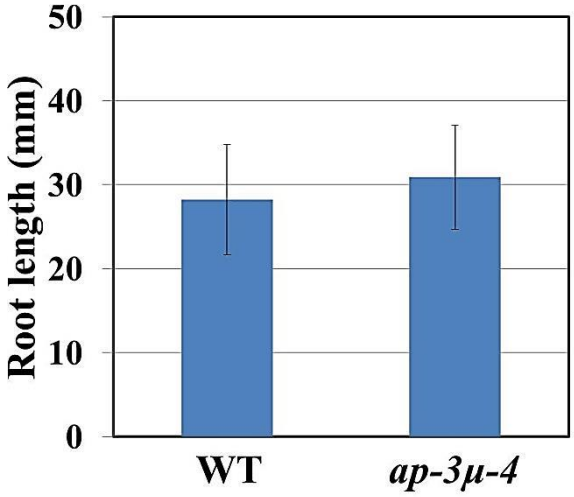

Figure 9. No difference between wild type and *ap-3μ-4* mutant was observed in the inhibition of root growth by ABA. Wild type and *ap-3μ-4* mutant seedlings were grown vertically on half-strength MS media without ABA for 3 days, and then transferred to half-strength MS media with 20 μM ABA and grown vertically for 10 days. The error bars represent SD. n = 24.

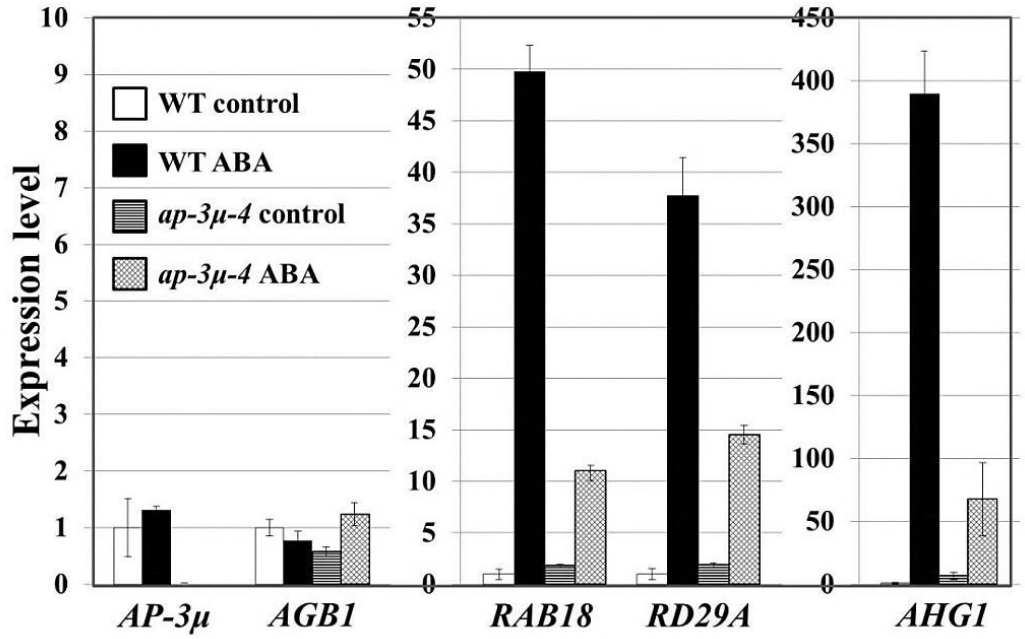

Figure 10. Expression of *AP-3μ*, *AGB1*, and ABA-responsive genes in wild-type and *ap-3μ-4* mutant by real-time quantitative RT-PCR. The sample of wild type in the absence of ABA (WT control) was used as a reference sample. Relative expression levels were calculated by the $\Delta\Delta C_T$ method using *Actin* as an internal control gene. Experiments were performed in triplicate. The error bars represent SD. Wild type and *ap-3μ-4* mutant were grown on half-strength MS media with 0 (control) or 1.0 μM ABA for 18 days and used for cDNA synthesis for RT-PCR.

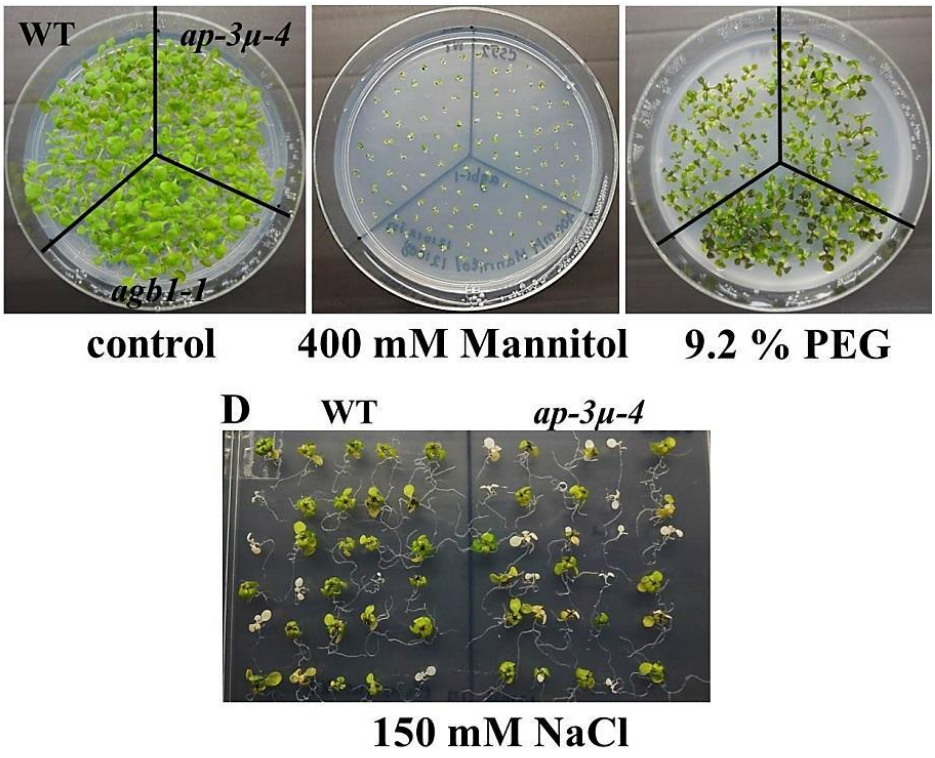

Figure 11. Responses of ap-3μ mutants to osmotic and salt stresses. Wild type and *ap-3μ-4* and *agb1-1* mutant seedlings were grown on half-strength MS media without treatment (A, control) or with 400 mM mannitol (B) or with 9.2% polyethylene glycol (PEG) (C). Photographs were taken on day 13 after transfer of seeds to light at 22˚C. (D) Wild type and *ap-3μ-4* mutant seedlings were grown on half-strength MS media without treatment for 6 days, transferred to half-strength MS media with 150 mM NaCl and further grown. Photographs were taken 11 days after plants were transferred to the NaCl media.

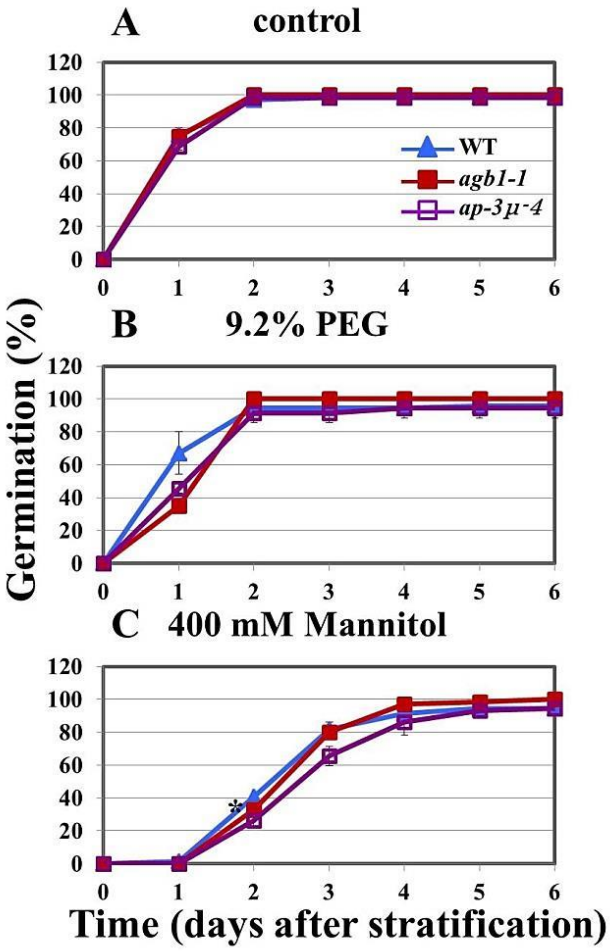

Figure 12. Germination rates of wild type seeds and *agb1-1* and *ap-3μ-4* mutant seeds in the presence of 400 mM mannitol or 9.2% polyethylene glycol. Germination rates of wild type seeds and *agb1-1* and *ap-3μ-4* mutant seeds in control media (A), in the presence of 400 mM mannitol (B) or 9.2% polyethylene glycol (C) over time (days after stratification). The experiment was repeated three times and data were averaged. n = 35/genotype for each experiment. The error bars represent SD. *, $p < 0.05$ as determined by *t* test in comparison between wild type and each mutant.

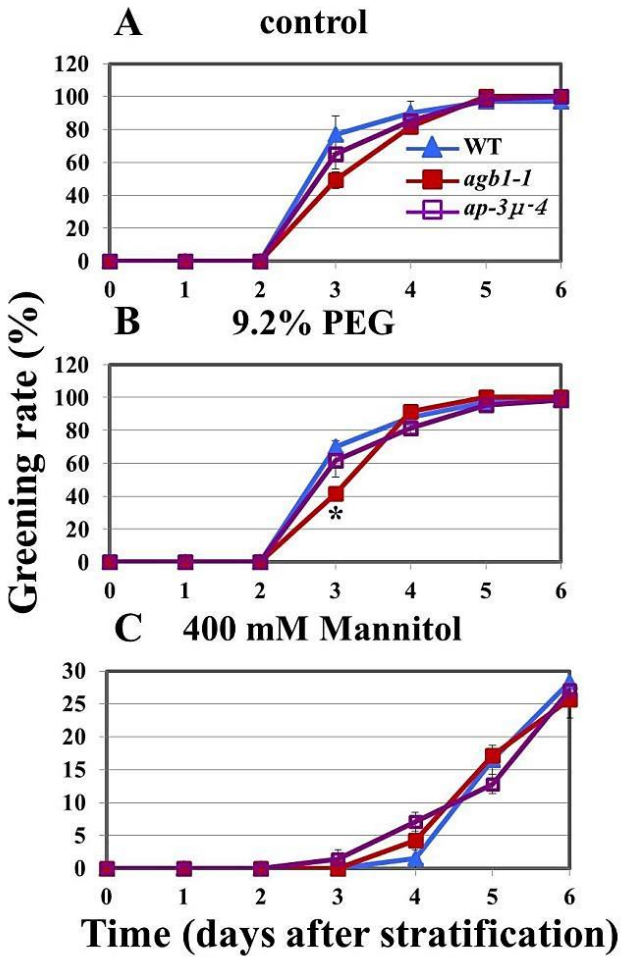

Figure 13. Greening rates of wild type and *agb1-1* and *ap-3μ-4* mutants in the presence of 400 mM mannitol or 9.2% polyethylene glycol. Greening rates of wild type and *agb1-1* and *ap-3μ-4* mutants in control media (A), in the presence of 400 mM mannitol (B) or 9.2% polyethylene glycol (C) over time (days after stratification). The experiment was repeated three times and data were averaged. n = 35/genotype for each experiment. The error bars represent SD. *, $p < 0.05$ as determined by *t* test in comparison between wild type and each mutant.

2.3.4 Phenotypes of *agb1/ap-3μ* double mutants

To investigate the interaction between *AP-3μ* and *AGB1* at the genetic level, I generated *agb1/ap-3μ* double mutants (DMs). A total of four DMs were obtained; DM#1-5-1, DM#1-5-2, DM#1-5-3, and DM#2-8-5-5 (Fig.14). Because DM#1-5-1, DM#1-5-2, and DM#1-5-3 are descended from the same line, DM#1-5-3 and DM#2-8-5-5 were selected for further analysis.

In the presence of 0.25 μM ABA, the germination rates of all the DMs were similar to the germination rate of *agb1-1* mutant (Fig. 15B). In the presence of 0.5 μM ABA, the germination rates of all the DMs were higher than the germination rate of the *agb1-1* mutant (Fig. 15C), suggesting that AP-3μ positively regulates the ABA response independently of AGB1 in seed germination. In the presence of 0.25 μM ABA, the greening rate of DM#1-5-3 was significantly higher than the greening rate of *agb1-1* mutant only at day 6, while no significant difference was observed between DM#2-8-5-5 and *agb1-1* mutant in their greening rates at any time points (Fig. 15E and see Fig. 16E for t test in comparison between *agb1-1* mutant and each genotypes). In the presence of 0.5 μM ABA, cotyledon greening was strongly inhibited in both the DMs and *agb1-1* mutant (Fig. 15F; see Fig. 17 for growth phenotypes in the presence of ABA). And the greening rate of DM#1-5-3 was significantly but only slightly higher than the greening rate of *agb1-1* mutant at day 9, while no significant difference was observed between DM#2-8-5-5 and *agb1-1* mutant in their greening rates at any time points (Fig. 16F). These results suggest that the AP-3μ-dependent alleviation of the effects of ABA is at least partially dependent on AGB1 at the post germination stage.

Although *agb1* mutants have an increased number of lateral roots (Ullah *et al.*, 2003), the numbers of lateral roots were not significantly different between the wild

type and *ap-3μ-4* mutant in the presence of 0 and 2 μM ABA. Similarly, the numbers of lateral roots were not different between *agb1-1* mutant and *agb1/ap-3μ* DMs (Fig. 18), suggesting that AP-3μ is not involved in regulating lateral root formation. Although lateral root formation can be controlled by auxin (Fukaki *et al*., 2007) and AGB1 is known to be involved in the auxin-dependent control of lateral root formation (Ullah *et al*., 2003), the *ap-3μ* mutants and the wild type did not differ in their responses to an auxin, IAA (indole acetic acid) and an auxin-transport inhibitor, NPA (N-(1- Naphthyl) phthalamic acid) (data not shown). These results suggest that AP-3μ is not involved in the control of lateral root growth by auxin.

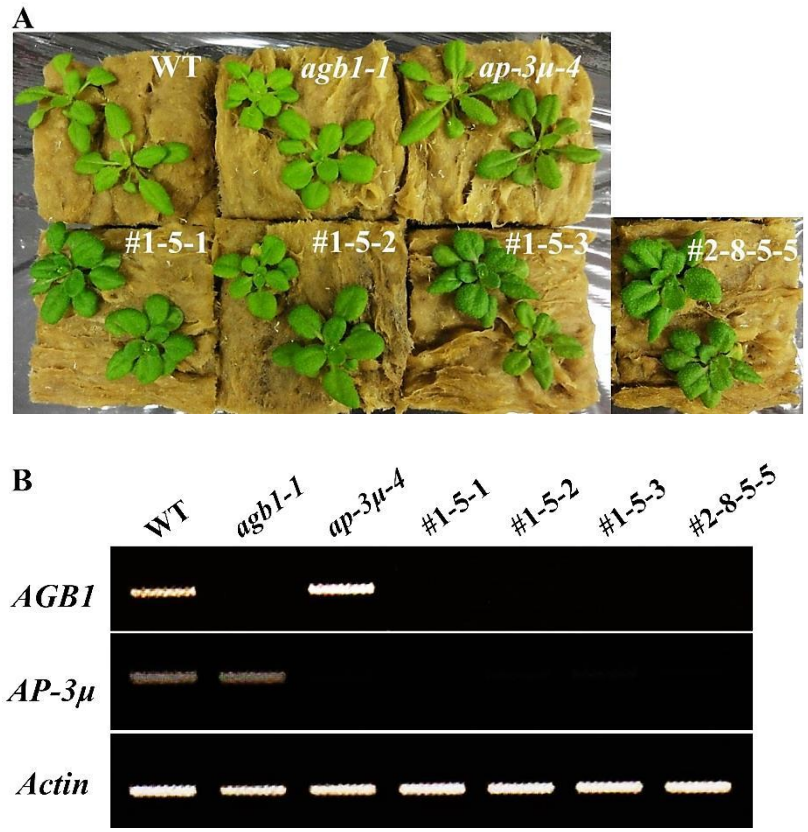

Figure 14. Generation of *agb1/ap-3μ* double mutants. (A) Total of four double mutant lines (DM) were generated; DM#1-5-1, DM#1-5-2, DM#1-5-3, and DM#2-8-5-5. Wild type, *agb1-1*, *ap-3μ-4*, and *agb1/ap-3μ* double mutants were grown on half-strength MS media plates containing 1% Suc for 10 days and transferred onto rockwool cubes and grown further with 0.2× MS solution regularly supplied. The photographs of three-week-old plants were taken. (B) RT-PCR using the primers specific to *AGB1* or *AP-3μ* gene confirmed the absence of transcripts of *AGB1* or *AP-3μ*. *Actin* was used as a reference transcript.

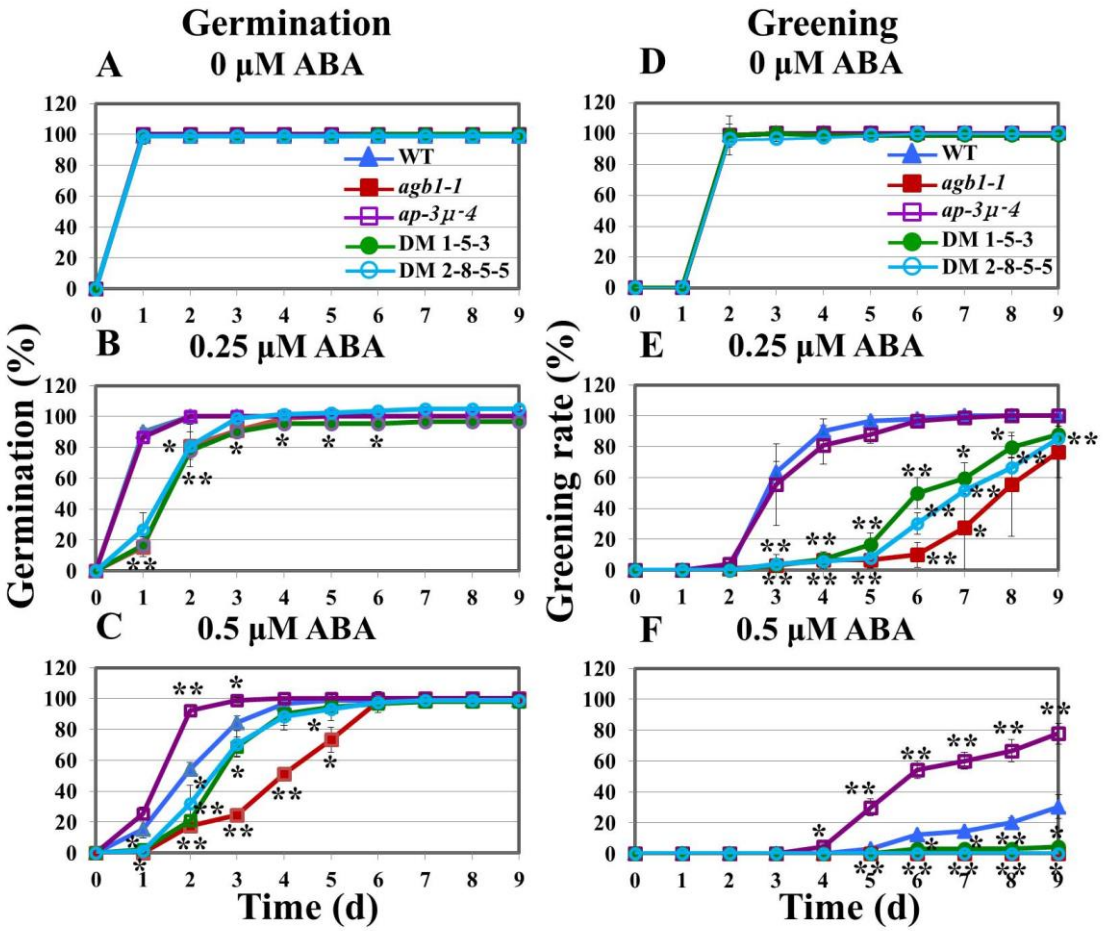

Figure 15. ABA sensitivity of *agb1/ap-3μ* double mutants during germination and post-germination growth. Germination rates (A to C) and greening rates (D to F) of wild type, *agb1-1*, *ap-3μ-4*, and *agb1/ap-3μ* double mutants in the presence of 0 (A and D), 0.25 (B and E) or 0.5 μM ABA (C and F) at the time indicated (days after stratification). The experiment was repeated three times and data were averaged. n = 30/genotype for each experiment. The error bars represent SD. *, $p < 0.05$, **, $p < 0.005$ as determined by *t* test in comparison between wild type and each mutants.

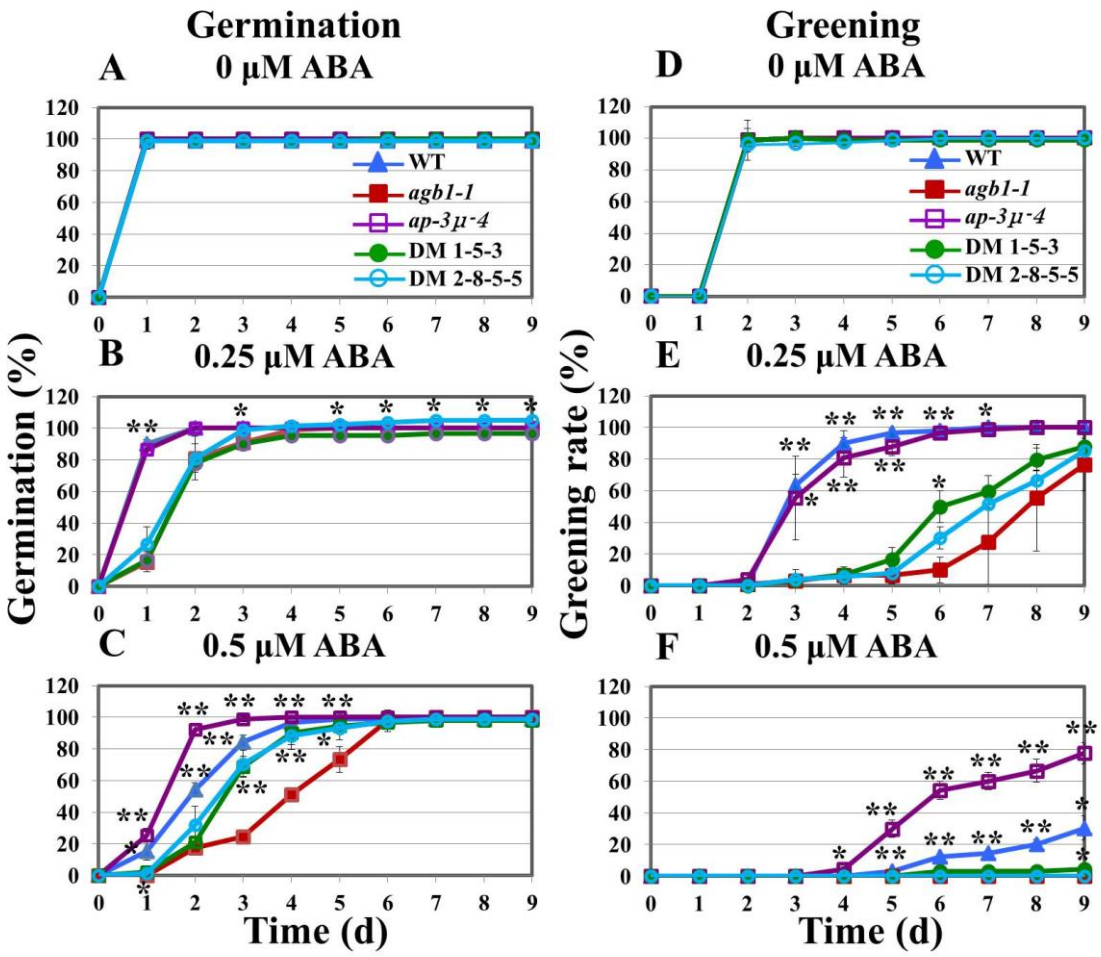

Figure 16. T test for germination rates and greening rates in comparison between *agb1-1* mutant and each *agb1/ap-3μ* double mutants. Germination rates (A to C) and greening rates (D to F) of wild type, *agb1-1*, *ap-3μ-4*, and *agb1/ap-3μ* double mutants in the presence of 0 (A and D), 0.25 (B and E) or 0.5 μM ABA (C and F) at the time indicated (days after stratification). The experiment was repeated three times and data were averaged. n = 30/genotype for each experiment. The error bars represent SD. *, $p < 0.05$, **, $p < 0.005$ as determined by *t* test in comparison between *agb1-1* mutant and each genotypes.

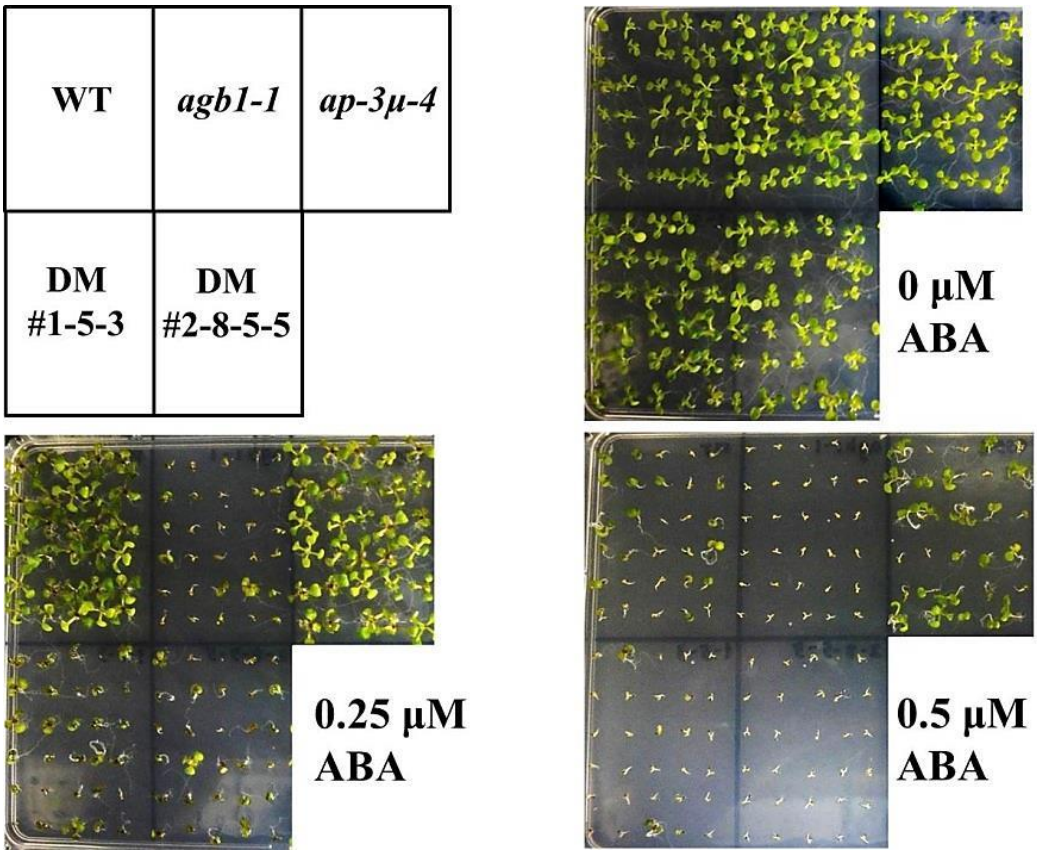

Figure 17. *agb1/ap-3μ* double mutants display ABA-hypersensitive phenotype in post-germination growth similar to that of *agb1* mutants. Plants were grown in the presence of 0, 0.25 or 0.5 μM ABA. Photographs were taken on day 9.

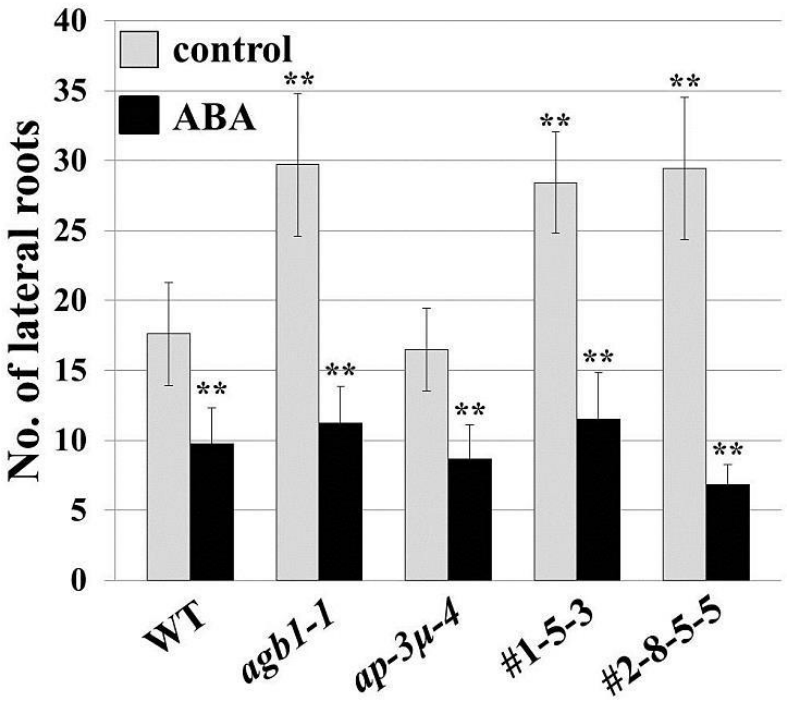

Figure 18. Numbers of lateral roots of wild type, *agb1-1*, *ap-3μ-4*, and *agb1/ap-3μ* double mutants in the absence or in the presence of ABA. Seeds germinated on 0.5× MS plates were transferred after 3 d to control plates (no ABA) or plates containing 2 μM ABA and seedlings were allowed to grow vertically for 12 d under 16-h light/8-h dark condition. Number of lateral roots was counted. Figure shows number of lateral roots in different genotypes in presence or absence of ABA. The error bars represent SD. n = 9-12. *, $p < 0.05$, **, $p < 0.005$ as determined by *t* test in comparison with wild type control.

2.3.5 Mutants of AP-3δ subunit and clathrin heavy chain (CHC) show ABA-hyposensitive phenotypes in post-germination growth

The *ap-3δ* and *chc1* mutants harbor T-DNA insertions in exon 1 of the *AP-3δ* gene and exon 24 of the *CHC1* gene, respectively (Fig. 19A and 19B). Genomic PCR analyses confirmed that the T-DNA plants were homozygous (Fig. 19A and 19B). RT-PCR using primers specific for *AP-3δ* confirmed the absence of transcripts in *ap-3δ* (Fig. 19A) and RT-PCR using primers specific for *CHC1* confirmed the absence of transcripts in *chc1* (Fig. 19B).

In the presence of 1.0 μM ABA, the rates of seed germination in *ap-3δ* and *chc1* were significantly but only slightly different from that in the wild type (Fig. 20B). However, in the greening test, only 23% of wild type seedlings developed green cotyledons on day 10 at 1.0 μM ABA, whereas about 43% of the *ap-3δ* mutant seedlings and 50% of the *chc1* mutant seedlings developed green cotyledons (Fig. 20D). These results suggest that AP-3δ and CHC, as well as AP-3μ, function in the ABA response during post-germination growth.

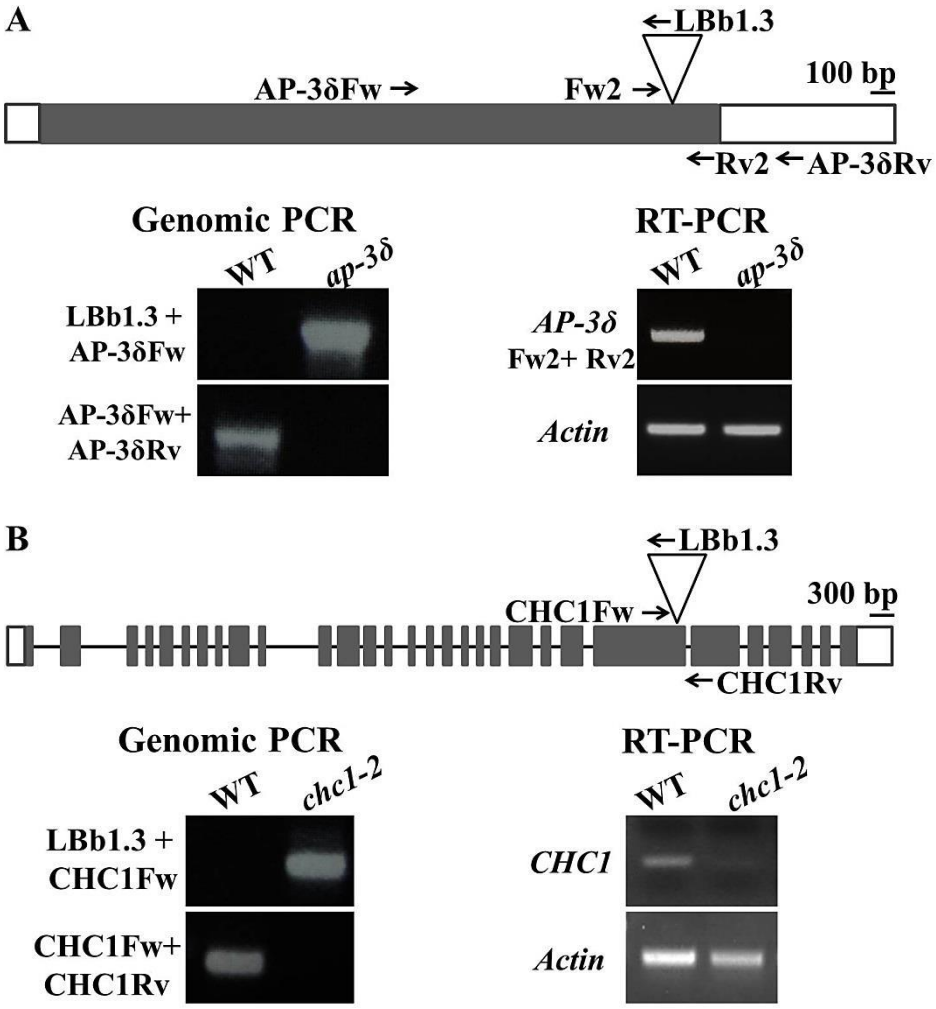

Figure 19. T-DNA insertional mutants of AP-3δ and CHC1. Schematic representations of the *AP-3δ* (A) and *CHC1* gene (B). Gray boxes and white boxes represent exons and UTR regions, respectively. The positions of the T-DNA insertions are indicated. Primer pairs used in genomic PCR are indicated. Genomic PCR analyses verified homozygosity of each mutants (left panels). Gene-specific primers used in RT-PCR to confirm absence of full-length transcripts in mutants (right panels). *Actin* was used as a reference transcript.

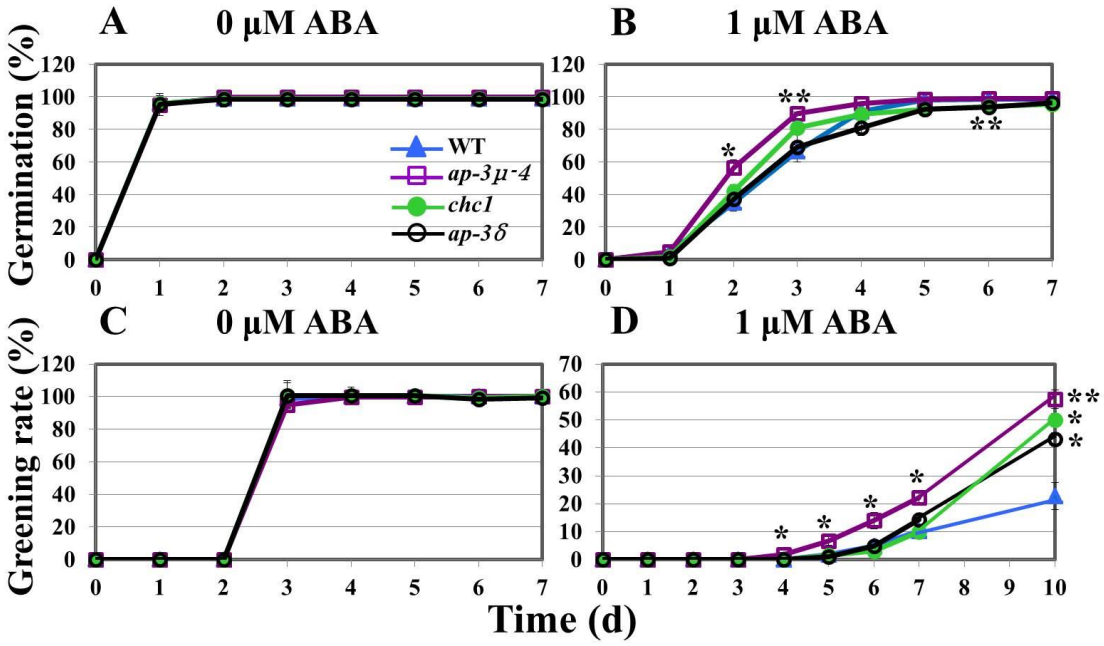

Figure 20. Mutants of AP-3δ subunit and Clathrin heavy chain show ABA-hyposensitive phenotype in post-germination growth. Germination rates (A and B) and greening rates (C and D) of wild type and *ap-3µ-4*, *ap-3δ* and *chc1* mutants in the absence of ABA (A and C) or in the presence of 1.0 µM ABA (B and D) over time (days after stratification). The experiment was repeated three times for wild type and *ap-3µ-4* and *ap-3δ* mutants, and twice for *chc1* mutant. Data were averaged, n = 70/genotype for each experiment. The error bars represent SD. *, $p < 0.05$, **, $p < 0.005$ as determined by *t* test in comparison between wild type and each mutants.

2.4 Discussion

2.4.1 AP-3μ interacts with AGB1 and negatively regulates AGB1

I have shown that AP-3μ both physically and genetically interacts with AGB1, and regulates the ABA-dependent seed germination and cotyledon greening. Because AGB1 is a negative regulator of ABA responses (Pandey *et al*., 2006), and because AP-3μ-dependent positive regulation of ABA responses during post-germination growth requires AGB1 (Fig. 15 and 16), AP-3μ is thought to be an upstream negative regulator of AGB1 in the suppression of the inhibition of post-germination growth by ABA (Fig. 21). Although no information about the physical interaction between AGB1 and AP-3μ was available in *Arabidopsis* G-Signaling Interactome Database (AGIdb, http://bioinfolab.unl.edu/AGIdb), my results strongly support the idea that AP-3μ participates in the AGB1-mediated signaling.

Although ABA is known to be involved in acquiring tolerances to osmotic stress and salt stress, no difference was observed between the wild type and *ap-3μ* in osmotic stress or salt stress treatments (Fig. 11, 12, and 13). These data suggest that AP-3μ is not involved in the responses to either osmotic stress or salt stress. Osmotic stresses can retard plant growth independently of ABA, because osmotic stresses inhibit cellular water uptake. In the case of salt stress, ion toxicity can also inhibit plant growth. It is possible that those ABA-independent plant growth inhibitions were much more significant than the ABA-mediated plant growth inhibition in my experiments in which the plants were subjected to osmotic/salt stresses.

In mammals, GPCRs are internalized to desensitize in response to excessive and/or continuous stimuli (Lefkowitz, 2004). An animal GPCR, β2 adrenergic receptor, has been suggested to be internalized via clathrin-mediated endocytosis when it binds

its ligand (Ferguson *et al*., 1996; Schmid *et al*., 2006; McMahon and Boucrot, 2011 for review). The classical function of clathrin-mediated endocytosis in the regulation of signal transduction is to terminate the signal by physically removing activated receptors from the cell surface (Sorkin and von Zastrow, 2009; Scita and Di Fiore, 2010). The internalization of ligand-receptor complexes into endosomes and then lysosomes may lead to their degradation, which results in termination of signaling. In plants, the internalization of AtRGS1 (regulator of G-protein signaling 1), which is the prototype of a seven-transmembrane receptor fused with an RGS domain, was reported (Urano *et al*., 2012). AtRGS1 is known to be internalized when cells are treated with sugars such as D-glucose. Endocytosis of AtRGS1 physically uncouples the GTPase-accelerating activity of AtRGS1 from GPA1, permitting sustained activation of G protein signaling on the plasma membrane (Urano *et al*., 2013 for review). It is unclear whether the internalization of AtRGS1 is dependent on clathrin. Because AP-3μ is a component of a clathrin complex and interacts with AGB1, it will be interesting to examine whether AP-3μ is involved in the internalization of AtRGS1. Alternatively, it is possible that AGB1 is a direct target of the clathrin-mediated endocytosis. However, in either the presence or the absence of ABA, no difference was observed in the patterns of GFP-fused AGB1 (GFP-AGB1) signals between the wild type and *ap-3μ-4* mutant (Fig. 22). It is possible that AP-3μ is involved in AGB1 internalization, but at least it could not be detected in this transient expression experiment. The level of AGB1, which negatively regulates ABA responses, might be higher in the absence of AP-3μ than in its presence, and this may be why the *ap-3μ* mutants showed hyposensitivities to ABA (Fig. 6 and 10). To my knowledge, this study is the first article reporting possibility of internalization of β subunit of G protein in plants. However, further studies are required

to elucidate whether AP-3μ is involved in endocytosis of AGB1 and other components of G-protein signaling.

The finding that the numbers of lateral roots were not significantly different between the wild-type and *ap-3μ-4* mutant in either the absence or the presence of ABA (Fig. 18), IAA or NPA (data not shown) suggests that AP-3μ does not function in regulating lateral root formation or in the control of lateral root growth by auxin. Therefore, the interaction between AP-3μ and AGB1 seems not to be involved in the control of lateral root formation and growth. In addition to the involvement in ABA-dependent inhibition of post-germination growth, the interaction between AP-3μ and AGB1 may be required in other processes. AGB1 mediates developmental processes and hormone responses. In addition to showing altered sensitivities to ABA and auxin, *agb1* mutants show altered sensitivities to gibberellin (GA) (Chen *et al*., 2004), brassinosteroid (BR) (Chen *et al*., 2004; Tsugama *et al*., 2013) and jasmonic acid (JA) (Trusov *et al*., 2006).

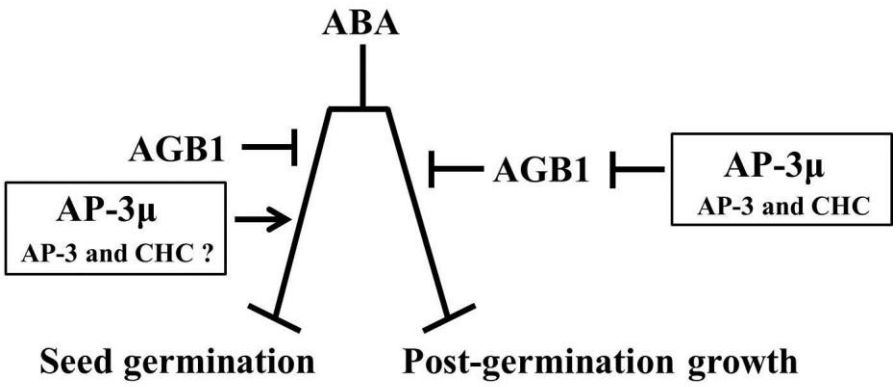

Figure 21. Schemes of AP-3µ modes of action. Contrary to AGB1, AP-3µ positively regulates the inhibition of seed germination and post-germination growth by ABA. AGB1 and AP-3µ function independently in ABA regulation of seed germination, but AP-3µ is a negative regulator of AGB1 in ABA regulation of post-germination growth. AP-3µ seems to function in these processes with other subunits of AP-3 complex mediating clathrin-based trafficking. AP-3: AP-3 complex, CHC: clathrin heavy chain.

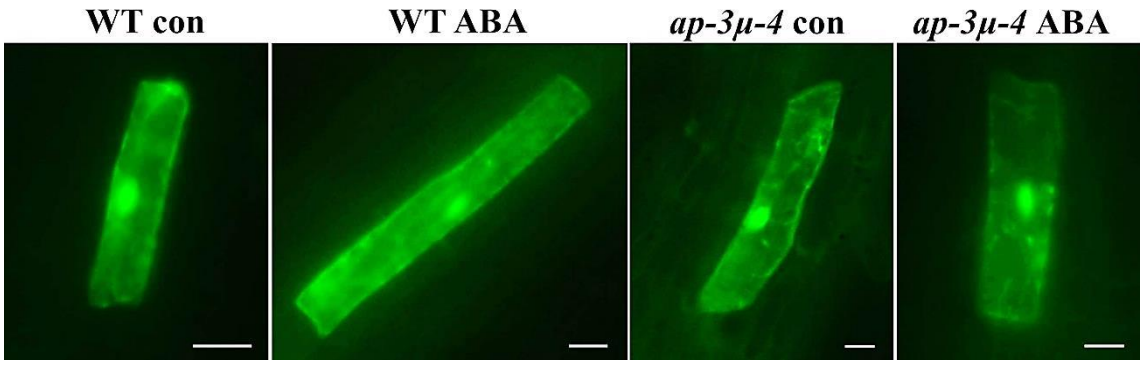

Figure 22. Subcellular localization of AGB1 in wild type and *ap-3μ* mutant. Wild type and *ap-3μ* mutant were grown on 0.5× MS plates for 10 d and transferred to control plates (no ABA, con) or plates containing 1 μM ABA for 24 h and seedlings were used for transient expression of pBS-35S-GFP-AGB1 (Tsugama *et al*., 2012a). More than 10 cells were observed and a representative cell is shown. Scale bars = 20 μm.

2.4.2 AP-3 complex and clathrin are involved in ABA regulation of post-germination development

AP-3 exists in Arabidopsis as a complex (Zwiewka *et al.*, 2011). The CHC is also associated with AP-3β (Zwiewka *et al*., 2011). AP-3β-GFP was found to localize predominantly in the cytoplasm (Feraru *et al*., 2010). AP-3μ is present in the cytoplasm and nucleus (Fig. 4A). Each component of the AP-3 complex plays similar roles in regulating biogenesis and the functions of vacuoles in plants (Feraru *et al*., 2010; Zwiewka *et al*., 2011). Furthermore, *ap-3μ*, *ap-3δ* and *ap-3β* all suppress the shoot gravitropism abnormality of the *zig1/vti11* mutant, which is defective in protein trafficking to the vacuoles (Sanmartín *et al*., 2007; Niihama *et al*., 2009). Similar phenotypes of the mutants defective in the different subunits of the same AP-3 complex suggest that these proteins act in the same process, possibly in the same complex. Also, the post-germination growth of the *ap-3μ*, *ap-3δ* and *chc1* mutants were hyposensitive to ABA (Fig. 20D), supporting the idea that each subunit of AP-3 complex acts in the same process, probably mediating clathrin-based trafficking. However, the hyposensitivity to ABA during post-germination growth was greater in the *ap-3μ* mutants than in the *ap-3δ* and *chc1* mutants (Fig. 20D) and the rates of seed germination at 1 μM ABA in *ap-3δ* and *chc1* were significantly but only slightly different from that in the wild-type (Fig. 20B). One possible explanation for these observations is that the homolog genes are redundant. The Arabidopsis genome encodes two *CHCs* that have 97% amino acid sequence identity (Kitakura *et al*., 2011). The homologs of AP-3δ in other AP complexes may compensate for the loss of AP-3δ. Another possibility is that although each subunit of the AP-3 complex acts in the same process in the ABA response during post-germination growth, AP-3μ is the predominant regulator in the

process. To my knowledge, this study is the first report on the involvement of AP-3 complex and clathrin in the regulation of post-germination growth by ABA (Fig. 21). Further studies are needed to understand how the AP-3 complex and clathrin are involved in the ABA regulation of post-germination growth.

Chapter 3

Studies on Nonphototropic hypocotyl 3 (NPH3)

3.1 Arabidopsis G protein β subunit AGB1 interacts with Nonphototropic hypocotyl 3 (NPH3) and is involved in phototropism.

3.1.1 Introduction

Previous studies of my group have identified interacting partners of AGB1with a yeast two-hybrid screen (Kobayashi *et al*., 2012; Tsugama *et al*., 2012a; Kansup *et al*., 2013; Tsugama *et al*., 2013a). One of these proteins, phototropin-interacting protein nonphototropic hypocotyl 3 (NPH3, At5g64330) is required for the phototropic response, leaf positioning and leaf flattening (Motchoulski and Liscum, 1999; Inoue *et al*., 2008; Wan *et al*., 2012). NPH3 is a member of a plant-specific family of proteins (Motchoulski and Liscum, 1999), designated the NRL (for NPH3/RPT2-Like) family (Holland *et al*., 2009). Three characteristics define members of the NRL family of proteins: 1) an N-terminal BTB (*broad complex*, *tramtrack*, and *bric a `brac*) domain, 2) a centrally located NPH3 domain, designated domain I-IV, and 3) a C-terminal coiled coil domain (Pedmale *et al*., 2010). *NPH3* has two transcript variants, *NPH3.1* and *NPH3.2*. NPH3.1 consists of N-terminal BTB domain, central NPH3 domain and C-terminal coiled-coil domain. NPH3.2 corresponds to the C-terminal region-truncated version of NPH3.1. The coiled-coil domain of NPH3.1 interacts with phot1 (Motchoulski and Liscum, 1999), and the BTB domain interacts with CULLIN3 (CUL3), a scaffold protein for ubiquitin ligase complex (Roberts *et al*., 2011). Both of these interactions are involved in regulating the NPH3-mediated blue light responses (Motchoulski and Liscum, 1999; Roberts *et al*., 2011).

In animals, G proteins are involved in phototransduction in rod photoreceptor cells (Arshavsky *et al*., 2002). Arabidopsis G proteins have been suggested to play roles in light responses. For example, blue light-induced phenylalanine production in etiolated seedlings is impaired in an Arabidopsis Gα (GPA1)-null mutant *gpa1-3* (Wei *et al*., 2008). Another GPA1-null mutant, *gpa1-4*, and an AGB1-null mutant, *agb1-2*,

are both less sensitive to blue light and far-red light in seed germination (Botto *et al*., 2009). *gpa1-4* is less sensitive to the cell death mediated by a red light receptor, phyA, while *agb1-2* is more sensitive to the phyA-mediated cell death (Warpeha *et al*., 2006). However, it is unclear whether G proteins are involved in the phototropic responses mediated by phot1 and NPH3.

Here I show that AGB1 physically interacts with NPH3 and is involved in the NPH3-dependent phototropic responses.

3.1.2 Materials and methods

3.1.2.1 Plant material, growth conditions and analysis of phototropism

Arabidopsis thaliana ecotype Columbia-0 (Col-0) was used throughout the experiments. Seeds of *nph3-7* (SALK_110039), *nph3-8* (CS322676), *agb1-1* (CS3976) (Lease *et al*., 2001) and *agb1-2* (CS6536) (Ullah *et al*., 2003) were obtained from the Arabidopsis Biological Research Center (ABRC). For SALK_110039 and CS322676, T-DNA insertion was confirmed by genomic PCR analysis (Figure 29B). Primers used for the genomic PCR analysis are shown in Table 3.

Seeds were surface sterilized and sown on 0.8% agar medium containing 0.5× Murashige and Skoog (MS) salts (Wako, Japan), 1% (w/v) sucrose and 0.5 g/L MES, pH 5.8, chilled at 4°C in the dark for 3 d (stratified), and germinated at 22°C. Plants were grown at 22°C under 16-h-light/8-h-dark photoperiod for RT-PCR and genomic PCR analyses. To measure phototropic curvature, plants were grown for three days in the dark and were irradiated with unilateral blue light for 20 h (Knauer *et al*., 2011).

3.1.2.2 Yeast two-hybrid (Y2H) analysis

A cDNA clone of *NPH3.2* (*AT5G64330.2*) (clone name: RAFL14-45-N16) was obtained from RIKEN BRC Experimental Plant Division (Seki *et al*., 2002). This clone had a base substitution (at the position 1556 from the start codon) and an 80-bp region corresponding to the 4th intron of the putative full-length cDNA of *NPH3.1*. To obtain the full-length ORF of *NPH3.1*, the 5’ region of *NPH3.1* ORF was amplified by PCR using the RIKEN cDNA clone as template and the following primer pair: 5’-CCGGTCTAGAATGATGTGGGAATCTGAGAGCGACGGTGGGG-3’ and 5’-CAAAACCTGAAACTTTGTCAACGGCAAATTCCGATCTCTAGCAACTTCGG

TGAGATAACT-3'. The 3' region of *NPH3.1* ORF was amplified by PCR using a yeast clone that was obtained in the yeast two-hybrid screen and harbored the 3' region of *NPH3.1* as template and the following primer pair: 5'-GCGAGGCTTGTGGATAGTTATCTCACCGAAGTTGCTAGAGATCGGAATTTG CCGTTGACA-3' and 5'-GGCCTCTAGATGAAATTGAGTTCCTCCATCGTCTTGGTTTCCTGGGGGGT-3 '. The two kinds of PCR products (corresponding to the 5' and 3' regions of *NPH3.1* ORF) were mixed and used as template for PCR using the following primer pair: 5'-CCGGTCTAGAATGATGTGGGAATCTGAGAGCGACGGTGGGG-3' and 5'-GGCCTCTAGATGAAATTGAGTTCCTCCATCGTCTTGGTTTCCTGGGGGGT-3' (*Xba*I sites are underlined). The resultant PCR products, which contain the full-length ORF of *NPH3.1*, were cloned into the *Xba*I site of pBluescript II SK$^-$, generating pBluescript II SK$^-$ NPH3.1.

pBluescript II SK$^-$ NPH3.1, which contains full-length *NPH3.1*, was digested by *EcoR*V and *Sac*I, and the resultant fragment containing the 3' region (the position 1546-2241 from the start codon) of the open reading frame (ORF) of *NPH3.1* was inserted into the *Sma*I-*Sac*I site of pGADT7-Rec (Clontech, Japan), generating pGAD-NPH3.1C. pBluescript II SK$^-$ NPH3.1 was digested by *EcoR*I and *Xba*I, and the resultant fragment containing the full-length ORF of *NPH3.1* was inserted into the *EcoR*I-*Xba*I site of pGADT7-Rec, generating pGAD-NPH3.1. pGBK-AGB1 (Tsugama *et al*., 2012a) and each pGAD construct were co-introduced into the *Saccharomyces cerevisiae* strain AH109. Reporter gene activation in the transformed yeast cells was examined by growing them on the SD (synthetic dextrose) medium lacking histidine and adenine as previously reported (Tsugama *et al*., 2012a).

3.1.2.3 *In vitro* pull-down assay

To express glutathione S-transferase (GST)-fused NPH3 variants in *Escherichia coli*, the ORFs of *NPH3.1*, *NPH3.2* and their truncated versions were inserted into pGEX-5X-1 (GE Healthcare, UK), generating pGEX-5X-NPH3.1, pGEX-5X-NPH3.2, pGEX-5X-BTB+I+II and pGEX-5X-III+IV, as described below.

To express GST-fused NPH3.1 (GST-NPH3.1), pBluescript II SK$^-$ NPH3.1 was digested by *Eco*RI and *Not*I, and the resultant ORF fragments of *NPH3.1* were inserted into the *Eco*RI-*Not*I site of pGEX-5X-1, in-frame to the coding sequence of GST, generating pGEX-5X-NPH3.1.

To express GST-fused NPH3.2 (GST-NPH3.2), the ORF of *NPH3.2* was cloned. To obtain the ORF of *NPH3.2* without the one-base substitution, the 3' region of *NPH3.2* ORF was amplified by PCR using the RIKEN cDNA clone as template and the following primer pair: 5'-GCGAGGCTTGTGGATAGTTATCTCACCGAAGTTGCTAGAGATCGGAATTTGCCGTTGACA-3' and 5'-CCGGTCTAGAATATATATATACCTTGAGATATGAATCAATGGCT-3'. The resultant PCR product and the above-described PCR product containing the 5' region of *NPH3.1* ORF, which corresponds to the 5' region of *NPH3.2* ORF as well, were mixed and used as template for PCR using the following primer pair: 5'-CCGGTCTAGAATGATGTGGGAATCTGAGAGCGACGGTGGGG-3' and 5'-CCGGTCTAGAATATATATATACCTTGAGATATGAATCAATGGCT-3' (*Xba*I sites are underlined). The resultant PCR products, which contain the ORF of *NPH3.2*, were cloned into the *Xba*I site of pBluescript II SK$^-$, generating pBluescript II SK$^-$ NPH3.2. pBluescript II SK$^-$ NPH3.2 was digested by *Eco*RI and *Not*I, and the resultant ORF

fragments containing *NPH3.2* were inserted into the *Eco*RI-*Not*I site of pGEX-5X-1, in-frame to the coding sequence of GST, generating pGEX-5X-NPH3.2.

To express GST-fused BTB domain and I and II domains of NPH3 (GST-BTB+I+II), pBluescript II SK$^-$ NPH3.1 was digested by *Eco*RI and *Xho*I, and the resultant fragments including BTB domain and I and II domains of NPH3 were inserted into the *Eco*RI-*Xho*I site of pGEX-5X-1, in-frame to the coding sequence of GST, generating pGEX-5X- BTB+I+II.

To express GST-fused III and IV domains of NPH3 (GST-III+IV), pBluescript II SK$^-$ NPH3.2 was digested by *Xho*I and *Not*I, and the resultant fragments including III and IV domains of NPH3 were inserted into the *Xho*I-*Not*I site of pGEX-5X-1, in-frame to the coding sequence of GST, generating pGEX-5X-III+IV.

These constructs were transformed into the *E. coli* strain BL21 (DE3), and transformed cells were cultured at 37°C in LB medium until OD_{600} reached 0.5. IPTG was then added to the medium at 0.5 mM final concentration (for pGEX-5X-NPH3.1 and pGEX-5X-NPH3.2) or 0.3 mM final concentration (for pGEX-5X-BTB+I+II and pGEX-5X-III+IV), and the cells were further cultured at 28 °C for 4 h (for pGEX-5X-NPH3.1 and pGEX-5X-NPH3.2) or 3 h (for pGEX-5X-BTB+I+II and pGEX-5X-III+IV). The cells were then harvested by centrifugation and resuspended in 1× PBS (phosphate-buffered saline: 137 mM NaCl, 8.10 mM $Na_2HPO_4 \cdot 12H_2O$, 2.68 mM KCl, 1.47 mM KH_2PO_4, pH 7.4) with 2 mg/ml lysozyme (Wako, Japan). The cell suspension was frozen at - 80 °C and thawed at room temperature. Freezing and thawing were repeated two more times to lyse the cells, and two units of recombinant DNase I (Takara, Japan) was added to the solution. The solution was incubated at room temperature until the solution became fluid due to DNA degradation. The solution was

then centrifuged at 12000 ×g for 5 min and the supernatant was used as crude extracts. The presence of the GST-fused proteins in the crude extracts was confirmed by Western blotting using a goat anti-GST antibody (GE Healthcare, UK) and a horseradish peroxidase (HRP)-conjugated rabbit anti-goat IgG antibody (MBL, Japan).

GST-fused proteins in the crude extracts were bound to Glutathione Sepharose 4 Fast Flow (GE Healthcare, UK) following the manufacturer's instructions, and the resin was washed 4 times by 1× PBS. The resin was then resuspended in a solution containing purified polyhistidine-tagged AGB1 (His-AGB1), which was prepared as previously described (Tsugama *et al*., 2012a), and incubated at room temperature for 60 min with gentle shaking. The resin was then washed 4 times by 1× PBS, resuspended in 20 mM reduced glutathione in 50 mM Tris–HCl, pH 8.0, and incubated at room temperature for 15 min to elute the GST-fused proteins. The slurry of the resin was centrifuged for 3 min at 12000 × g, and His-AGB1 in the supernatant was analyzed by Western blotting using HisProbe-HRP (Thermo Fisher Scientific, USA). When used, HisProbe-HRP was diluted 2000 times by 1× PBS. Signals were detected with SuperSignal West Pico Chemiluminescent Substrate (Thermo Fisher Scientific, USA) and the Las 1000 image analyzer (Fuji Film, Japan).

3.1.2.4 Bimolecular fluorescence complementation (BiFC) assay

To express cYFP (the C-terminal half of yellow fluorescent protein)-fused NPH3.1, pBluescript II SK$^-$ NPH3.1 was digested by *Xba*I, and the resultant *NPH3.1* ORF fragment was inserted into the *Spe*I site of pBS-35SMCS-cYFP (Tsugama *et al*., 2012a), generating pBS-35S-NPH3.1-cYFP. To express nYFP (the N-terminal half of YFP)-fused AGB1, pBS-35S-nYFP-AGB1 (Tsugama *et al*., 2012a) was used. A mixture

of pBS-35S-nYFP-AGB1 and pBS-35S-NPH3.1-cYFP (500 ng each) was used for particle bombardment to co-express NPH3.1-cYFP and nYFP-AGB1 in onion epidermal cells. Particle bombardment was performed as previously described, and YFP fluorescence was observed by fluorescence microscopy as previously described (Zhang CQ *et al*., 2008). Images were processed using Canvas X software (ACD Systems).

3.1.2.5 *In vivo* co-immunoprecipitation (Co-IP)

The constructs of pBI121-35S-His-AGB1 and pBI121-35S-NPH3.1-GFP, which express polyhistidine-tagged AGB1 (His-AGB1) and green fluorescent protein (GFP)-fused full length NPH3 (NPH3.1-GFP) respectively, were generated as described below.

To express polyhistidine-tagged AGB1 (His-AGB1), the open reading frame (ORF) of *AGB1* was amplified by PCR using pBI121-35S-AGB1-mCherry (Kansup *et al*., 2013) as template and the following primer pair: 5′-CCGGTCTAGAATGCATCATCATCATCATCATATGTCTGTCTCCGAGCTCAAA GAACGC-3′ and 5′-ATTCGTCGACTCAAATCACTCTCCTGTGTCCTCC-3′ (*Xba*I and *Sal*I sites are underlined). The PCR products were digested by *Xba*I and *Sal*I, and cloned into the *Xba*I-*Sal*I site of pBI121-35SMCS (Tsugama *et al*., 2012c), generating pBI121-35S- His-AGB1.

To express green fluorescent protein (GFP)-fused full length NPH3 (NPH3.1), pBluescript II SK$^-$ NPH3.1 was digested by *Xba*I, and the resultant ORF fragments of NPH3.1 were inserted into the *Spe*I site of pBS-35SMCS-GFP (Tsugama *et al*., 2012c), generating pBS-35S-NPH3.1-GFP. The resultant plasmid was digested by *Sal*I and *EcoR*I, and the resultant ORF fragments of NPH3.1-GFP were inserted into the

*Sal*I-*Eco*RI site of pBI121-35SMCS (Tsugama *et al*., 2012c), generating pBI121-35S-NPH3.1-GFP.

Agrobacterium strain EHA105 carrying pBI121-35S-His-AGB1 or pBI121-35S-NPH3.1-GFP was infiltrated into *Brassica rapa* var. *perviridis* leaves. Three days after agroinfection, the leaf tissue was harvested for extraction of total proteins with a native buffer that was composed of 20 mM Tris-MES, pH 7.5, 0.25 M Suc, 1 mM $MgCl_2$, 1 mM EGTA, 2 mM DTT, and protease inhibitor cocktail (28.6 μg/ml pancreasextract, 0.7 μg/ml thermolysin, 2.9 μg/ml chymotrypsin, 28.6 μg/ml trypsin and 471.4μg/ml papain; Roche, USA). After centrifugation at 20,000 ×g, 4°C for 30 min, the supernatant was collected. Ni-NTA His-Bind resin (Novagen, Germany) was added to the supernatant following the manufacturer's instructions, and the mixtures were incubated at room temperature for 60 min with gentle shaking. The resin was washed 4 times by 1× PBS and resuspended in 250 mM imidazole. The slurry of the resin was centrifuged for a few min at 12000 ×g. His-AGB1 and NPH3.1-GFP in the supernatant were analyzed by western blotting using a polyhistidine probe, HisProbe-horseradish peroxidase (HRP) (diluted 2,000-fold; Thermo Fisher Scientific, USA) and an anti-GFP antibody (diluted 2,000-fold; MBL, Japan). After detecting His-AGB1, the blot was washed three times by Tween–phosphate-buffered saline (PBS)–EDTA, which was made by adding 0.5 M EDTA, pH 8.0, to Tween–PBS (0.1% v/v Tween-20 in PBS) to 10 mM final concentration of EDTA, for deprobing the HisProbe-HRP. The blot was then washed twice by Tween–PBS and used for a western blot analysis using an anti-GFP antibody. To detect signals of His-AGB1 in the Co-IP assay, SuperSignal West Pico Chemiluminescent Substrate (Thermo Fisher Scientific, USA) was used. To detect signals of NPH3.1-GFP in the Co-IP assay, SuperSignal

West Femto Chemiluminescent Substrate (Thermo Fisher Scientific, USA) was used.

3.1.2.6 RT-PCR

For RT PCR, plants were grown for four weeks and sampled. Total RNA was prepared using RNeasy Plant Mini Kit (Qiagen, Netherlands), and cDNA was synthesized from 900 ng total RNA using High Capacity RNA-to-cDNA Kit (Applied Biosystems, USA). The cDNA was diluted 15 times by distilled water and used as template for RT-PCR. The expression of *NPH3* was examined by semi-quantitative RT-PCR, and the expression of *AGB1* was examined by quantitative real-time RT-PCR. The real-time PCR was performed using SYBR Premix EX Taq II (Perfect Real Time) (Takara, Japan) and the StepOne Real-Time PCR Systems (Applied Biosystems, USA). Primers used for RT-PCR are shown in Table 4.

3.1.2.7 Western blot analysis of NPH3 phosphorylation states

Crude protein extracts containing GST-fused BTB domain and I and II domains of NPH3 (GST-BTB+I+II) or GST-fused III and IV domains of NPH3 (GST-III+IV) were prepared as described above, using 1× TBS (Tris-buffered saline: 150 mM NaCl in 20 mM Tris–HCl, pH 7.5) instead of 1× PBS. GST-BTB+I+II or GST-III+IV was bound to Glutathione Sepharose 4 Fast Flow as described above. The resin was washed 4 times by 1× TBS and resuspended in 20 mM reduced glutathione in 50 mM Tris–HCl, pH 8.0 to elute GST-BTB+I+II or GST-III+IV. The slurry was centrifuged at 12000 ×g for 5 min and the supernatant was used as purified GST-BTB+I+II or GST-III+IV solution.

Seedlings of wild type or *agb1-2* mutant were homogenized by a pestle and a

mortar with liquid nitrogen. The extraction buffer (0.1 M MES-NaOH, pH 6.0) was added to the homogenate. Then the homogenate was centrifuged at 20,000 ×g, 4°C for 30 min. The supernatant was collected and mixed with the purified GST-BTB+I+II or GST-III+IV solution. After 30 min incubation at room temperature in dark or light condition, the mixtures were used for western blotting using an anti-GST antibody (GE Healthcare, UK) and Phostag Biotin BTL-104 (Wako, Japan; Kinoshita *et al*., 2006). Signals were detected using SuperSignal West Pico Chemiluminescent Substrate (Thermo Fisher Scientific, USA) and an LAS-1000 plus image analyzer (Fuji Film, Japan).

Table 3. Primer pairs used for genomic PCR

	Primer sequence (5' > 3')
NPH3	PF1: CCGGTCTAGAATGATGTGGGAATCTGAGAGCGACGGTGGGG PR1: TCAATGGCTCTGTATAGTCCATCGT
T-DNA border	LBb1.3: ATTTTGCCGATTTCGGAAC RB: GGCATGCACATACAAATGGACGAACGG

Table 4. Primer pairs used for RT-PCR analyses

Gene	Primer sequence (5' > 3')
Actin	Fw: GGTAACATTGTGCTCAGTGGTGG Rv: AACGACCTTAATCTTCATGCTGC
AGB1	Fw: TGGGATGTAACTACTGGTCTCA Rv: CAGCACGAGTGTCCCACAA
NPH3 (for real-time PCR)	Fw: TTTGCCGTTGACAAAGTTTCAGGT Rv: TGCGTCCATTGATAGTTTTTGACA
NPH3 (for RT-PCR)	Fw: TTTGCCGTTGACAAAGTTTCAGGT Rv: GGCCTCTAGATGAAATTGAGTTCCTCCATCGTCTTG GTTTCCTGGGGGGT

3.1.3 Results

3.1.3.1 AGB1 interacts with NPH3

My group and another group independently performed yeast two-hybrid (Y2H) screens using AGB1 as bait, and both identified NPH3 as a potential AGB1 interactor (Klopffleisch *et al*., 2011; Tsugama *et al*., 2012a). In the Y2H screen of my group, *NPH3* was detected as a 5' region-truncated form (the position 1546-2241 from the start codon) of *NPH3.1* (see Fig. 23 for the region of NPH3 used in Y2H analysis). Yeast cells could grow on the selection medium when they were co-transformed with the constructs that contain both *AGB1* and the 5' region-truncated version of *NPH3.1* (Fig. 24A, middle panel), but not when either *AGB1* or the truncated form of *NPH3.1* was absent in the constructs (Fig. 24A, right and left panels), confirming that AGB1 and the C-terminal region of NPH3.1 interact in yeast cells. Y2H analysis using full-length NPH3.1 and AGB1 was also attempted. However, yeast transformed with pGAD full-length NPH3.1 could not grow in the control medium (data not shown).

In an *in vitro* GST pull-down assay, polyhistidine-tagged AGB1 (His-AGB1) was detected when it was reacted with GST-fused NPH3.1, NPH3.2 or BTB+I+II, a C-terminal region-truncated form of NPH3, but not when reacted with III+IV (GST-fused form), which corresponds to the central region of NPH3 (Fig. 25 and 26; see Fig. 23 for diagrammatic representations of NPH3 proteins). These results suggest that the N-terminal region rather than the C-terminal region of NPH3 interacts with AGB1 *in vitro*.

In a bimolecular fluorescence complementation (BiFC) assay using onion cells, YFP (yellow fluorescent protein) fluorescence was recovered in cell periphery when nYFP (the N-terminal region of YFP)-fused AGB1 and cYFP (the C-terminal region of

YFP)-fused NPH3.1 were co-expressed (Fig. 27), suggesting that AGB1 and NPH3.1 interact in the plasma membrane in plant cells. Additionally, in co-immunoprecipitation experiments using *Brassica rapa* var. *perviridis* leaves expressing polyhistidine-tagged AGB1 (His-AGB1) and/or green fluorescent protein (GFP)-fused full length NPH3 (NPH3.1-GFP), NPH3.1-GFP was only detected when it was co-expressed with His-AGB1 (Fig. 28, lane 3). These results suggested that AGB1 and NPH3 interact *in planta*.

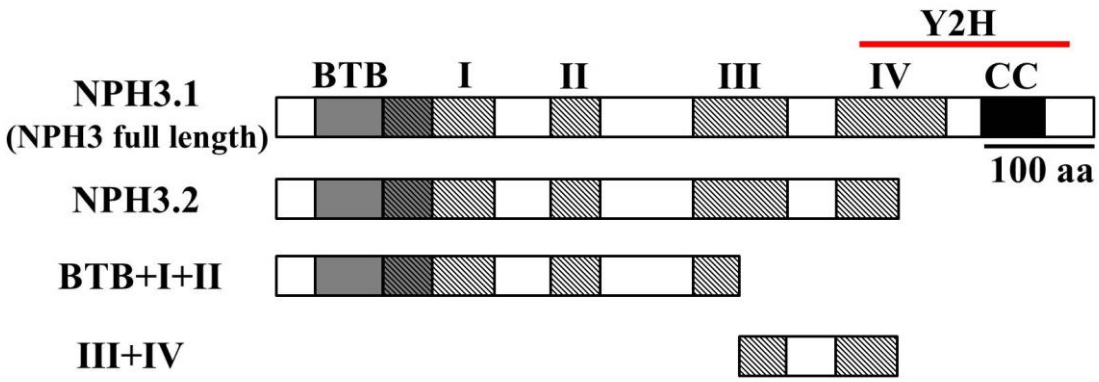

Figure 23. Diagrammatic representations of NPH3 proteins. Four domains (I to IV) conserved among NPH3 homologs are shown on NPH3 by cross-hatched blocks. The BTB (broad complex, tramtrack, bric a`brac) domain and the coiled-coil (CC) domain are shown in the dark gray block and black block, respectively. The gray cross-hatched block indicates the region which the BTB domain and domain I share. The region of NPH3 used in yeast two-hybrid (Y2H) analysis is indicated by the red line.

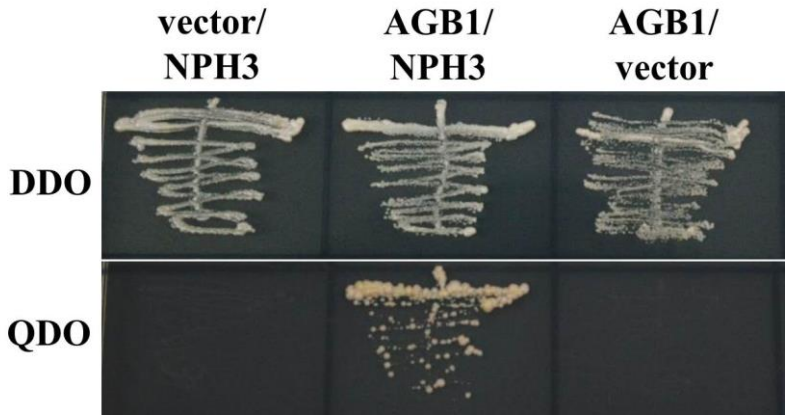

Figure 24. Interaction between NPH3 and AGB1 in yeast. Yeast two-hybrid analysis of the interaction between AGB1 and NPH3. The combinations of the plasmids used for transformation of the yeast strain AH109 are indicated at the top of each panel. vector: a pGBKT7 plasmid or a pGADT7-Rec plasmid containing no insert; AGB1: pGBKT7 containing *AGB1*; NPH3: pGADT7-Rec containing a 5' region-truncated form (the position 1546-2241) of *NPH3.1*. Transformed yeast cells were cultured on DDO (SD medium lacking tryptophan and leucine) and QDO (DDO lacking histidine and adenine) to check activation of the reporter genes *HIS3* and *ADE2*. At least 4 colonies for each genotype were tested and a representative result is shown.

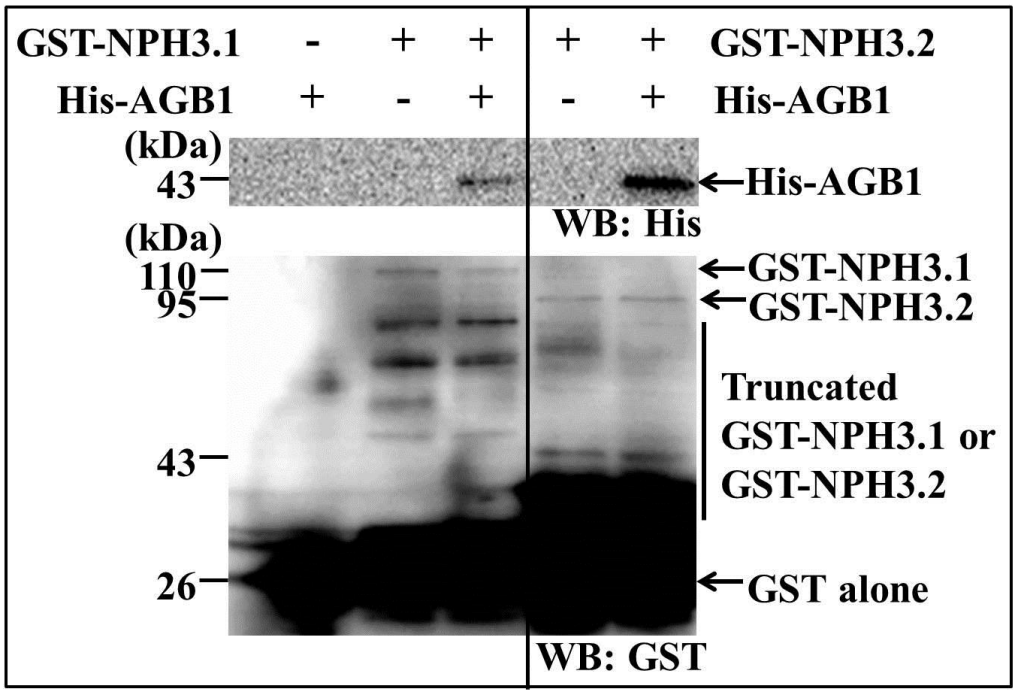

Figure 25. Interaction between NPH3 variants and AGB1 *in vitro*. *In vitro* GST pull-down assay between GST-fused NPH3.1 (GST-NPH3.1) or GST-fused NPH3.2 (GST-NPH3.2) and polyhistidine-tagged AGB1 (His-AGB1). GST-NPH3.1, GST-NPH3.2 and His-AGB1 were expressed in *E. coli* and used for the analysis. The presence or absence of each protein in the reaction mixture is shown as + or -, respectively. His-AGB1 was analysed by western blotting using a polyhistidine probe, HisProbe-HRP (WB: His). GST-NPH3.1 and GST-NPH3.2 were analysed by western blotting using anti-GST antibody (WB: GST). Experiments were performed 4 times and a representative result is shown.

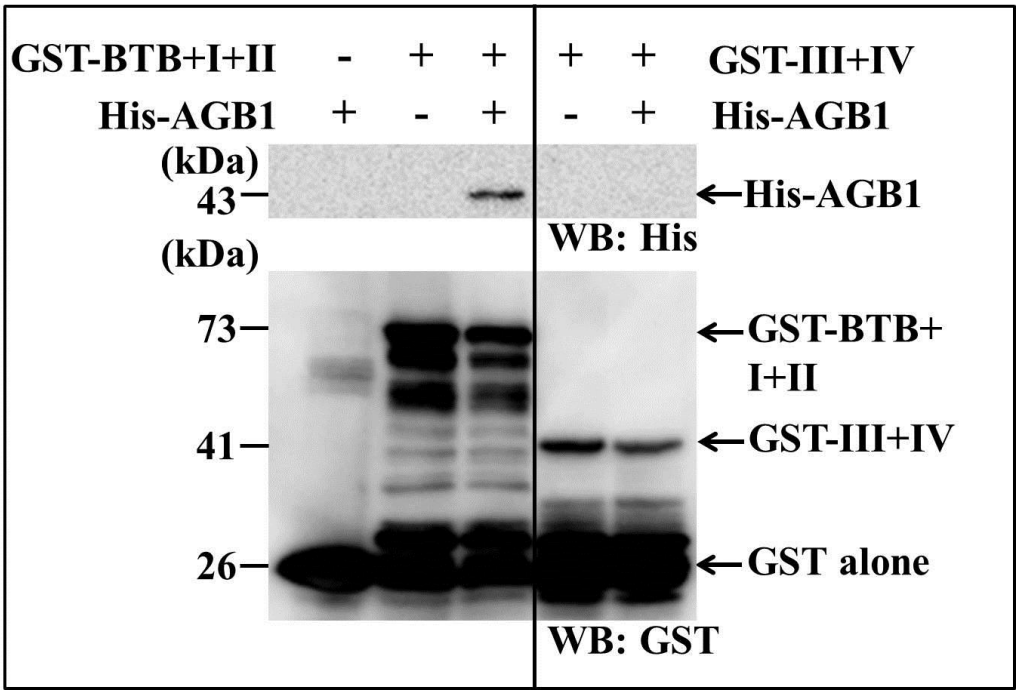

Figure 26. Interaction between NPH3 variants and AGB1 *in vitro*. *In vitro* GST pull-down assay between GST-fused BTB+I+II, a C-terminal region-truncated form of NPH3, (GST-BTB+I+II) or GST-fused III+IV, a variant containing only the central region of NPH3, (GST-III+IV) and polyhistidine-tagged AGB1 (His-AGB1). GST-BTB+I+II, GST-III+IV and His-AGB1 were expressed in *E. coli* and used for the analysis. The presence or absence of each protein in the reaction mixture is shown as + or -, respectively. His-AGB1 was analysed by Western blotting using a polyhistidine probe, HisProbe-HRP (WB: His). GST-BTB+I+II and GST-III+IV were analysed by western blotting using anti-GST antibody (WB:GST). Experiments were performed 4 times and a representative result is shown.

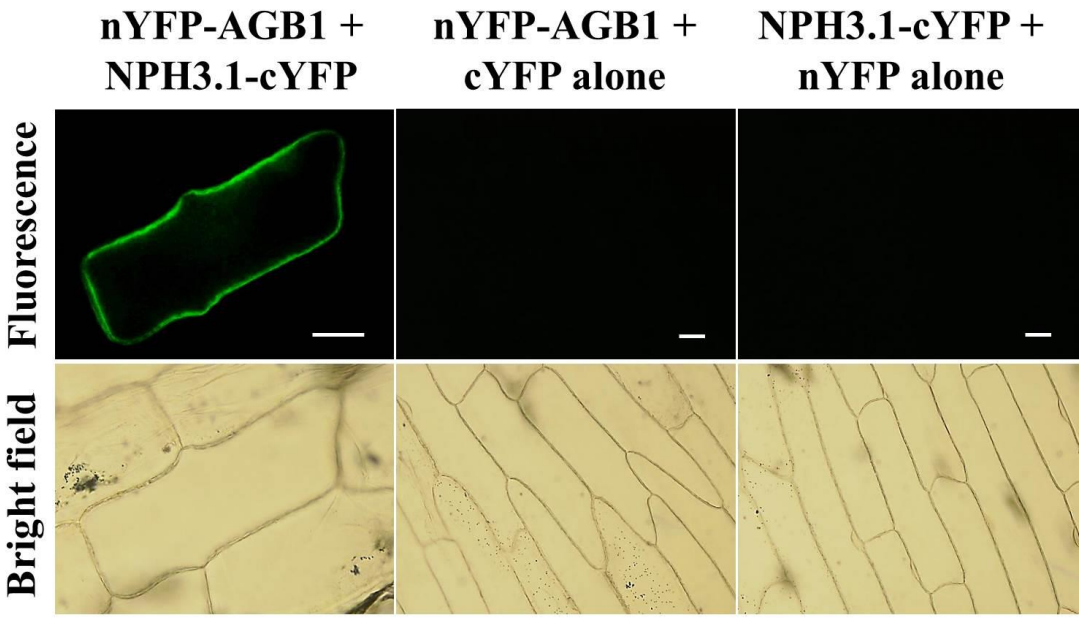

Figure 27. Interaction between NPH3 and AGB1 *in planta*. BiFC in onion epidermal cells. The ORF of *AGB1* was cloned in frame behind the coding sequence of the N-terminal region of YFP (nYFP) to express nYFP-fused AGB1 (nYFP-AGB1), and the ORF of *NPH3.1* was cloned in frame in front of the coding sequence of the C-terminal region of YFP (cYFP) to express cYFP-fused NPH3.1 (NPH3.1-cYFP). These constructs were co-introduced into onion epidermal cells via particle bombardment. Combinations of co-expressed proteins are shown at the top of each panel. cYFP alone and nYFP alone were used as controls. More than 20 cells were observed and a representative cell is shown. Scale bars = 50 μm.

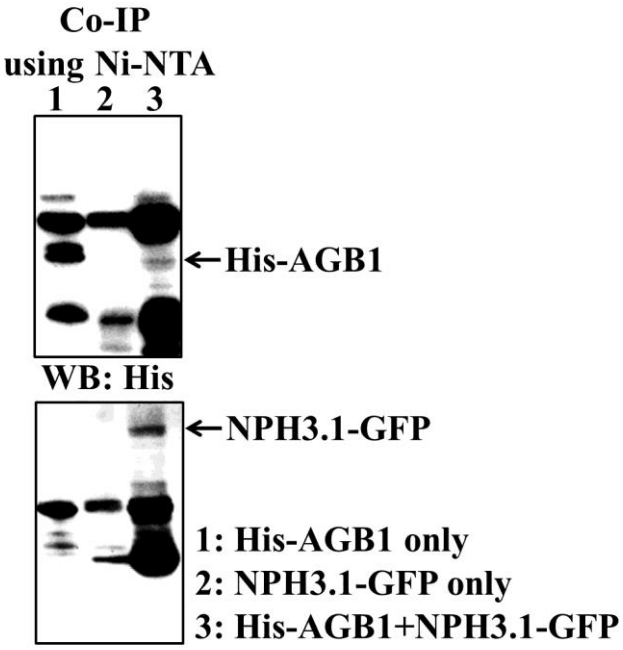

Figure 28. Interaction between NPH3 and AGB1 *in planta*. Co-immunoprecipitation of NPH3 with AGB1. Total extracts of *Brassica rapa* var. *perviridis* leaves expressing polyhistidine-tagged AGB1 (His-AGB1 only, lane 1) or green fluorescent protein (GFP)-fused full length NPH3 (NPH3.1-GFP only, lane 2) or His-AGB1 + NPH3.1-GFP (lane 3) were incubated with Ni-NTA His-Bind resin and probed with a HisProbe-HRP (WB: His) or anti-GFP antibodies (WB: GFP).

3.1.3.2 AGB1 is involved in phototropism

I obtained two different mutant lines of NPH3, *nph3-7* (Salk_110039) and *nph3-8* (CS322676), which carry T-DNA insertions in exon 3 and intron 3 of the *NPH3* gene, respectively (Fig. 29A). Genomic PCR analyses verified that the T-DNA alleles were homozygous (Fig. 29B). RT-PCR confirmed the absence of full-length transcripts (Fig. 29C). To generate *agb1/nph3* double mutants (DMs), I crossed the *nph3-7* mutant with *agb1-2* mutant (Ullah *et al*., 2003). Two DMs were obtained; DM#1-1-2 and DM#11-1-2 (Fig. 30).

In a previous study, *NPH3*-null mutations completely abolished the phototropic response of etiolated seedlings (Motchoulski and Liscum, 1999). In agreement with this result, the phototropic response of etiolated seedlings was abolished in both *nph3-7* and *nph3-8*. Interestingly, the *AGB1*-null mutants *agb1-1* and *agb1-2* both showed weaker phototropic responses than the wild type. The phototropic response was completely abolished in the *agb1-2/nph3-7* double mutants as in *nph3-7* and *nph3-8* (Fig. 31 and 32). These results suggest that AGB1 is involved in the phototropic responses.

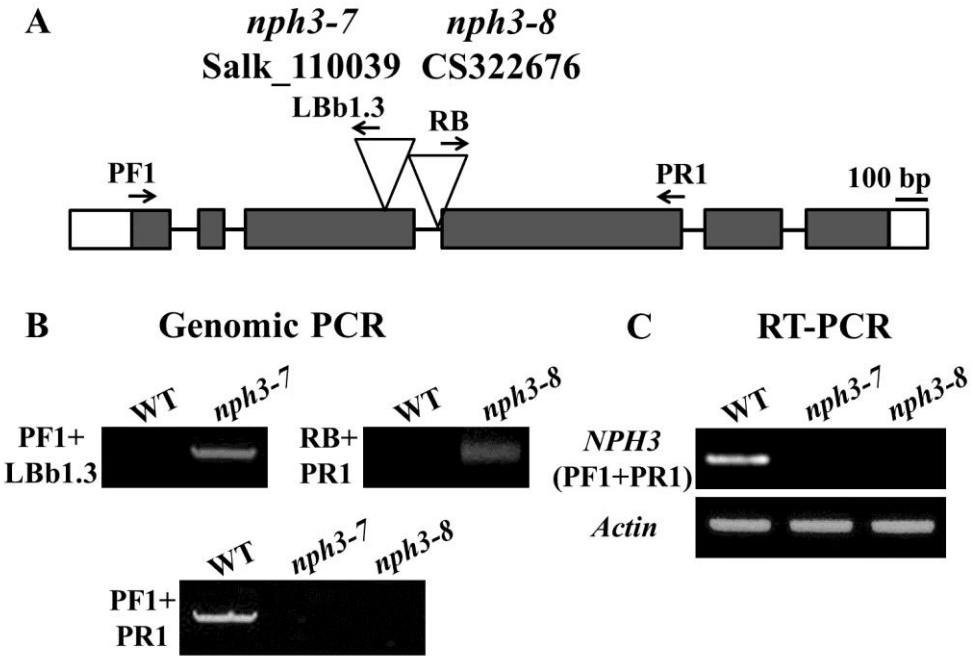

Figure 29. T-DNA insertional mutants of NPH3. (A) Positions of T-DNA insertion in *nph3* mutants. Gray boxes and white boxes represent exons and UTR regions, respectively. The positions of T-DNA insertions in *nph3-7* and *nph3-8* are indicated by arrowheads. Primer pairs used in genomic PCR and primer pairs used in RT-PCR to assess *NPH3* transcripts are indicated. Annealing sites of the primers used in (B) and (C) are indicated by arrows. (B) Genomic PCR analyses verified homozygosity for the T-DNA alleles. (C) RT-PCR analysis of *NPH3* transcript levels in *nph3* mutants. *Actin* was used as an internal control.

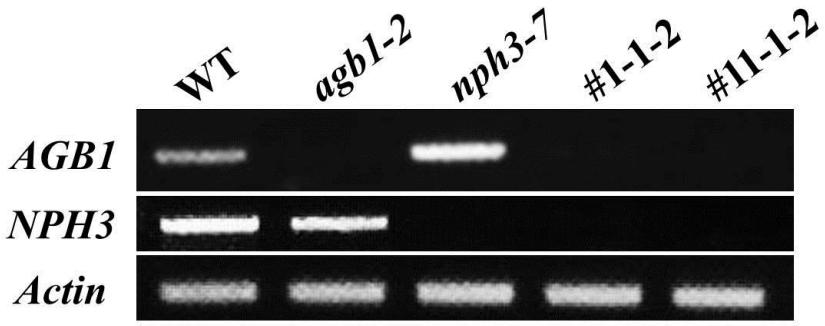

Figure 30. Generation of *agb1/nph3* double mutants. Two double mutant lines (DM) were generated; DM#1-1-2 and DM#11-1-2. RT-PCR using the primers specific to *AGB1* or *NPH3* gene confirmed the absence of transcripts of *AGB1* or *NPH3*. *Actin* was used as an internal control gene.

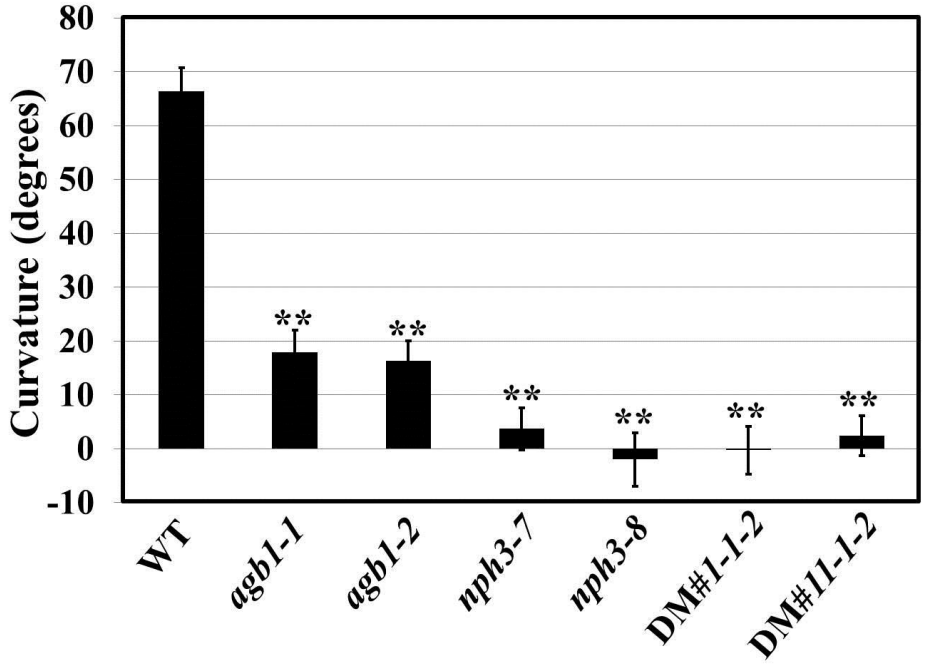

Figure 31. AGB1 is involved in phototropism. Plants of each genotype were grown in the dark for 3 days, exposed to unilateral blue light for 20 hours, and photographed to measure hypocotyl curvature. WT: wild type; DM#1-1-2 and DM#11-1-2: *agb1/nph3* double mutants. Data are means ± SE of 23 seedlings. **, $p < 0.005$ vs. wild type, *t*-test.

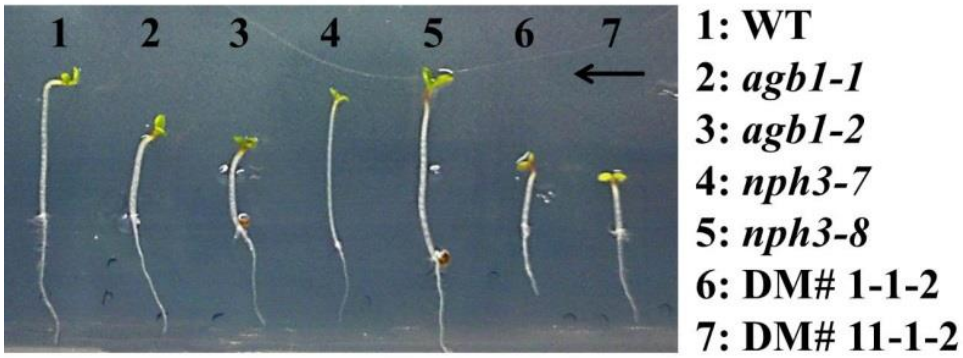

Figure 32. Hypocotyl phototropism in wild type (WT), *agb1* mutants, *nph3* mutants, and *agb1/nph3* double mutants. Plant were grown for 3 days in the dark, exposed to unilateral blue light, and photographed. Arrow shows the direction of blue light.

3.1.3.3 Expression of *AGB1* gene in *nph3* mutants

The expression level of *AGB1* gene was lower in the *nph3* mutants than in the wild type (Fig. 33), raising the possibility that NPH3 positively regulates the expression of *AGB1* gene. No difference in expression of *NPH3* gene was observed between the wild type and the *agb1* mutant (Fig. 34).

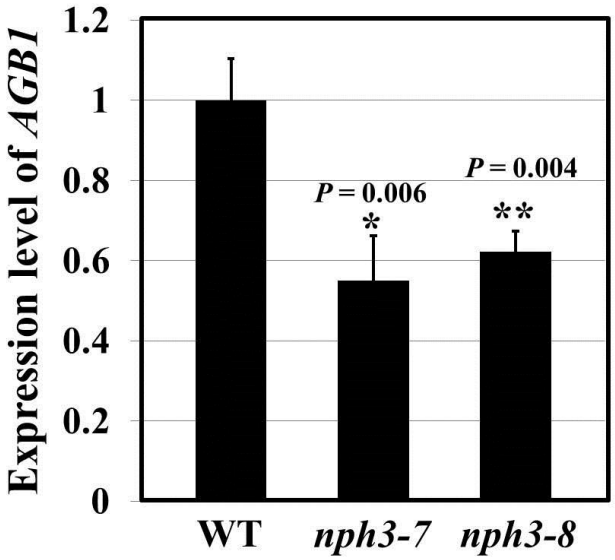

Figure 33. Expression of *AGB1* is lower in *nph3* mutants than in wild type. The expression of *AGB1* was analyzed by quantitative real-time RT-PCR. Relative expression levels were calculated by the $\Delta\Delta C_T$ method using *Actin* as an internal control gene and wild type sample as a reference sample. Experiments were performed in triplicate. Values are means ±SD. *, $p < 0.05$, **, $p < 0.005$ vs. wild type, *t*-test.

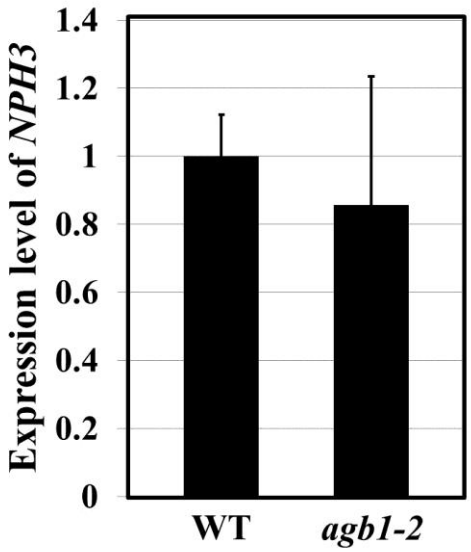

Figure 34. Expression of *NPH3* gene in wild type (WT) and *agb1-2*. The expression of *NPH3* was analyzed by real-time quantitative RT-PCR. Relative expression levels were calculated by the $\Delta\Delta C_T$ method using *Actin* as an internal control gene and wild type sample as a reference sample. Experiments were performed in triplicate. Values are means ±SD.

3.1.4 Discussion

3.1. 4.1 AGB1 interacts with NPH3

I have shown that AGB1 interacts with NPH3 *in vitro* and *in vivo* (Figs. 24-28). The N-terminal region rather than the C-terminal region of NPH3 interacts with AGB1 *in vitro* (Fig. 25 and 26). This is not consistent with the Y2H analysis, where the C-terminal region of NPH3.1 was responsible for the AGB1-NPH3 interaction (Fig. 24). It might be possible that the interaction between AGB1 and the C-terminal region of NPH3.1 requires cellular components. In yeast, the N-terminal region of NPH3 might mislocalize and/or destabilize NPH3.1.

BiFC assay revealed that AGB1 and NPH3.1 interact in the plasma membrane in plant cells (Fig. 27). AGB1 has been reported to be localized to the cytosol, the nucleus, the Golgi apparatus and the plasma membrane (Adjobo-Hermans *et al*., 2006; Anderson and Botella, 2007; Kansup *et al*., 2013; Tsugama *et al*., 2012a), while NPH3.1 is localized to the plasma membrane (Motchoulski and Liscum, 1999; Inoue *et al*., 2008). Thus, the localization of NPH3.1 is thought to limit the localization of the AGB1-NPH3.1 BiFC to the plasma membrane.

3.1. 4.2 AGB1 is involved in phototropism

Phenotypic analysis of *agb1* mutants and *agb1-2/nph3-7* double mutants revealed that AGB1 is involved in the phototropic responses (Fig. 31 and 32). In dark-grown seedlings, NPH3 exists as a phosphorylated protein and blue light stimulates its dephosphorylation (Pedmale and Liscum, 2007; Tsuchida-Mayama *et al*., 2008). This post-translational modification represents a crucial event in phot1-dependent phototropism (Pedmale and Liscum, 2007; Tsuchida-Mayama *et al*., 2008). To study whether AGB1 is involved in the phosphorylation state changes of NPH3, I examined the phosphorylation state of NPH3 in the presence of crude protein extracted from the wild type or *agb1-2* mutant using GST-fused NPH3 proteins. Because the size of GST-NPH3.1 protein was 110 kDa (Fig. 25, WB: GST) and non-specific bands with the size of 110 kDa and 80 kDa were detected in crude proteins extracted from WT or *agb1-2* mutant in western blot using Phos-tag (Fig. 35), I used GST-fused BTB domain and I and II domains of NPH3 (GST-BTB+I+II) and GST-fused III and IV domains of NPH3 (GST-III+IV), which were 73 kDa and 41 kDa, respectively (Fig. 26, WB: GST).

However, the phosphorylated GST-BTB+I+II and GST-III+IV were not detected in the presence of crude proteins extracted from WT or *agb1-2* mutant in light or dark condition (Fig 36). This may due to the excessive amount of GST-BTB+I+II in the mixture and the activity of kinase in the crude proteins extracted from the wild type or *agb1-2* mutant is insufficient. Alternatively, AGB1 is not involved in regulating the phosphorylation state of NPH3.

NPH3 regulates auxin polar transport as a downstream step in phototropic responses (Roberts *et al*., 2011; Sakai and Haga, 2012; Wan *et al*., 2012), and AGB1 is

involved in regulating auxin responses and/or transport (Lease *et al*., 2001; Ullah *et al*., 2003; Mudgil *et al*., 2009). Thus, AGB1 might play a role in the NPH3-dependent regulation of auxin polar transport.

In conclusion, AGB1 physically interacts with NPH3, and is involved in the hypocotyl phototropic response. Further studies are required to elucidate how AGB1 is involved in the NPH3-mediated regulation of phototropism.

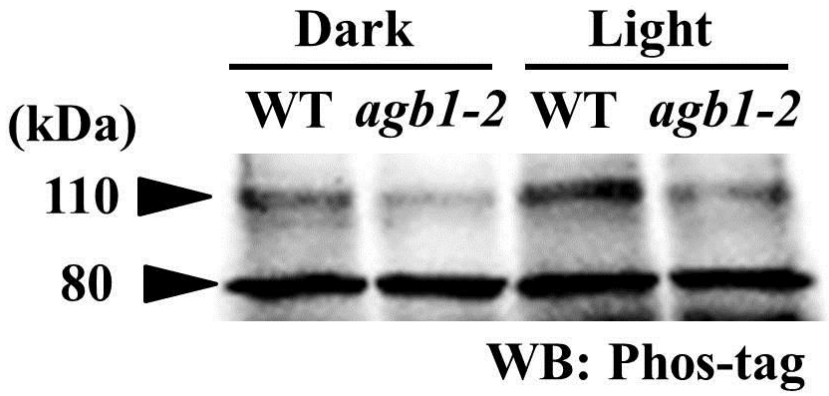

Figure 35. Non-specific bands were found in crude proteins extracted from the wild type or *agb1-2* mutant. Crude proteins extracted from wild type or *agb1-2* mutant were incubated for 30 min at room temperature in dark or light condition, and used for western blotting using Phos-tag Biotin BTL-104 (WB: Phos-tag). The positions of non-specific bands are indicated by arrowheads. Experiments were performed in triplicate and representative result is shown.

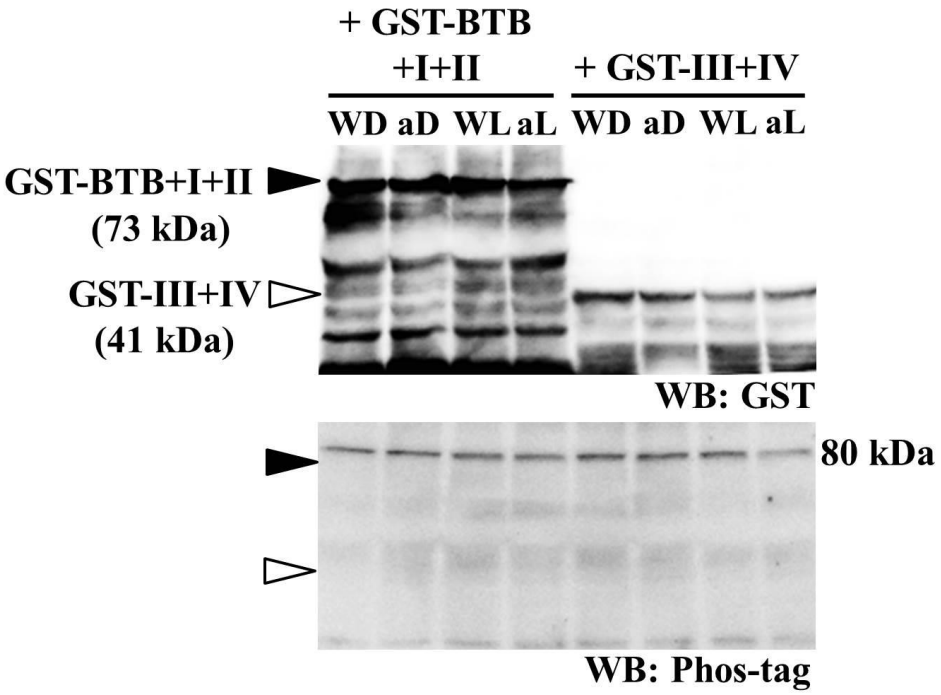

Figure 36. Western blot analysis of phosphorylation state of NPH3. Purified GST-BTB+I+II or GST-III+IV was mixed with crude proteins extracted from wild type (W) or *agb1-2* mutant (a) and incubated for 30 min at room temperature in dark (D) or light (L) condition. The mixtures were used for western blotting using anti-GST antibody (WB: GST) or Phos-tag Biotin BTL-104 (WB: Phos-tag). The positions of GST-BTB+I+II and GST-III+IV (in both the upper and lower panels) are indicated by black arrowheads and white arrowheads, respectively. Experiments were performed in triplicate and representative result is shown.

3.2 The involvement of NPH3 in hormonal responses

3.2.1 Introduction

G proteins are suggested to play roles in signal transduction of a phytohormone, brassinosteroid (BR). For example, Gα deficiency in *Arabidopsis* causes BR hyposensitivities in hypocotyl and root elongation (Ullah *et al*., 2002) and enhances the dwarf phenotypes of *bri1-5* and *det2-1*, which have defects in BR biosynthesis and BR perception, respectively (Gao *et al*., 2008). Arabidopsis seedlings lacking Gβ show BR hyposensitivities and BRZ (brassinazole, a BR biosynthesis inhibitor) hypersensitivities in hypocotyl elongation (Tsugama *et al*., 2013b). Furthermore, an AGB1-null mutant, *agb1-2*, is hyposensitive to BR in seed germination (Chen *et al*., 2004). In addition, *agb1-2* has rounder leaves, more highly branched root systems, shorter siliques (Ullah *et al*., 2003), and higher sensitivities to ABA (Pandey *et al*., 2006). All these phenotypes of *agb1*-2 are similar to the phenotypes of mutants that have defects in BR biosynthesis or BR signaling (Clouse, 2011). Recently, AGB1 was found to regulate BR responses via interaction with a glycogen synthase kinase 3/SHAGGY-like protein kinase (GSK), which is a component of BR signaling (Tsugama *et al*., 2013b).

A reduction in blue light (low blue) induces a set of phenotypic traits, such as shoot elongation, to consolidate light capture; these are called shade avoidance responses. A well-known phenotypic response to blue light depletion is elongation of hypocotyls (Ballaré *et al.*, 1991; Djakovic-Petrovic *et al.*, 2007; Pierik *et al.*, 2009). BR plays an important role in the regulation of enhanced hypocotyl elongation in response to blue light depletion (Keuskamp *et al*., 2011). Mutants that have defects in BR biosynthesis or BR signaling had a strongly reduced low-blue response. Furthermore, inhibition of BR biosynthesis via the application of BRZ led to impaired low-blue-induced hypocotyl elongation (Keuskamp *et al*., 2011).

NPH3 interacts with AGB1 and is involved in blue light signaling, such as phototropism (Chapter 3. 3.1; Kansup *et al*., 2014). However, the involvement of NPH3 in BR signaling and hypocotyl elongation is unknown. Furthermore, there is no report about the involvement of NPH3 in other hormone signaling except auxin (Wan *et al*., 2012). In this chapter, the subcellular localization and the function of NPH3 in hormone responses were characterized.

3.2.2 Materials and methods

3.2.2.1 Plant material and culture conditions

Arabidopsis thaliana ecotype Columbia-0 (Col-0) was used throughout the experiments. Seeds of *nph3-1* and *agb1-2* (Ullah *et al*., 2003) mutants were obtained from the Arabidopsis Biological Research Center (ABRC) with stock numbers of SALK_110039 and CS6536 respectively. The genetic backgrounds for all the mutant lines are Col-0.

To generate transgenic plants expressing splicing variant NPH3.2, which its C-terminus is truncated, fused with green fluorescent protein (GFP), pBluescript II SK$^-$ NPH3.2 was digested by *Xba*I, and the resultant ORF fragments of NPH3.2 were inserted into the *Spe*I site of pBS-35SMCS-GFP (Tsugama *et al*., 2012c), generating pBS-35S-NPH3.2-GFP. The resultant plasmid was digested by *Sal*I and *EcoR*I, and the resultant ORF fragments of NPH3.2-GFP were inserted into the *Sal*I-*EcoR*I site of pBI121-35SMCS (Tsugama *et al*., 2012c), generating pBI121-35S-NPH3.2-GFP.

The wild type plants were transformed with pBI121-35S-GFP (Kansup *et al*., 2013) or pBI121-35S-NPH3.1-GFP or pBI121-35S-NPH3.2-GFP by the *Agrobacterium*-mediated floral dip method (Clough and Bent, 1998). GFP expression in T2 plants was checked by fluorescence microscopy as previously described (Zhang CQ *et al*., 2008), and only GFP-positive plants were used for measuring hypocotyl lengths, scoring germination rates and western blotting.

Seeds were surface sterilized and sown on 0.8% agar containing 0.5× Murashige and Skoog (MS) salts (Wako, Japan), 1% (w/v) Suc, and 0.5 g/L MES, pH 5.8, with or without the brassinosteroid brassinolide (BR) (Brassino Co., Ltd., Japan), brassinazole (BRZ) (Tokyo Kasei, Japan), bikinin (Calbiochem), or ABA (Wako,

Japan) (concentrations are shown in the figures), chilled at 4°C in the dark for 3 d (stratified), and germinated at 22°C. Plants were grown at 22°C under 16-h-light/8-h-dark conditions.

3.2.2.2 Western blot analysis

Wild type plants and transgenic plants expressing GFP or NPH3.1-GFP or NPH3.2-GFP were grown in the presence or absence of BR, BRZ, or bikinin as described above. The plants were sampled at the time points indicated in the figures and and used for western blotting using anti-GFP antibody (MBL, Japan) or Phostag Biotin BTL-104 (Wako, Japan) (Kinoshita *et al*., 2006). Signal detection and image processing were performed as described above.

3.2.2.3 Quantitative real-time RT-PCR

The expressions of *CPD*, which is a BR-responsive gene, in the wild type and *nph3-7* mutant were tested. Plants of each genotype were grown for 16 days on 0.8% agar containing 0.5× Murashige and Skoog (MS) salts (Wako, Japan), 1% (w/v) Suc, and 0.5 g/L MES, pH 5.8, and sampled.

The expressions of the *NPH3* in the wild type and *ap-3μ* mutant grown in the absence or in the presence of ABA were tested. Plants of each genotype were grown for 18 days on 0.8% agar containing 0.5× Murashige and Skoog (MS) salts (Wako, Japan), 1% (w/v) Suc, and 0.5 g/L MES, pH 5.8, with 0 or 1.0 μM ABA and sampled.

Total RNA was prepared using RNeasy Plant Mini Kit (Qiagen, Netherlands) and cDNA was synthesized from 2 μg of the total RNA with High Capacity RNA-to-cDNA Kit (Applied Biosystems, USA) according to the manufacturer's

instructions. The reaction mixtures were diluted 20 times with distilled water and used as a template for PCR. The primer sequences are given in Table 5 (Tsugama *et al*., 2013b, Kansup *et al*., 2013). Quantitative real-time RT-PCR was performed using SYBR® *Premix Ex Taq*™ II (Perfect Real Time) (Takara, Japan) and the StepOne Real-Time PCR System (Applied Biosystems, USA).

Table 5. Primer pairs used for RT-PCR analyses

Gene	Primer sequence (5' > 3')
CPD	Fw: GGGCCAAGGCTATGTCCCGG Rv: ACGGCGCTTCACGAAGATCGG
NPH3	Fw: TTTGCCGTTGACAAAGTTTCAGGT Rv: TGCGTCCATTGATAGTTTTTGACA
Actin	Fw: GGTAACATTGTGCTCAGTGGTGG Rv: AACGACCTTAATCTTCATGCTGC

3.2.3 Results

3.2.3.1 Subcellular localization of NPH3 proteins

To determine the subcellular localizations of NPH3 proteins, I constructed NPH3.1-GFP and NPH3.2-GFP fusion genes expressed under the control of a CaMV 35S promoter. When expressed in onion epidermal cells, NPH3.1-GFP was detected at the plasma membrane (Fig. 37A) as previously reported (Inoue *et al*., 2008), while NPH3.2-GFP was detected in the cytoplasm and nucleus (Fig. 37B).

Arabidopsis plants stably transformed with NPH3.1-GFP or NPH3.2-GFP under the control of the CaMV 35S promoter were generated. Three lines of NPH3.1-GFP (WT/NPH3.1-GFP#5, WT/NPH3.1-GFP#9 and WT/NPH3.1-GFP#10) and 3 lines of NPH3.2-GFP (WT/NPH3.2-GFP#1, WT/NPH3.2-GFP#4 and *nph3-8*/NPH3.2-GFP#2) were obtained (Fig. 38A and 38B). The line of *nph3-8*/NPH3.2-GFP#2 was in the *nph3-8* background, while the other lines were in the wild type background.

Epifluorescence microscopy imaging of epidermal cells of the Arabidopsis leaves revealed that NPH3.1-GFP was localized at the plasma membrane (Fig 39A), while NPH3.2-GFP was localized in the cytoplasm and nucleus (Fig. 39B), suggesting that the region inside the latter half of IV domain, coiled-coil domain and C-terminus of NPH3 is required for the localization at the plasma membrane. This is consistent with the previous report that the region including coiled-coil domain and C-terminus of NPH3 is sufficient for the plasma membrane localization of NPH3 (Inoue *et al*., 2008).

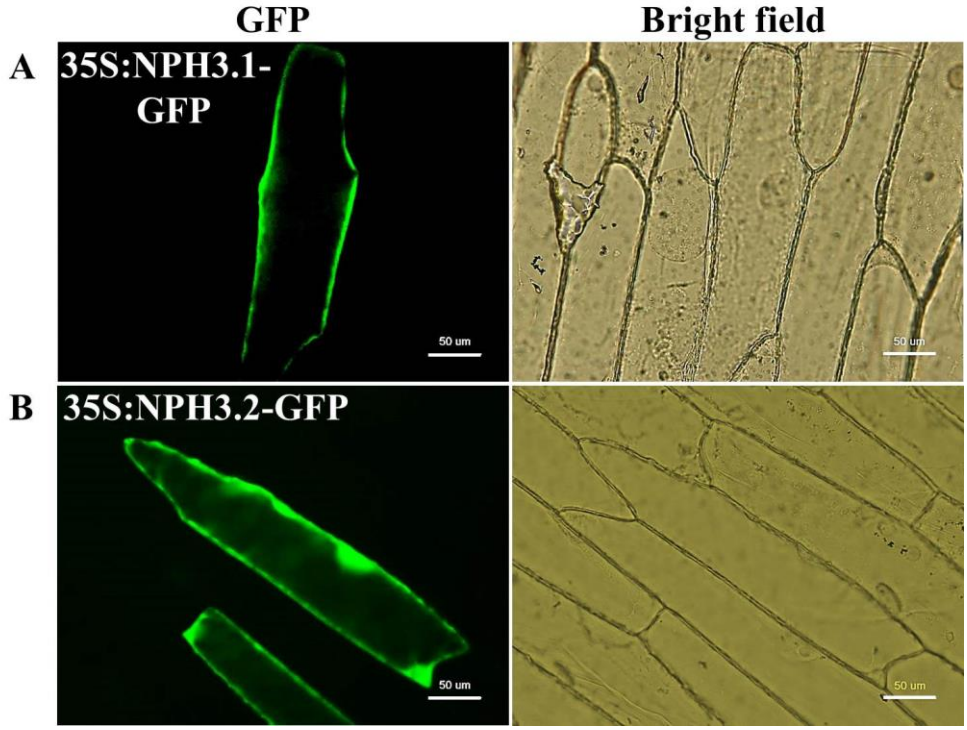

Figure 37. Subcellular localizations of NPH3.1 and NPH3.2. GFP-fused NPH3.1 (NPH3.1-GFP) (A) or GFP-fused NPH3.2 (NPH3.2-GFP) (B) was transiently expressed in onion epidermal cells under the control of CaMV 35S promoter (35S:). More than 10 cells were observed, and a representative cell is shown in each panel. Scale bars = 50 μm.

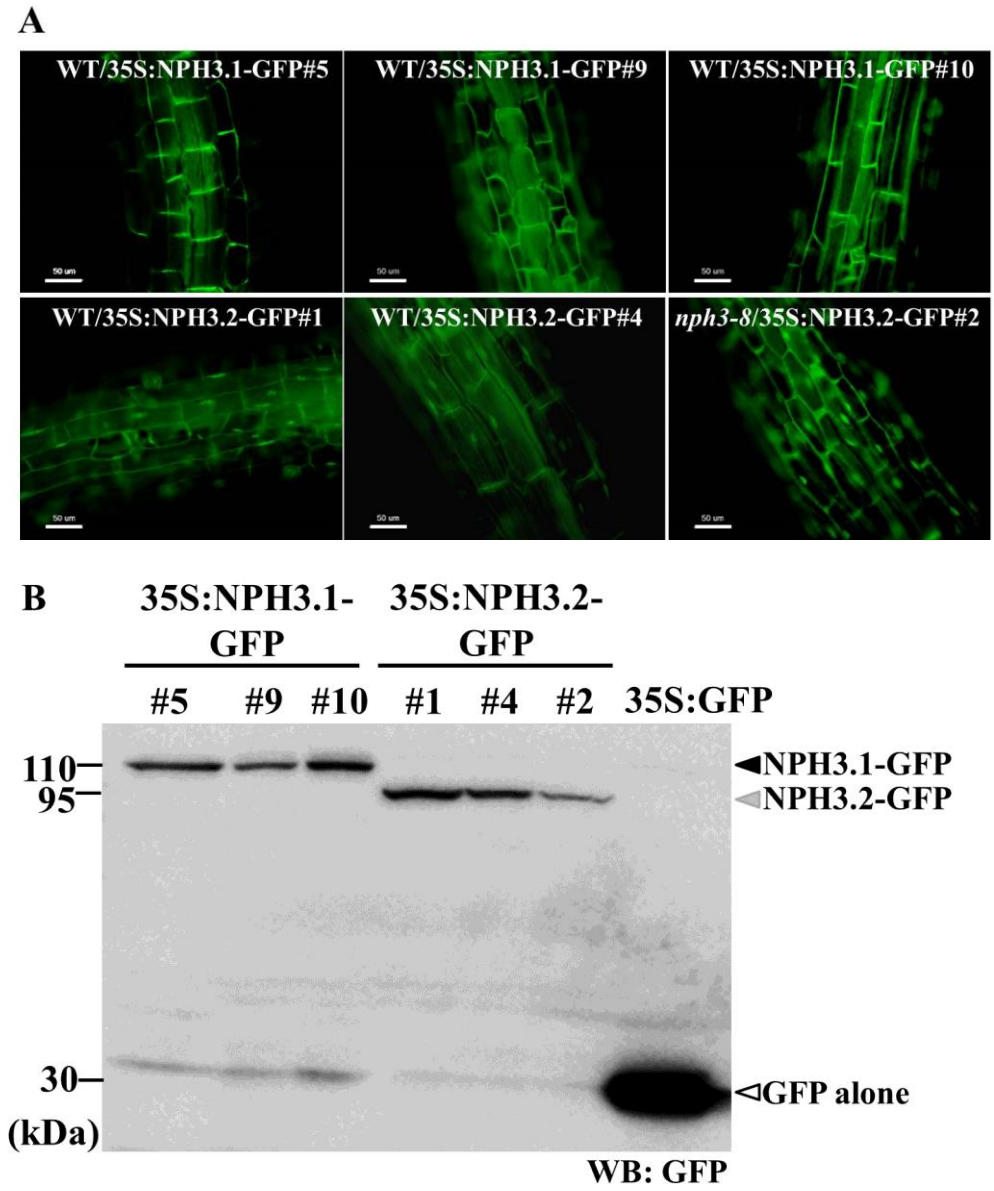

Figure 38. Generation of NPH3.1-GFP and NPH3.2-GFP overexpression lines. Plants were stably transformed with a construct containing CaMV 35S promoter-NPH3.1-GFP or CaMV 35S promoter-NPH3.2-GFP. Three lines of NPH3.1-GFP (WT/NPH3.1-GFP#5, WT/NPH3.1-GFP#9 and WT/NPH3.1-GFP#10) and 3 lines of NPH3.2-GFP (WT/NPH3.2-GFP#1, WT/NPH3.2-GFP#4 and *nph3-8*/NPH3.2-GFP#2) were obtained. (A) Petioles of 10-day-old seedlings were observed by epifluorescence microscopy. Scale bar = 50 μm. (B) Eighteen-d-old

seedlings were subjected to immunoblot analysis using anti-GFP antibody. Transgenic plants expressing GFP alone (35S:GFP) were used as a control. The positions of NPH3.1-GFP, NPH3.2-GFP and GFP are indicated by black arrowhead, gray arrowhead and white arrowhead, respectively.

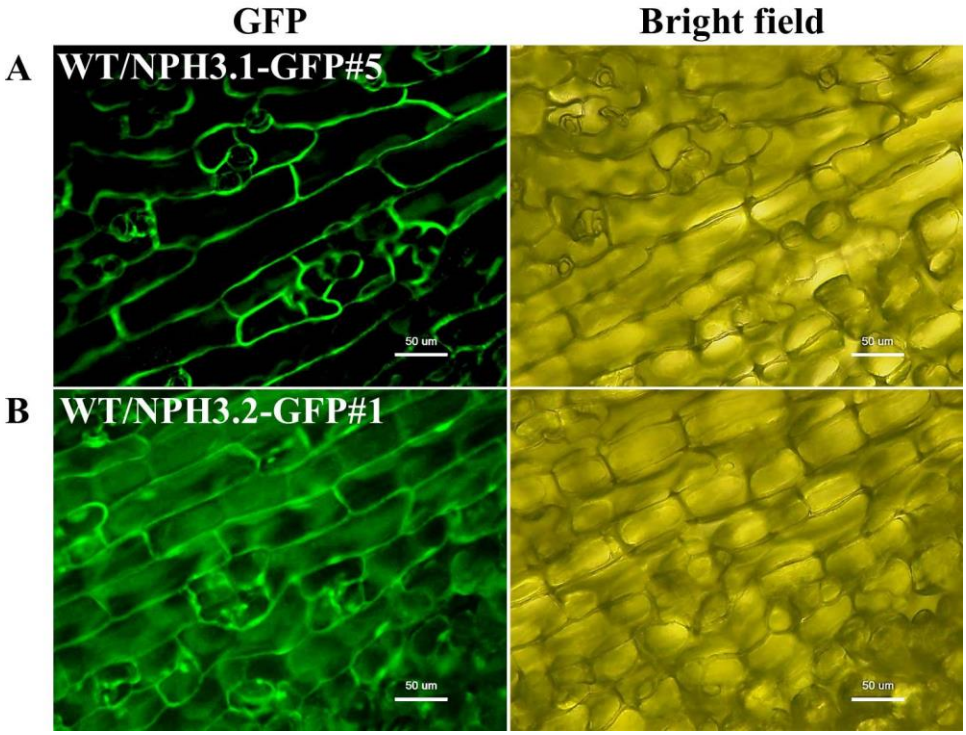

Figure 39. Subcellular localizations of NPH3.1 and NPH3.2 observed in NPH3 overexpression lines. Leaves of NPH3.1-GFP- or NPH3.2-GFP-overexpressing plants were observed by epifluorescence microscopy. (A) WT/NPH3.1-GFP#5. (B) WT/NPH3.2-GFP#1. Scale bar = 50 μm.

3.2.3.2 The involvement of NPH3 in BR signaling

The sensitivities of *nph3* mutant to brassinosteroid brassinolide and a BR biosynthesis inhibitor, brassinazole (BRZ), were examined. Brassinosteroids can promote hypocotyl elongation under light and dark conditions, but concentrations above 0.1 μM can inhibit growth in the dark (Neff *et al*.,1999; Vandenbussche *et al*., 2007). The relative hypocotyl lengths in the presence of 0.1 μM BR in the dark were in the order of WT < *agb1-2* = *nph3-7* < DM#1-1-2 = DM#11-1-2 showing significant differences (Fig. 40). BRZ inhibits hypocotyl elongation. The relative hypocotyl lengths in the presence of 1 μM BRZ in the dark were in the order of WT > *agb1-2* = *nph3-7* > DM#1-1-2 = DM#11-1-2 showing significant differences (Fig. 41). These data suggested that *agb1* and *nph3* mutants are hyposensitive to BR and hypersensitive to BRZ. The effect of AGB1 deficiency and the effect of NPH3 deficiency in *agb1/nph3* double mutants are additive in the presence of 0.1 μM BR (Fig. 40) or 1 μM BRZ (Fig. 41) in dark, suggesting that AGB1 and NPH3 function independently in BR signaling. The expression of *CPD*, which is a BR-responsive gene (He *et al*., 2005), was higher in *nph3-7* mutant than in the wild type (Fig. 42), which is consistent with the finding that *nph3* is hyposensitive to BR.

The expression levels and the phosphorylation states of NPH3 proteins in the absence or in the presence of 20 nM BR or 5 μM BRZ or 40 μM bikinin, which is a glycogen synthase kinase 3/SHAGGY-like protein kinases (GSKs) inhibitor (De Rybel *et al*., 2009), were examined using NPH3.1-GFP and NPH3.2-GFP overexpression lines. No difference was observed between the control and 20 nM BR or 5 μM BRZ or 40 μM bikini with respect to the expression levels and the phosphorylation states of the NPH3 proteins (Fig. 43 and 44).

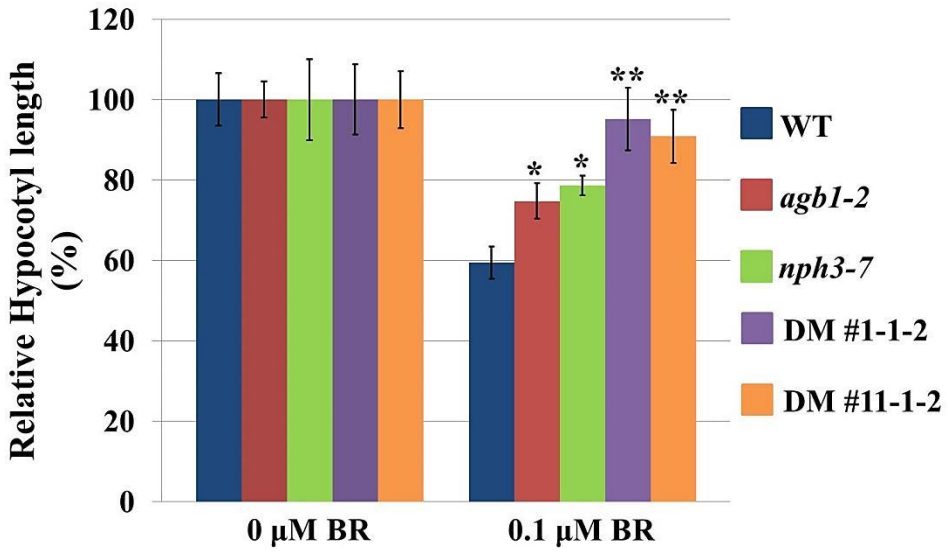

Figure 40. BR hyposensitivity of *nph3 mutant*. Plants were grown for 3 d in the dark in the presence of 0 or 0.1 µM BR. Relative hypocotyl lengths are shown. Values are means ±SE (n=7–20). *P < 0.05, **P < 0.005 vs. the WT by t test.

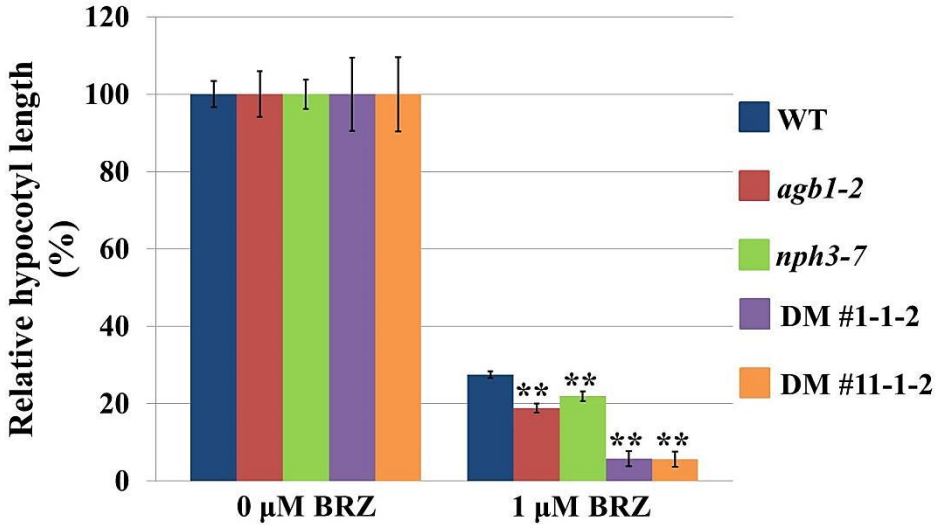

Figure 41. BRZ hypersensitivity of *nph3 mutant*. Plants were grown for 5 d in the dark in the presence of 0 or 1 μM BRZ. Relative hypocotyl lengths are shown. Values are means ±SE (*n*=18–20). ***P* < 0.005 vs. the WT by *t* test.

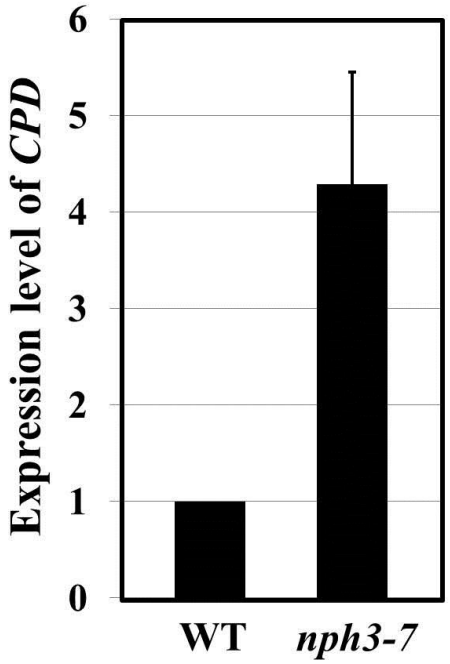

Figure 42. Expression of *CPD* gene in wild type and *nph3-7* mutant by real-time quantitative RT-PCR. Relative expression levels were calculated by the $\Delta\Delta C_T$ method using *Actin* as an internal control gene and wild type sample as a reference sample. Experiments were performed in triplicate. Values are means ±SD.

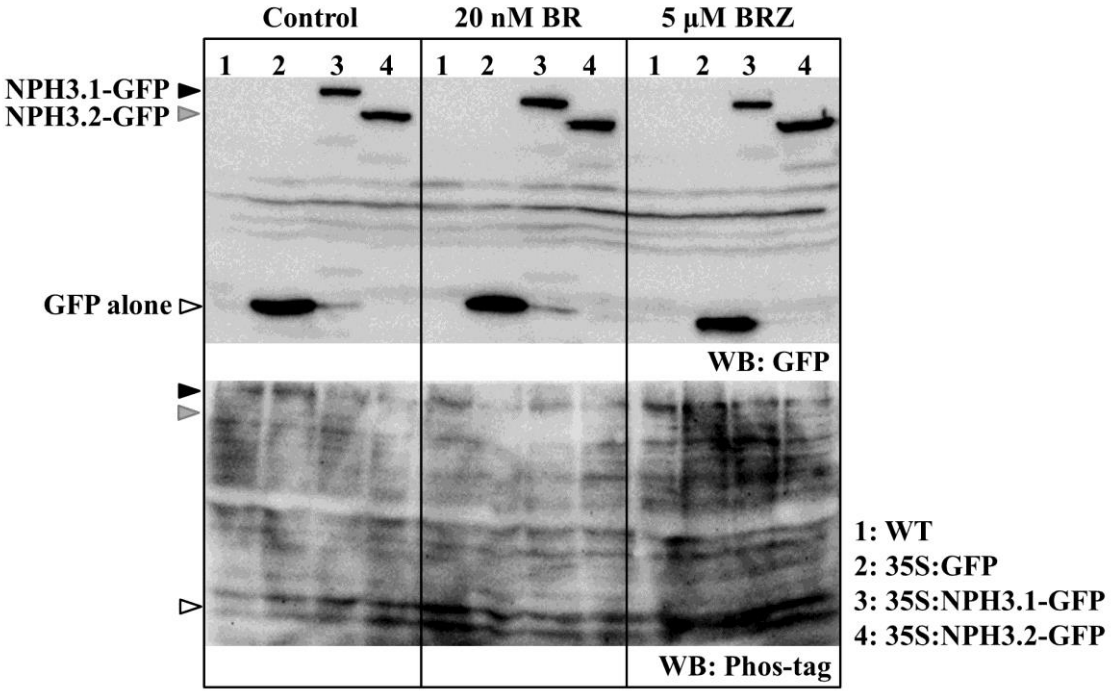

Figure 43. Immunoblot of NPH3.1-GFP and NPH3.2-GFP in the presence of BR or BRZ. Wild type, 35S:GFP, WT/35S:NPH3.1-GFP#5 and WT/35S:NPH3.2-GFP#1 were grown in the presence of 20 nM BR or 5 μM BRZ or in the absence of BR and BRZ (Control) for 12 d, and used for western blotting using an anti-GFP antibody (WB: GFP) or a Phos-tag (WB: Phos-tag). The positions of NPH3.1-GFP, NPH3.2-GFP and GFP are indicated by black arrowheads, gray arrowheads and white arrowheads, respectively.

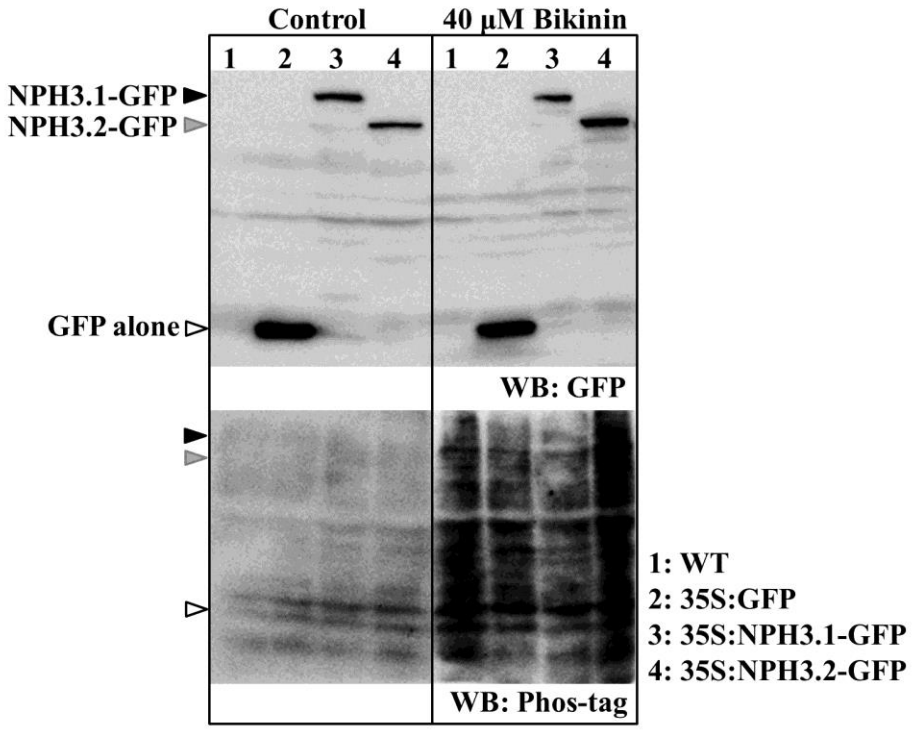

Figure 44. Immunoblot of NPH3.1-GFP and NPH3.2-GFP in the presence of bikinin. Wild type, 35S:GFP, WT/35S:NPH3.1-GFP#5 and WT/35S:NPH3.2-GFP#1 were grown in the presence of 0 (Control) or 40 μM bikinin for 15 d, and used for western blotting using an anti-GFP antibody (WB: GFP) or a Phos-tag (WB: Phos-tag). The positions of NPH3.1-GFP, NPH3.2-GFP and GFP are indicated by black arrowheads, gray arrowheads and white arrowheads, respectively.

3.2.3.3 NPH3.1 overexpression lines show ABA hyposensitive phenotypes in seed germination

To study whether NPH3 has the other functional roles in plants, *nph3* mutants and NPH3.1-GFP and NPH3.2-GFP overexpression lines were tested with various hormones and a biotic stress (flg22, an elicitor). No difference was observed between the wild type and *nph3* mutants or NPH3 overexpression lines in the presence of 10 μM 1-aminocyclopropane-1-carboxylic acid (ACC, metabolic precursor of ethylene) or 20 μM jasmonic acid (JA) or 5 μM gibberellic acid (GA3) or 1 mg/L flg22 (data not shown).

In the presence of 1.0 μM ABA, NPH3.1-GFP seeds germinated earlier than wild type seeds did (Fig. 45). However, the germination rates of *nph3* mutants and NPH3.2-GFP overexpression lines were similar to the germination rate of the wild type in the presence of 1.0 μM ABA (data not shown). The effect of ABA on the post-germination growth of seedlings was analyzed. No difference was observed between the wild type and *nph3* mutants or NPH3 overexpression lines in the presence of 1.0 μM ABA with respect to the greening rates (data not shown). The expression of *NPH3* gene was induced by ABA treatment (Fig. 46). These data suggested the possibility that NPH3 is involved in the ABA regulation of seed germination. AP-3μ does not affect the expression of *NPH3* gene (Fig. 46).

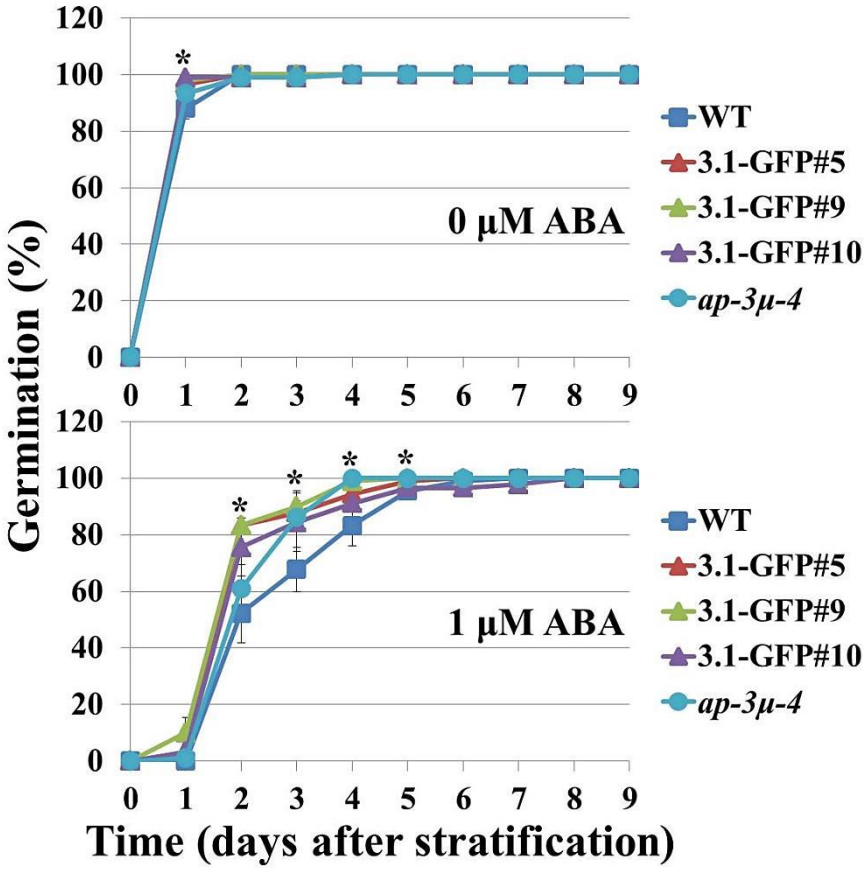

Figure 45. Seed germinations of NPH3.1 overexpression lines are hyposensitive to ABA. Germination rates of the wild type (WT) seeds and WT/NPH3.1-GFP#5, WT/NPH3.1-GFP#9 and WT/NPH3.1-GFP#10 overexpressing seeds and *ap-3µ-4* mutant seeds in the presence of 0 (A) or 1.0 µM ABA (B). Germinated seeds were counted at the indicated time points. The experiment was repeated three times and data were averaged. n = 30/genotype for each experiment. The error bars represent SD. **P* < 0.05 vs. the WT by *t* test.

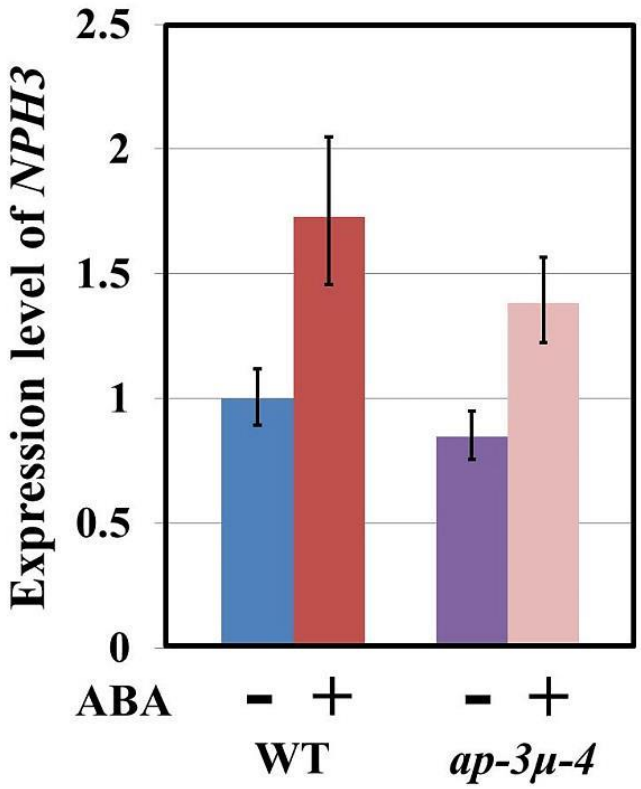

Figure 46. Expression of *NPH3* gene in wild-type and *ap-3μ-4* mutant by real-time quantitative RT-PCR. The sample of wild type in the absence of ABA (-ABA) was used as a reference sample. Relative expression levels were calculated by the $\Delta\Delta C_T$ method using *Actin* as an internal control gene. Experiments were performed in triplicate. Values are means ±SD. The wild type and *ap-3μ-4* mutant were grown on half-strength MS media with 0 (-ABA) or 1.0 μM ABA (+ABA) for 18 days and used for cDNA synthesis for RT-PCR.

3.2.4 Discussion

3.2.4.1 NPH3 is involved in brassinosteroid (BR) signaling independently of AGB1

The *nph3* mutants showed the altered sensitivities to BR and BRZ (Fig. 40, 41 and 42), suggesting that NPH3 is involved in BR signaling and functions as a positive regulator. The additive phenotypes of *agb1/nph3* double mutants in BR sensitivities (Fig. 40 and 41) suggest that AGB1 and NPH3 function independently in BR signaling. Western blot analysis revealed that the expression levels and the phosphorylation states of NPH3 proteins were not affected by BR, BRZ or bikinin (Fig. 43 and Fig. 44).

Light and BR antagonistically regulate the developmental switch from etiolation in the dark to photomorphogenesis in the light in plants. A group of proteins termed constitutive photomorphogenic/de-etiolated/fusca (COP/DET/FUS), which are components of the ubiquitination system, integrate light signal and downstream light-responsive gene expression (Kwok *et al*.,1996; Jiao *et al*., 2007). The E3 ligase COP1 targets positive regulators of photomorphogenesis, such as HYPOCOTYL5, LONG AFTER FAR-RED LIGHT1, and PHYTOCHROME A, for ubiquitin-mediated degradation by the 26S proteasome in order to repress photomorphogenic developmental processes, including hypocotyl elongation (Osterlund *et al*., 2000; Seo *et al*., 2003; Seo *et al*., 2004). On the contrary, BR-deficient mutants show typical de-etiolation phenotypes in the dark, with elevated expression of many light-induced genes (Chory *et al*., 1991; Szekeres *et al*., 1996; Song *et al*., 2009). Recently NPH3, which is carrying BTB domain, was found to function as a substrate adaptor in a CULLIN-based E3 ligase for ubiquitination and subsequent degradation of phototropin 1 (Roberts *et al*., 2011). In BR signaling, NPH3 may act as a substrate adaptor for ubiquitination of some positive regulators of photomorphogenesis.

3.2.4.2 NPH3 is involved in ABA signaling

The ABA hyposensitivities of NPH3.1 overexpression lines during seed germination (Fig. 45) and the induction of *NPH3* gene expression by ABA (Fig. 46) suggest that NPH3 is involved in the ABA regulation of seed germination. However, the altered sensitivity to ABA during seed germination was not observed in *nph3* mutants. This may due to functional redundancy of other members of the NRL family.

Alternatively, the overexpression of NPH3 causes the ABA hyposensitivity in an indirect manner. ABA enhances the activity of an auxin-responsive promoter in embryonic elongation zone and represses embryonic axis (radicle and hypocotyl) elongation by potentiating auxin, consequently represses seed germination and post-germination growth (Belin *et al*., 2009). *pin2* and *aux1* (AUXIN RESISTANT1; a cellular auxin influx carrier) mutants are insensitive to ABA-dependent repression of the embryonic axis elongation (Belin *et al*., 2009). NPH3 plays a role in PIN2 subcellular localization and consequently regulates blue light-induced auxin flux (Wan *et al*., 2012). The overexpression of NPH3.1 may cause the altered auxin flux leading to the ABA hyposensitivity.

To my knowledge, this study is the first report on the involvement of NPH3 in the regulation of seed germination by ABA. Further studies are needed to understand how NPH3 is involved in the ABA signaling and whether the involvement of NPH3 in the ABA signaling is mediated by AGB1.

Chapter 4

General Discussion

4.1 AGB1 regulates hormone signalings via AP-3μ and NPH3.

G proteins modulate many hormone responses, such as auxin, gibberellin (GA), abscisic acid (ABA) and brassinosteroid (BR). So far, only two G protein-interacting proteins, namely AtPIRIN1 and PLDα1, have been reported to function in ABA signaling. AtPIRIN1, which is a member of the cupin protein superfamily, binds GPA1 and negatively regulates ABA signaling in seed germination and early seedling development (Lapik and Kaufman, 2003; Warpeha *et al*., 2007). PLDα1, which is a major isoform of phospholipase D, binds GPA1 and positively regulates ABA-inhibited stomate opening (Zhao and Wang, 2004; Mishra *et al*., 2006). In this study, AP-3μ and NPH3 were identified as two novel AGB1-interacting proteins that are involved in ABA signaling. Furthermore, BIN2 is the only one protein which has been reported to interact with AGB1 and function in BR signaling (Klopffleisch *et al*., 2011; Tsugama *et al*., 2013b; Urano *et al*., 2013). Further studies to elucidate how NPH3 is involved in BR signaling will provide insights into the interaction between G proteins and BR signaling, as well as, the interaction between light and BR signaling.

Because AGB1 and NPH3 are involved in phototropism and BR signaling, the involvement of AP-3μ in these processes was examined. However, no difference was observed between the wild type and *ap-3μ* mutants in response to unilateral blue light (Fig. 47) or in the presence of 1.0 μM BRZ (Fig. 48), suggesting that AP-3μ is not involved in phototropism and BR signaling.

This study revealed that AGB1 specifically interacts with AP-3μ or NPH3

depending on the cues from the environment, and regulates many processes in plant, including ABA signaling, BR signaling and phototropism (Fig. 49). The interaction between AP-3μ and NPH3 was examined by BiFC assay. However, there was no interaction between them (data not shown). Further studies, such as yeast two-hybrid (Y2H) analysis and *in vitro* GST-pull down assay, are required to determine whether AP-3μ and NPH3 interact. Furthermore, the generation of *ap-3μ/nph3* double mutants may help to clarify whether AP-3μ and NPH3 function together in ABA signaling. Recently, the clathrin adaptor complex AP-2 was found to mediate endocytosis of BRASSINOSTEROID INSENSITIVE1 in Arabidopsis (Di Rubbo *et al*., 2013). In addition, the clathrin-mediated endocytosis has been linked to the regulation of auxin transport (Dhonukshe *et al*., 2007; Robert *et al*., 2010; Kitakura *et al*., 2011). AP-3μ may be involved in the endocytosis or the intracellular trafficking of the factors that function downstream of NPH3.

AGB1 interacts with NPH3 and regulates phototropism together with NPH3. However, in BR signaling, AGB1 and NPH3 function independently. It is unclear whether the involvement of NPH3 in ABA signaling is required the mediation of AGB1 (Table 6). The overexpression of NPH3 in *agb1* mutants may help to understand the mechanism.

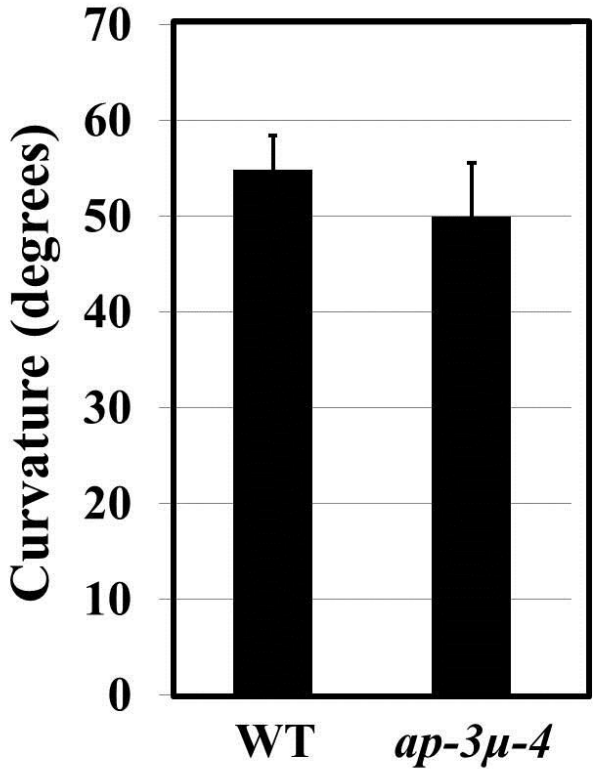

Figure 47. AP-3μ is not involved in phototropism. Hypocotyl phototropism in wild type and *ap-3μ-4* mutant exposed to 20 h of unilateral blue light. Values are means ± SE of 10 seedlings of each genotype.

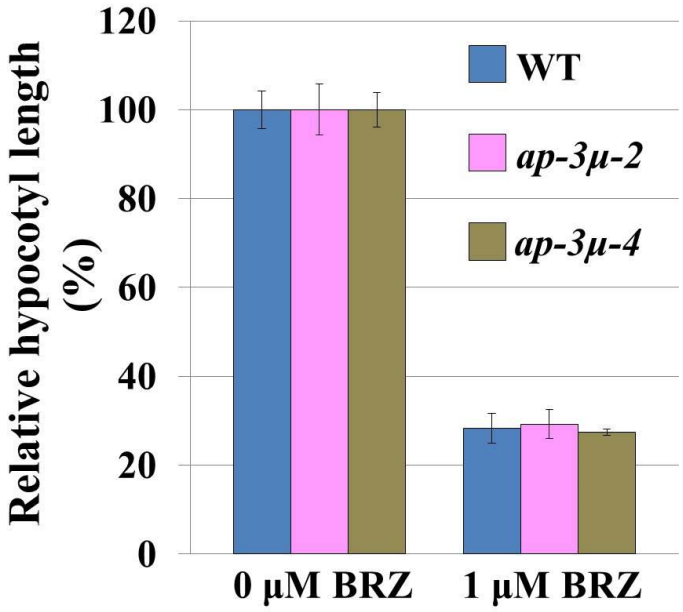

Figure 48. AP-3μ is not involved in BR signaling. The BRZ sensitivities of *ap-3μ* mutants are similar to that of the wild type. Plants were grown for 5 d in the dark in the presence of 0 or 1 μM BRZ. Relative hypocotyl lengths are shown. Values are means ±SE (*n* = 10–15).

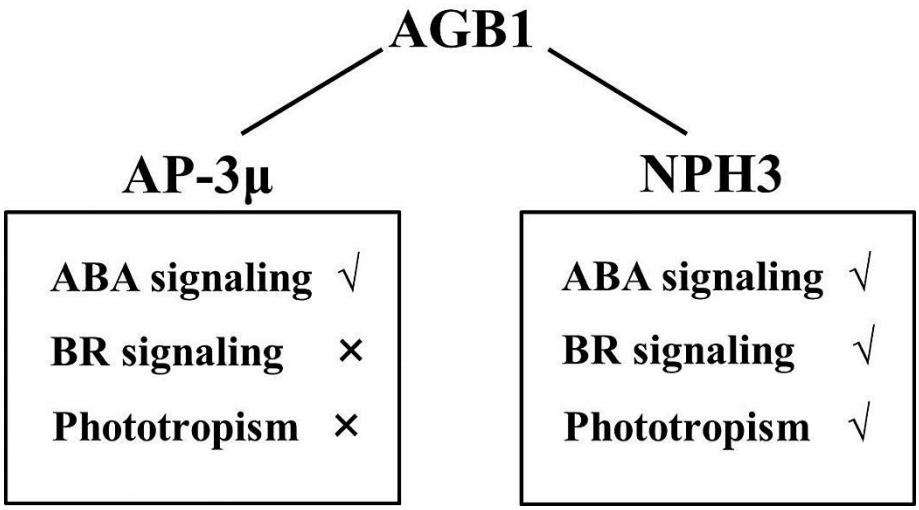

Figure 49. Schemes of functions of AGB1, AP-3μ and NPH3 proposed by this study.

Cellular process	The mediation of AGB1 to NPH3 function
ABA signaling	?
BR signaling	×
Phototropism	√

Table 6. The requirement of the mediation of AGB1 to NPH3 function depends on cellular processes.

4.2 The hormonal crosstalk between ABA and BR.

Phytohormones have essential roles in coordinately regulating a large array of developmental processes. Some studies have elucidated specific molecular mechanisms of hormonal crosstalk. They include the role of auxin and ethylene in regulating root meristem development (Teale *et al*., 2008), the antagonistic relationship between abscisic acid (ABA) and gibberellins (GAs) on seed dormancy and germination (Razem *et al*., 2006; Finkelstein *et al*., 2008), an integration of the primary signaling pathways of auxin and brassinosteroids (BRs) by auxin response factor 2 (ARF2) (Vert *et al*., 2008), and the combined actions between BR and auxin in shade avoidance response (Kozuka *et al*., 2010; Keuskamp *et al*., 2011). Compared with these combinations of hormonal cross-talk, the information about the molecular mechanism of the interaction between BR and ABA is scanter.

Studies have indicated that ABA is required to establish seed dormancy during embryo maturation and to inhibit seed germination (Finkelstein *et al*., 2008), whereas BRs promote seed germination, likely through enhancing the embryo growth potential to antagonize the effect of ABA (Leubner-Metzger, 2001; Steber and McCourt, 2001; Finkelstein *et al*., 2008). An established model of the BR signaling consists of specific types of protein kinases, protein phosphatases, and transcription factors. BRs are perceived by a cell surface receptor, BRI1, a leucine-rich-repeat receptor-like kinase. BRI1 binding to BR inactivates BIN2, a glycogen synthase kinase-3, and possibly activates the phosphatase BSU1. BIN2 negatively regulates transcription factors BZR1 and BES1 by phosphorylating them, while BSU1 positively regulates BR signaling by dephosphorylating BZR1 and BES1. The dephosphorylated BZR1 and BES1 regulate their target gene expression, which leads to BR responses (Wang *et al*., 2012 for review).

Analysis using biochemical and molecular markers of BR signaling and ABA biosynthetic mutants revealed that exogenous ABA rapidly inhibits BR signaling outputs as indicated by the phosphorylation status of BES1 and BR-responsive gene expression (Zhang *et al*., 2009).

Recently it was demonstrated that overexpression of BZR1 alleviated the effects of ABA in both the wild type and *agb1-1* (Tsugama *et al*., 2013b). However, AGB1 did not affect the phosphorylation state of BZR1 *in vivo*. AGB1 interacted with BIN2 *in vitro*, but did not affect the phosphorylation state of BIN2. These results suggest that AGB1 interacts with BIN2, but regulates the BR signaling in a BZR1-independent manner (Tsugama *et al*., 2013b). In this study, NPH3 was found to be a positive regulator of BR response and a negative regulator of ABA response, similar to AGB1 (Fig. 50). However, the function of NPH3 in these responses remains to be elucidated.

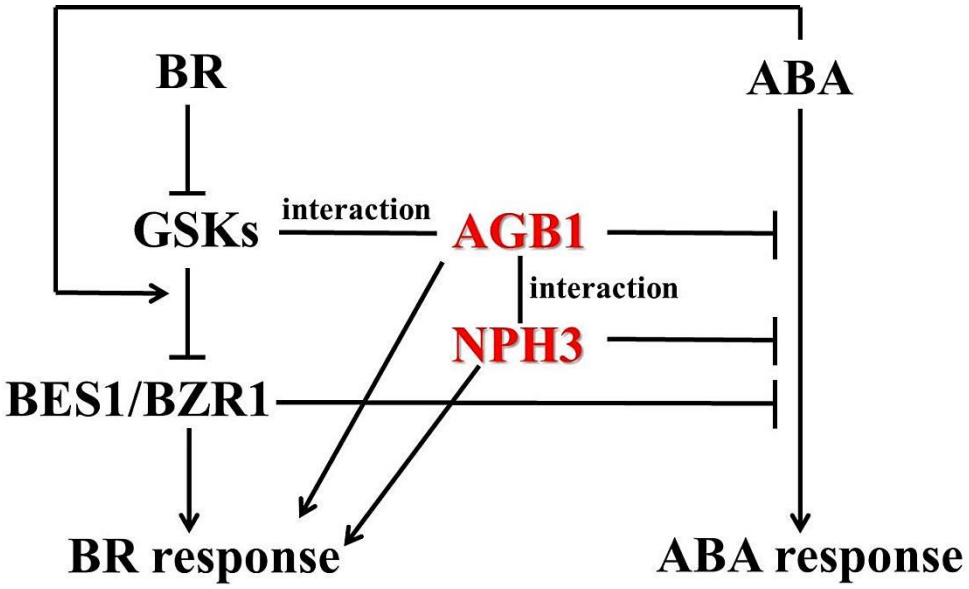

Figure 50. The involvement of AGB1 and NPH3 in BR and ABA signaling.

Chapter 5

General Summary

Heterotrimeric G proteins (G proteins) have been implicated in ubiquitous signaling mechanisms in eukaryotes. G proteins consist of three subunits, Gα, Gβ and Gγ. In animals, G proteins transmit the ligand-binding signals from G protein-coupled receptors (GPCRs) to downstream pathways to affect numerous cellular behaviours. In plants, G proteins have structural similarities to the corresponding molecules in animals but transmit signals by atypical mechanisms and effector proteins to modulate hormonal and stress responses, and regulate diverse developmental processes. However, the molecular mechanisms of their functions are largely unknown.

Gβ of Arabidopsis is named AGB1. *agb1-1* and *agb1-2*, which are the loss-of-function mutants of AGB1, show morphological aberrations (Lease *et al*., 2001; Ullah *et al*., 2001; Chen *et al*., 2004), an etiolated and light-grown phenotype under dark conditions (Ullah *et al*., 2003), increased stomatal density (Zhang L *et al*., 2008), altered phytohormone responsiveness (Pandey *et al*., 2006; Fan *et al*., 2008) and reduced responsiveness to pathogens (Trusov *et al*., 2006; Trusov *et al*., 2008). The multiple phenotypes of *agb1* mutants suggest that AGB1 is a key factor of several signaling pathways. Although the roles of AGB1 in plants are becoming clearer, the downstream effectors of AGB1 and other components of the AGB1 signaling pathways remain largely unknown. To identify interacting partners of AGB1, a yeast two-hybrid screen was performed (Tsugama *et al*., 2012a). Some novel interacting partners of AGB1 were identified, for example, a plasma membrane 2C-type protein phosphatase PP2C52 (Tsugama *et al*., 2012a; Liu *et al*., 2013), a U-box E3 ubiquitin ligase PUB20

(Kobayashi *et al*., 2012), and a bZIP protein VIP1, which is a regulator of osmosensory signaling (Tsugama *et al*., 2012b; Tsugama *et al*., 2013a).

In this study, two novel AGB1-interacting proteins, an adaptor protein 3μ (AP-3μ, At1g56590) and a phototropin-interacting protein nonphototropic hypocotyl 3 (NPH3, At5g64330), were functionally characterized. Furthermore, the physiological roles of the interaction between AGB1 and AP-3μ or NPH3 were examined.

1. The Arabidopsis adaptor protein AP-3μ interacts with the G protein β subunit AGB1 and is involved in abscisic acid regulation of germination and post-germination development.

AP-3μ (At1g56590) is an adaptor protein. Adaptor proteins (APs) are key regulators of endocytosis and secretory pathways. AP complexes (AP-1, AP-2, AP-3, AP-4, and AP-5) have been characterized so far in eukaryotes. The AP-3 complex consists of two large subunits (δ and β3), a medium subunit (μ3), and a small subunit (σ3) (Boehm and Bonifacino, 2002; Dell' Angelica, 2009). The interaction between AGB1 and AP-3μ was confirmed by an *in vitro* pull-down assay and bimolecular fluorescence complementation (BiFC) assay. When co-expressed in onion epidermal cells, GFP-fused AP-3μ (AP-3μ-GFP) was detected in the cytoplasm and nucleus, while mCherry-fused AGB1 (AGB1-mCherry) was detected in the cytoplasm, nucleus, and the plasma membrane, suggesting the possibility that AP-3μ and AGB1 are co-localized in the cytoplasm and nucleus.

Two *ap-3μ* T-DNA insertional mutants were obtained. The abscisic acid (ABA) sensitivities of *ap-3μ* mutants were examined. *ap-3μ* mutants were hyposensitive to ABA during germination and post-germination growth, whereas *agb1* mutants were

hypersensitive to ABA. To investigate the interaction between *AP-3μ* and *AGB1* at the genetic level, *agb1/ap-3μ* double mutants (DMs) were generated and the ABA sensitivities of them were examined. During seed germination, *agb1/ap-3μ* double mutants were more sensitive to ABA than the wild type but less sensitive than *agb1* mutants. However, in post-germination growth, the double mutants were as sensitive to ABA as *agb1* mutants. These data suggest that AP-3μ positively regulates the ABA responses independently of AGB1 in seed germination, while AP-3μ does require AGB1 to regulate ABA responses during post-germination growth.

Furthermore, mutants of AP-3δ subunit and clathrin heavy chain (CHC) were obtained. *ap-3δ* and *chc1* mutants showed ABA-hyposensitive phenotypes in post-germination growth, suggesting that AP-3δ and CHC, as well as AP-3μ, function in the ABA response during post-germination growth.

2. Studies on Nonphototropic hypocotyl 3 (NPH3)

2.1 Arabidopsis G protein β subunit AGB1 interacts with Nonphototropic hypocotyl 3 (NPH3) and is involved in phototropism.

(NPH3, At5g64330) is a phototropin-interacting protein and is required for the phototropic response, leaf positioning and leaf flattening (Motchoulski and Liscum, 1999; Inoue *et al*., 2008). The interaction between AGB1 and NPH3 was confirmed by an *in vitro* pull-down assay, a bimolecular fluorescence complementation assay in onion epidermal cells, and an *in vivo* co-immunoprecipitation using *Brassica rapa* var. *perviridis* leaves. Two novel *nph3* T-DNA insertional mutants were obtained and their non-phototropic phenotypes were confirmed by exposure of unilateral blue light. On the contrary, *agb1* mutants showed a smaller phototropic response than the wild type. To

investigate the interaction between *NPH3* and *AGB1* at the genetic level, *agb1/nph3* double mutants were generated. *agb1/nph3* double mutants displayed non-phototropic phenotypes similar to those of *nph3* mutants. These data suggest that AGB1 function is required for normal phototropism and that AGB1 and NPH3 function in the same pathway during the phototropic response. The expression level of *AGB1* gene was lower in the *nph3* mutants than in the wild type, raising the possibility that NPH3 positively regulates the expression of *AGB1* gene.

It is known that in dark-grown seedlings, NPH3 exists as a phosphorylated protein and blue light stimulates its dephosphorylation (Pedmale and Liscum, 2007; Tsuchida-Mayama *et al*., 2008). This post-translational modification represents a crucial event in phot1-dependent phototropism (Pedmale and Liscum, 2007; Tsuchida-Mayama *et al*., 2008). To study whether AGB1 is involved in the phosphorylation state changes of NPH3, the phosphorylation state of NPH3 in the presence of crude protein extracted from the wild type or *agb1-2* mutant using GST-fused NPH3 proteins were examined. However, the phosphorylated GST-fused NPH3 proteins were not detected in the presence of crude proteins extracted from the wild type or *agb1-2* mutant in light or dark condition. This may due to the excessive amount of GST-fused NPH3 proteins in the mixture and the activity of kinase in the crude proteins extracted from the wild type or *agb1-2* mutant is insufficient for the amount. Alternatively, AGB1 is not involved in regulating the phosphorylation state of NPH3.

NPH3 regulates auxin polar transport as a downstream step in phototropic responses (Roberts *et al*., 2011; Sakai and Haga, 2012; Wan *et al*., 2012), and AGB1 is involved in regulating auxin responses and/or transport (Lease *et al*., 2001; Ullah *et al*., 2003; Mudgil *et al*., 2009). Thus, AGB1 might play a role in the NPH3-dependent

regulation of auxin polar transport.

To my knowledge, this is the first report on the involvement of AGB1 in phototropism. However, further studies are needed to understand how AGB1 is involved in the NPH3-mediated regulation of phototropism.

2.2 The involvement of NPH3 in hormonal responses

In my study, NPH3 was found to be an interacting partner of Arabidopsis G protein β subunit AGB1, which plays roles in many hormonal signalings, such as auxin, abscisic acid (ABA) and brassinosteroid (BR). Functional role of NPH3 in the hormonal signaling is poorly understood. In this part, the subcellular localization and the function of NPH3 in hormone responses were characterized.

Transient and stable subcellular localization analysis confirmed the plasma membrane localization of NPH3. *nph3* mutants exhibit BR hyposensitivities and BRZ hypersensitivities similar to *agb1* mutants. However, *agb1/nph3* double mutants show additive phenotypes in the BR hyposensitivities and the BRZ hypersensitivities, suggesting that NPH3 is involved in brassinosteroid (BR) signaling independently of AGB1. NPH3 overexpression lines show ABA hyposensitivity during seed germination. Furthermore, the expression of NPH3 is induced by ABA. These data suggest that NPH3 is involved in the ABA regulation of seed germination. The functional roles of NPH3 in BR signaling and ABA signaling are discussed.

Acknowledgement

I would like to express my deepest appreciation to my supervisor, Professor Dr. Tetsuo Takano, for his valuable guidance, generous assistance in monitoring this research study and gentle encouragement I received throughout the research work. His support through continuous discussion from the initial to the final level enabled me to develop an understanding of my research.

I am heartily thankful to the entire member of Laboratory of Environmental Stress Tolerance Mechanism, for the assistance they provided at all levels of my research and also for kindness and hospitality during my study in Japan.

I am deeply grateful to my colleagues in Biotechnology Research and Development Office, Department of Agriculture (Thailand), for their support through my study. I would also like to thank my family for support, encouragement and love they provided me through my entire life.

Lastly, I offer my regards and blessing to all of those who supported me in any respect during the completion of this research.

References

Adjobo-Hermans MJ, Goedhart J, Gadella TW Jr. 2006. Plant G protein heterotrimers require dual lipidation motifs of Galpha and Ggamma and do not dissociate upon activation. Journal of Cell Science 119, 5087-5097.

Alvarez S, Roy Choudhury S, Hicks LM, Pandey S. 2013. Quantitative proteomics-based analysis supports a significant role of GTG proteins in regulation of ABA response in Arabidopsis roots. Journal of Proteome Research 12, 1487-1501.

Anderson DJ, Botella JR. 2007. Expression analysis and subcellular localization of the Arabidopsis thaliana G-protein beta-subunit AGB1. Plant Cell Reports 26, 1469-1480.

Arshavsky VY, Lamb TD, Pugh EN Jr. 2002. G proteins and phototransduction. Annual Review of Physiology 64, 153-187.

Ballaré CL, Casal JJ, Kendrick RE. 1991. Responses of light-grown wild-type and long-hypocotyl mutant cucumber seedlings to natural and simulated shade light. Photochemistry and Photobiology 54, 819–826.

Bassham DC, Brandizzi F, Otegui MS, Sanderfoot AA. 2008. The secretory system of Arabidopsis. The Arabidopsis Book. 6, e0116.

Belin C, Megies C, Hauserová E, Lopez-Molina L. 2009. Abscisic acid represses growth of the Arabidopsis embryonic axis after germination by enhancing auxin signaling. The Plant Cell 21, 2253-2268.

Bisht NC, Jez JM, Pandey S. 2010. An elaborate heterotrimeric G-protein family from soybean expands the diversity of plant G-protein networks. New Phytologist 190, 35-48.

Boehm M, Bonifacino JS. 2002. Genetic analyses of adaptin function from yeast to mammals. Gene 286, 175-186.

Botto JF, Ibarra S, Jones AM. 2009. The heterotrimeric G-protein complex modulates light sensitivity in Arabidopsis thaliana seed germination. Photochemistry and

Photobiology 85, 949-954.

Busk PK, Pagès M. 1998. Regulation of abscisic acid-induce transcription. Plant Molecular Biology 37, 425-435.

Chakravorty D, Trusov Y, Zhang W, Acharya BR, Sheahan MB, McCurdy DW, Assmann SM, Botella JR. 2011. An atypical heterotrimeric G-protein γ-subunit is involved in guard cell K^+-channel regulation and morphological development in Arabidopsis thaliana. The Plant Journal 5, 840-851.

Chen JG, Pandey S, Huang J, Alonso JM, Ecker JR, Assmann SM, Jones AM. 2004. GCR1 can act independently of heterotrimeric G-protein in response to brassinosteroids and gibberellins in Arabidopsis seed germination. Plant Physiology 135, 907-915.

Chen JG. 2008. Heterotrimeric G-proteins in plant development. Frontiers in Bioscience 13, 3321-3333.

Chomczynski P, Sacchi N. 1987. Single-step method of RNA isolation by acid guanidinium thiocyanate–phenol–chloroform extraction. Analytical Biochemistry 162, 156–159.

Chory J, Nagpal P, Peto CA. 1991. Phenotypic and Genetic Analysis of det2, a New Mutant That Affects Light-Regulated Seedling Development in Arabidopsis. The Plant Cell 3, 445-459.

Choudhury SR, Bisht NC, Thompson R, Todorov O, Pandey S. 2011. Conventional and novel Gγ protein families constitute the heterotrimeric G-protein signaling network in soybean. PLOS ONE 6, e23361.

Clough SJ, Bent AF. 1998. Floral dip: a simplified method for Agrobacterium-mediated transformation of Arabidopsis thaliana. The Plant Journal 16, 735-743.

Clouse SD. 2011. Brassinosteroids. The Arabidopsis book 9, e0151.

Cowles CR, Odorizzi G, Payne GS, Emr SD. 1997. The AP-3 adaptor complex is essential for cargo-selective transport to the yeast vacuole. Cell 91, 109-118.

Dell'Angelica EC, Ohno H, Ooi CE, Rabinovich E, Roche KW, Bonifacino JS. 1997. AP-3: an adaptor-like protein complex with ubiquitous expression. The EMBO Journal 16, 917-928.

Dell'Angelica EC. 2009. AP-3 dependent trafficking and disease: The first decade. Current Opinion in Cell Biology 21, 552–559.

De Rybel B, Audenaert D, Vert G, Rozhon W, Mayerhofer J, Peelman F, Coutuer S, Denayer T, Jansen L, Nguyen L, Vanhoutte I, Beemster GT, Vleminckx K, Jonak C, Chory J, Inzé D, Russinova E, Beeckman T. 2009. Chemical inhibition of a subset of Arabidopsis thaliana GSK3-like kinases activates brassinosteroid signaling. Chemistry and Biology 16, 594-604.

Dhonukshe P, Aniento F, Hwang I, Robinson DG, Mravec J, Stierhof YD, Friml J. 2007. Clathrin-mediated constitutive endocytosis of PIN auxin efflux carriers in Arabidopsis. Current Biology 17, 520-527.

Di Rubbo S, Irani NG, Kim SY, Xu ZY, Gadeyne A, Dejonghe W, Vanhoutte I, Persiau G, Eeckhout D, Simon S, Song K, Kleine-Vehn J, Friml J, De Jaeger G, Van Damme D, Hwang I, Russinova E. 2013. The clathrin adaptor complex AP-2 mediates endocytosis of brassinosteroid insensitive1 in Arabidopsis. The Plant Cell 25, 2986-2997.

Djakovic-Petrovic T, Wit MD, Voesenek LACJ, Pierik R. 2007. DELLA protein function in growth responses to canopy signals. The Plant Journal 51, 117–126.

Fan LM, Zhang W, Chen JG, Taylor JP, Jones AM. 2008. Abscisic acid regulation of guard-cell K+ and anion channels in Gβ- and RGS-deficient Arabidopsis lines. Proceedings of the National Academy of Sciences of the United States of America 105, 8476–8481.

Feraru E, Paciorek T, Feraru MI, Zwiewka M, De Groodt R, De Rycke R, Kleine-Vehn J, Friml J. 2010. The AP-3 β adaptin mediates the biogenesis and function of lytic vacuoles in Arabidopsis. The Plant Cell 22, 2812-2824.

Ferguson SS, Downey WE 3rd, Colapietro AM, Barak LS, Ménard L, Caron MG. 1996.

Role of β-arrestin in mediating agonist-promoted G protein-coupled receptor internalization. Science 271, 363-366.

Finkelstein R, Reeves W, Ariizumi T, Steber C. 2008. Molecular aspects of seed dormancy. Annual Review of Plant Physiology 59, 387-415.

Friedman EJ, Wang HX, Jiang K, Perovic I, Deshpande A, Pochapsky TC, Temple BR, Hicks SN, Harden TK, Jones AM. 2011. Acireductone dioxygenase 1 (ARD1) is an effector of the heterotrimeric G protein β subunit in Arabidopsis. The Journal of Biological Chemistry 286, 30107-30118.

Fukaki H, Okushima Y, Tasaka M. 2007. Auxin-mediated lateral root formation in higher plants. International Review of Cytology 256, 111-137.

Gao Y, Wang S, Asami T, Chen JG. 2008. Loss-of-function mutations in the Arabidopsis heterotrimeric G-protein alpha subunit enhance the developmental defects of brassinosteroid signaling and biosynthesis mutants. Plant and Cell Physiology 49, 1013-1024.

Garciarrubio A, Legaria JP, Covarrubias AA. 1997. Abscisic acid inhibits germination of mature Arabidopsis seeds by limiting the availability of energy and nutrients. Planta 203, 182 – 187.

Gookin TE, Kim J, Assmann SM. 2008. Whole proteome identification of plant candidate G-protein coupled receptors in Arabidopsis, rice, and poplar: computational prediction and in-vivo protein coupling. Genome Biology 9, R120.

He JX, Gendron JM, Sun Y, Gampala SS, Gendron N, Sun CQ, Wang ZY. 2005. BZR1 is a transcriptional repressor with dual roles in brassinosteroid homeostasis and growth responses. Science 307, 1634-1638.

Holland JJ, Roberts D, Liscum E. 2009. Understanding phototropism: from Darwin to today. Journal of Experimental Botany 60, 1969-1978.

Inoue S, Kinoshita T, Takemiya A, Doi M, Shimazaki K. 2008. Leaf positioning of Arabidopsis in response to blue light. Molecular Plant 1, 15-26.

Jiao Y, Lau OS, Deng XW. 2007. Light-regulated transcriptional networks in higher plants. Nature Reviews Genetics 8, 217-230.

Jones AM, Assmann SM. 2004. Plants: the latest model system for G-protein research. EMBO reports 6, 572-578.

Kansup J, Tsugama D, Liu S, Takano T. 2013. The Arabidopsis adaptor protein AP-3μ interacts with the G-protein β subunit AGB1 and is involved in abscisic acid regulation of germination and post-germination development. Journal of Experimental Botany 64, 5611-5621.

Kansup J, Tsugama D, Liu S, Takano T. 2014. Arabidopsis G-protein β subunit AGB1 interacts with NPH3 and is involved in phototropism. Biochemical and Biophysical Research Communications. [In press, DOI: 10.1016/j.bbrc.2014.01.106]

Keuskamp DH, Sasidharan R, Vos I, Peeters AJ, Voesenek LA, Pierik R. 2011. Blue-light-mediated shade avoidance requires combined auxin and brassinosteroid action in Arabidopsis seedlings. The Plant Journal 67, 208-217.

Kinoshita E, Kinoshita-Kikuta E, Takiyama K, Koike T. 2006. Phosphate-binding tag, a new tool to visualize phosphorylated proteins. Molecular and Cellular Proteomics 5, 749-757.

Kitakura S, Vanneste S, Robert S, Löfke C, Teichmann T, Tanaka H, Friml J. 2011. Clathrin mediates endocytosis and polar distribution of PIN auxin transporters in Arabidopsis. The Plant Cell 23, 1920-1931.

Klopffleisch K, Phan N, Augustin K, Bayne RS, Booker KS, Botella JR, Carpita NC, Carr T, Chen JG, Cooke TR, Frick-Cheng A, Friedman EJ, Fulk B, Hahn MG, Jiang K, Jorda L, Kruppe L, Liu C, Lorek J, McCann MC, Molina A, Moriyama EN, Mukhtar MS, Mudgil Y, Pattathil S, Schwarz J, Seta S, Tan M, Temp U, Trusov Y, Urano D, Welter B, Yang J, Panstruga R, Uhrig JF, Jones AM. 2011. Arabidopsis G-protein interactome reveals connections to cell wall carbohydrates and morphogenesis. Molecular Systems Biology 7, 532.

Knauer T, Dümmer M, Landgraf F, Forreiter C. 2011. A negative effector of blue light-induced and gravitropic bending in Arabidopsis. Plant Physiology 156, 439-447.

Kobayashi S, Tsugama D, Liu S, Takano T. 2012. A U-Box E3 Ubiquitin Ligase, PUB20, interacts with the Arabidopsis G-Protein β Subunit, AGB1. PLoS One 7, e49207.

Kozuka T, Kobayashi J, Horiguchi G, Demura T, Sakakibara H, Tsukaya H, Nagatani A. 2010. Involvement of auxin and brassinosteroid in the regulation of petiole elongation under the shade. Plant Physiology 153, 1608-1618.

Kretzschmar D, Poeck B, Roth H, Ernst R, Keller A, Porsch M, Strauss R, Pflugfelder GO. 2000. Defective pigment granule biogenesis and aberrant behavior caused by mutations in the Drosophila AP-3beta adaptin gene ruby. Genetics 155, 213-223.

Kwok SF, Piekos B, Misera S, Deng XW. 1996. A complement of ten essential and pleiotropic arabidopsis COP/DET/FUS genes is necessary for repression of photomorphogenesis in darkness. Plant Physiology 110, 731-742.

Lapik YR, Kaufman LS. 2003. The Arabidopsis cupin domain protein AtPirin1 interacts with the G protein alpha-subunit GPA1 and regulates seed germination and early seedling development. The Plant Cell 15, 1578-1590.

Lease KA, Wen J, Li J, Doke JT, Liscum E, Walker JC. 2001. A mutant Arabidopsis heterotrimeric G-protein β subunit affects leaf, flower and fruit development. The Plant Cell 13, 2631–2641.

Lefkowitz RJ. 2004. Historical review: a brief history and personal retrospective of seven-transmembrane receptors. Trends in Pharmacological Sciences 25, 413-422.

Leubner-Metzger G. 2001. Brassinosteroids and gibberellins promote tobacco seed germination by distinct pathways. Planta 213, 758-763.

Leung J, Giraudat J. 1998. ABSCISIC ACID SIGNAL TRANSDUCTION. Annual Review of Plant Physiology and Plant Molecular Biology 49, 199-222.

Liu H, Tsugama D, Liu S, Takano T. 2013. Functional analysis of a type-2C protein

phosphatase (AtPP2C52) in Arabidopsis thaliana. Genomics and Applied Biology 4, 1-7.

Ma H, Yanofsky MF, Meyerowitz EM. 1990. Molecular cloning and characterization of GPA1, a G protein α subunit gene from Arabidopsis thaliana. Proceedings of the National Academy of Sciences of the United States of America 87, 3821-3825.

Mason MG, Botella JR. 2000. Completing the heterotrimer: Isolation and characterization of an Arabidopsis thaliana G protein γ-subunit cDNA. Proceedings of the National Academy of Sciences of the United States of America 97, 14784-14788.

Mason MG, Botella JR. 2001. Isolation of a novel G protein γ-subunit from Arabidopsis thaliana and its interaction with Gβ. Biochimica *et* Biophysica Acta 1520, 147-153.

McMahon HT, Boucrot E. 2011. Molecular mechanism and physiological functions of clathrin-mediated endocytosis. Nature Reviews Molecular Cell Biology 12, 517-533.

Mishra G, Zhang W, Deng F, Zhao J, Wang X. 2006. A bifurcating pathway directs abscisic acid effects on stomatal closure and opening in Arabidopsis. Science 312, 264-266.

Motchoulski A, Liscum E. 1999. Arabidopsis NPH3: A NPH1 photoreceptor-interacting protein essential for phototropism. Science 286, 961-964.

Mudgil Y, Uhrig JF, Zhou J, Temple B, Jiang K, Jones AM. 2009. Arabidopsis N-MYC DOWNREGULATED-LIKE1, a positive regulator of auxin transport in a G protein-mediated pathway. The Plant Cell 21, 3591-3609.

Neff MM, Nguyen SM, Malancharuvil EJ, Fujioka S, Noguchi T, Seto H, Tsubuki M, Honda T, Takatsuto S, Yoshida S, Chory J. 1999. BAS1: A gene regulating brassinosteroid levels and light responsiveness in Arabidopsis. Proceedings of the National Academy of Sciences of the United States of America 96, 15316-15323.

Niihama M, Takemoto N, Hashiguchi Y, Tasaka M, Morita MT. 2009. ZIP genes encode proteins involved in membrane trafficking of the TGN-PVC/vacuoles. Plant and Cell Physiology 50, 2057-2068.

Nishimura N, Yoshida T, Kitahata N, Asami T, Shinozaki K, Hirayama T. 2007. ABA-Hypersensitive Germination1 encodes a protein phosphatase 2C, an essential component of abscisic acid signaling in Arabidopsis seed. The Plant Journal 50, 935-949.

Osterlund MT, Hardtke CS, Wei N, Deng XW. 2000. Targeted destabilization of HY5 during light-regulated development of Arabidopsis. Nature 405, 462-466.

Owen DJ, Evans PR. 1998. A structural explanation for the recognition of tyrosine-based endocytotic signals. Science 282, 1327-1332.

Pandey S, Chen JG, Jones AM, Assmann SM. 2006. G-protein complex mutants are hypersensitive to abscisic acid regulation of germination and postgermination development. Plant Physiology 141, 243-256.

Pandey S, Nelson DC, Assmann SM. 2009. Two novel GPCR-type G proteins are abscisic acid receptors in Arabidopsis. Cell 136, 136-148.

Pedmale UV, Celaya RB, Liscum E. 2010. Phototropism: mechanism and outcomes. Arabidopsis Book. 8:e0125. doi: 10.1199/tab.0125.

Pedmale UV, Liscum E. 2007. Regulation of phototropic signaling in Arabidopsis via phosphorylation state changes in the phototropin 1-interacting protein NPH3. Journal of Biological Chemistry 282, 19992-20001.

Pierce KL, Premont RT, Lefkowitz RJ. 2002. Seven-transmembrane receptors. Nature Reviews Molecular Cell Biology 3, 639-650.

Pierik R, Djakovic-Petrovic T, Keuskamp DH, De Wit M, Voesenek LACJ. 2009. Auxin and ethylene regulate elongation responses to neighbor proximity signals independent of gibberellin and DELLA proteins in *Arabidopsis.* Plant Physiology 149, 1701–1712.

Razem FA, Baron K, Hill RD. 2006. Turning on gibberellin and abscisic acid signaling. Current Opinion in Plant Biology 9, 454-459.

Roberts D, Pedmale UV, Morrow J, Sachdev S, Lechner E, Tang X, Zheng N, Hannink M, Genschik P, Liscum E. 2011. Modulation of phototropic responsiveness in Arabidopsis through ubiquitination of phototropin 1 by the CUL3-Ring E3 ubiquitin ligase CRL3(NPH3). The Plant Cell 23, 3627-3640.

Robert S, Kleine-Vehn J, Barbez E, Sauer M, Paciorek T, Baster P, Vanneste S, Zhang J, Simon S, Čovanová M, Hayashi K, Dhonukshe P, Yang Z, Bednarek SY, Jones AM, Luschnig C, Aniento F, Zažímalová E, Friml J. 2010. ABP1 mediates auxin inhibition of clathrin-dependent endocytosis in Arabidopsis. Cell 143, 111-121.

Sakai T, Haga K. 2012. Molecular genetic analysis of phototropism in Arabidopsis. Plant and Cell Physiology 53, 1517-1534.

Sanmartín M, Ordóñez A, Sohn EJ, Robert S, Sánchez-Serrano JJ, Surpin MA, Raikhel NV, Rojo E. 2007. Divergent functions of VTI12 and VTI11 in trafficking to storage and lytic vacuoles in Arabidopsis. Proceedings of the National Academy of Sciences of the United States of America 104, 3645-3650.

Schmid EM, Ford MG, Burtey A, Praefcke GJ, Peak-Chew SY, Mills IG, Benmerah A, McMahon HT. 2006. Role of the AP2 β - appendage hub in recruiting partners for clathrin-coated vesicle assembly. PLoS Biology 4, e262.

Scita G, Di Fiore PP. 2010. The endocytic matrix. Nature 463, 464-473.

Seki M, Narusaka M, Kamiya A, Ishida J, Satou M, Sakurai T, Nakajima M, Enju A, Akiyama K, Oono Y, Muramatsu M, Hayashizaki Y, Kawai J, Carninci P, Itoh M, Ishii Y, Arakawa T, Shibata K, Shinagawa A, Shinozaki K. 2002. Functional annotation of a full-length Arabidopsis cDNA collection. Science 296, 141-145.

Seo HS, Watanabe E, Tokutomi S, Nagatani A, Chua NH. 2004. Photoreceptor ubiquitination by COP1 E3 ligase desensitizes phytochrome A signaling. Genes and Development 18, 617-622.

Seo HS, Yang JY, Ishikawa M, Bolle C, Ballesteros ML, Chua NH. 2003. LAF1 ubiquitination by COP1 controls photomorphogenesis and is stimulated by SPA1. Nature 423, 995-999.

Song L, Zhou XY, Li L, Xue LJ, Yang X, Xue HW. 2009. Genome-wide analysis revealed the complex regulatory network of brassinosteroid effects in photomorphogenesis. Molecular Plant 2, 755-772.

Sorkin A, von Zastrow M. 2009. Endocytosis and signalling: intertwining molecular networks. Nature Reviews Molecular Cell Biology 10, 609-622.

Steber CM, McCourt P. 2001. A role for brassinosteroids in germination in Arabidopsis. Plant Physiology 125, 763-769.

Stepp JD, Huang K, Lemmon SK. 1997. The yeast adaptor protein complex, AP-3, is essential for the efficient delivery of alkaline phosphatase by the alternate pathway to the vacuole. The Journal of Cell Biology 139, 1761-1774.

Szekeres M, Németh K, Koncz-Kálmán Z, Mathur J, Kauschmann A, Altmann T, Rédei GP, Nagy F, Schell J, Koncz C. 1996. Brassinosteroids rescue the deficiency of CYP90, a cytochrome P450, controlling cell elongation and de-etiolation in Arabidopsis. Cell 85, 171-182.

Teale WD, Ditengou FA, Dovzhenko AD, Li X, Molendijk AM, Ruperti B, Paponov I, Palme K. 2008. Auxin as a model for the integration of hormonal signal processing and transduction. Molecular Plant 1, 229-237.

Trusov Y, Rookes JE, Chakravorty D, Armour D, Schenk PM, Botella JR. 2006. Heterotrimeric G proteins facilitate Arabidopsis resistance to necrotrophic pathogens and are involved in jasmonate signaling. Plant Physiology 140, 210-220.

Trusov Y, Sewelam N, Rookes JE, Kunkel M, Nowak E, Schenk PM, Botella JR. 2008. Heterotrimeric G proteins-mediated resistance to necrotrophic pathogens includes mechanisms independent of salicylic acid-, jasmonic acid/ethyleneand abscisic acid-mediated defense signaling. Plant Journal 58, 69–81.

Tsuchida-Mayama T, Nakano M, Uehara Y, Sano M, Fujisawa N, Okada K, Sakai T. 2008. Mapping of the phosphorylation sites on the phototropic signal transducer, NPH3. Plant Science 174, 626–633.

Tsugama D, Liu H, Liu S, Takano T. 2012a. Arabidopsis heterotrimeric G protein β subunit interacts with a plasma membrane 2C-type protein phosphatase, PP2C52. Biochimica et Biophysica Acta 1823, 2254-2260.

Tsugama D, Liu S, Takano T. 2012b. A bZIP protein, VIP1, is a regulator of osmosensory signaling in Arabidopsis. Plant Physiology 159, 144-155.

Tsugama D, Liu S, Takano T. 2012c. A putative myristoylated 2C-type protein phosphatase, PP2C74, interacts with SnRK1 in Arabidopsis. FEBS Letters 586, 693-698.

Tsugama D, Liu S, Takano T. 2013a. A bZIP protein, VIP1, interacts with Arabidopsis heterotrimeric G protein β subunit, AGB1. Plant Physiology and Biochemistry 9, 240-246.

Tsugama D, Liu S, Takano T. 2013b. Arabidopsis heterotrimeric G protein β subunit, AGB1, regulates brassinosteroid signalling independently of BZR1. Journal of Experimental Botany 64, 3213-3223.

Ullah H, Chen JG, Temple B, Boyes DC, Alonso JM, Davis KR, Ecker JR, Jones AM. 2003. The β-subunit of the Arabidopsis G protein negatively regulates auxin-induced cell division and affects multiple developmental processes. The Plant Cell 15, 393-409.

Ullah H, Chen JG, Wang S, Jones AM. 2002. Role of a heterotrimeric G protein in regulation of Arabidopsis seed germination. Plant Physiology 129, 897-907.

Ullah H, Chen JG, Young JC, Im KH, Sussman MR, Jones AM. 2001. Modulation of cell proliferation by heterotrimeric G protein in Arabidopsis. Science 292, 2066-2069.

Urano D, Chen JG, Botella JR, Jones AM. 2013. Heterotrimeric G protein signalling in the plant kingdom. Open Biology 3:120186.

Urano D, Phan N, Jones JC, Yang J, Huang J, Grigston J, Taylor JP, Jones AM. 2012. Endocytosis of the seven-transmembrane RGS1 protein activates G-protein-coupled signalling in Arabidopsis. Nature Cell Biology 14, 1079-1088.

Vandenbussche F, Habricot Y, Condiff AS, Maldiney R, Van der Straeten D, Ahmad M. 2007. HY5 is a point of convergence between cryptochrome and cytokinin signalling pathways in Arabidopsis thaliana. The Plant Journal 49, 428-441.

Vert G, Walcher CL, Chory J, Nemhauser JL. 2008. Integration of auxin and brassinosteroid pathways by Auxin Response Factor 2. Proceedings of the National Academy of Sciences of the United States of America 105, 9829-9834.

Wang HX, Weerasinghe RR, Perdue TD, Cakmakci NG, Taylor JP, Marzluff WF, Jones AM. 2006. A golgi-localized hexose transporter is involved in heterotrimeric G protein-mediated early development in Arabidopsis. Molecular Biology of the Cell 17, 4257- 4269.

Wang ZY, Bai MY, Oh E, Zhu JY. 2012. Brassinosteroid signaling network and regulation of photomorphogenesis. Annual Review of Genetics 46, 701-724.

Wan Y, Jasik J, Wang L, Hao H, Volkmann D, Menzel D, Mancuso S, Baluška F, Lin J. 2012. The signal transducer NPH3 integrates the phototropin1 photosensor with PIN2-based polar auxin transport in Arabidopsis root phototropism. The Plant Cell 24, 551-565.

Warpeha KM, Lateef SS, Lapik Y, Anderson M, Lee BS, Kaufman LS. 2006. G-protein-coupled receptor 1, G-protein Galpha-subunit 1, and prephenate dehydratase 1 are required for blue light-induced production of phenylalanine in etiolated Arabidopsis. Plant Physiology 140, 844-855.

Warpeha KM, Upadhyay S, Yeh J, Adamiak J, Hawkins SI, Lapik YR, Anderson MB, Kaufman LS. 2007. The GCR1, GPA1, PRN1, NF-Y signal chain mediates both blue light and abscisic acid responses in Arabidopsis. Plant Physiology 143, 1590-1600.

Wei Q, Zhou W, Hu G, Wei J, Yang H, Huang J. 2008. Heterotrimeric G-protein is involved in phytochrome A-mediated cell death of Arabidopsis hypocotyls. Cell Research 18, 949-960.

Weiss CA, Garnaat CW, Mukai K, Hu Y, Ma H. 1994. Isolation of cDNAs encoding

guanine nucleotidebinding protein β-subunit homologues from maize (ZGB1) and Arabidopsis (AGB1). Proceedings of the National Academy of Sciences of the United States of America 91, 9554-9558.

Wettschureck N, Offermanns S. 2005. Mammalian G proteins and their cell type specific functions. Physiological Reviews 85, 1159-1204.

Zhang CQ, Nishiuchi S, Liu S, Takano T. 2008. Characterization of two plasma membrane protein 3 genes (PutPMP3) from the alkali grass, Puccinellia tenuiflora, and functional comparison of the rice homologues, OsLti6a/b from rice. Biochemistry and Molecular Biology Reports 41, 448-454.

Zhang L, Hu G, Cheng Y, Huang J. 2008. Heterotrimeric G protein α and β subunits antagonistically modulate stomatal density in Arabidopsis thaliana. Developmental Biology 324, 68–75.

Zhang S, Cai Z, Wang X. 2009. The primary signaling outputs of brassinosteroids are regulated by abscisic acid signaling. Proceedings of the National Academy of Sciences of the United States of America 106, 4543-4548.

Zhao J, Wang X. 2004. Arabidopsis phospholipase Dalpha1 interacts with the heterotrimeric G-protein alpha-subunit through a motif analogous to the DRY motif in G-protein-coupled receptors. The Journal of Biological Chemistry 279, 1794-1800.

Zwiewka M, Feraru E, Möller B, Hwang I, Feraru MI, Kleine-Vehn J, Weijers D, Friml J. 2011. The AP-3 adaptor complex is required for vacuolar function in Arabidopsis. Cell Research 21, 1-12.